Accepted Manuscript

Novel 1,4-naphthoquinone-based sulfonamides: synthesis, QSAR, anticancer and antimalarial studies

Ratchanok Pingaew, Veda Prachayasittikul, Apilak Worachartcheewan, Chanin Nantasenamat, Supaluk Prachayasittikul, Somsak Ruchirawat, Virapong Prachayasittikul

PII: S0223-5234(15)30245-2

DOI: 10.1016/j.ejmech.2015.09.001

Reference: EJMECH 8098

To appear in: *European Journal of Medicinal Chemistry*

Received Date: 18 June 2015

Revised Date: 11 August 2015

Accepted Date: 2 September 2015

Please cite this article as: R. Pingaew, V. Prachayasittikul, A. Worachartcheewan, C. Nantasenamat, S. Prachayasittikul, S. Ruchirawat, V. Prachayasittikul, Novel 1,4-naphthoquinone-based sulfonamides: synthesis, QSAR, anticancer and antimalarial studies, European Journal of Medicinal Chemistry (2015), doi: 10.1016/j.ejmech.2015.09.001.

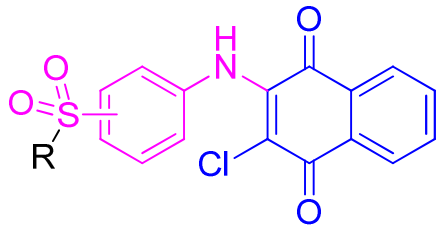

R = -NHCH$_2$CH$_2$2-Py

-NHCH$_2$CH$_2$Ph

-NHCH$_2$CH$_2$Ph(3,4-dimethoxy)

-NHCH$_2$2-Py

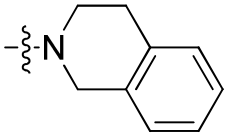

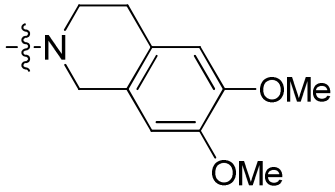

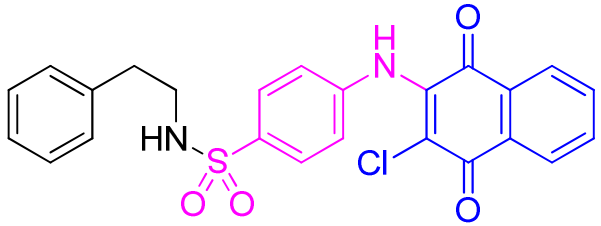

34

IC_{50} = 2.18-11.24 μM (cancer cell lines)
IC_{50} > 107.08 μM (noncancerous cell line)

Novel 1,4-naphthoquinone-based sulfonamides: synthesis, QSAR, anticancer and antimalarial studies

Ratchanok Pingaew [a,*], Veda Prachayasittikul [b,c], Apilak Worachartcheewan [c,d], Chanin Nantasenamat [b,c], Supaluk Prachayasittikul [c], Somsak Ruchirawat [e,f], Virapong Prachayasittikul [b,*]

[a]*Department of Chemistry, Faculty of Science, Srinakharinwirot University, Bangkok 10110, Thailand*

[b] *Department of Clinical Microbiology and Applied Technology, Faculty of Medical Technology, Mahidol University, Bangkok 10700, Thailand*

[c] *Center of Data Mining and Biomedical Informatics, Faculty of Medical Technology, Mahidol University, Bangkok 10700, Thailand*

[d] *Department of Clinical Chemistry, Faculty of Medical Technology, Mahidol University, Bangkok 10700, Thailand*

[e] *Laboratory of Medicinal Chemistry, Chulabhorn Research Institute, and Program in Chemical Biology, Chulabhorn Graduate Institute, Bangkok 10210,Thailand*

[f] *Center of Excellence on Environmental Health and Toxicology, Commission on Higher Education (CHE), Ministry of Education, Thailand*

---

*Corresponding authors:

E-mail: ratchanok@swu.ac.th (R. Pingaew)

Tel: 662-649-5000 ext 18253; Fax: 662-260-0128

E-mail: virapong.pra@mahidol.ac.th (V. Prachayasittikul)

Tel: 662-441-4376; Fax: 662-441-4380

Abstract

A novel series of 1,4-naphthoquinones (**33-44**) tethered by opened and closed chain sulfonamide moieties were designed, synthesized and evaluated for their cytotoxic and antimalarial activities. All quinone-sulfonamide derivatives displayed a broad spectrum of cytotoxic activities against all of the tested cancer cell lines including HuCCA-1, HepG2, A549 and MOLT-3. Most quinones (**33-36** and **38-43**) exerted higher anticancer activity against HepG2 cell than that of the etoposide. The opened chain analogs **36** and **42** were shown to be the most potent compounds. Notably, the restricted sulfonamide analog **38** with 6,7-dimethoxy groups exhibited the most potent antimalarial activity (IC_{50} = 2.8 μM). Quantitative structure-activity relationships (QSAR) study was performed to reveal important chemical features governing the biological activities. Five constructed QSAR models provided acceptable predictive performance (R_{cv} 0.5647 - 0.9317 and $RMSE_{cv}$ 0.1231 - 0.2825). An additional set of structurally modified compounds were generated *in silico* (**34a-34d**, **36a-36k**, **40a-40d** and **42a-42k**) in which their activities were predicted using the constructed QSAR models. A comprehensive discussion of the structure-activity relationships was made and a set of promising compounds (i.e., **33**, **36**, **38**, **42**, **36d**, **36f**, **42e**, **42g** and **42f**) were suggested for further development as anticancer and antimalarial agents.

Keywords: Naphthoquinone; Sulfonamide; QSAR; Anticancer activity; Antimalarial activity

1. Introduction

Quinones are widely distributed in nature [1,2], and are represented in many clinically used drugs (e.g. doxorubicin, daunorubicin, bleomycins, mitomycin-C) [3]. Apparently, 1,4-naphthoquinones have been found to possess a diverse range of biological activities including anticancer and antimalarial activities [4-6]. For example, calothrixins A and B isolated from cyanobacterial *Calothrix* exhibited potent anticancer and antimalarial activities [7]. Biological properties of quinones have been related by a wide range of molecular targets thus rendering them to be promising lead molecules for various therapeutic applications. Two carbonyl groups of quinone have been well-documented to act as electrophile and electron acceptor, therefore, alkylation and reactive oxygen species (ROS) production have been stimulated on the two carbonyl sites (1,4-C), respectively [8-10]. In addition, cytotoxic quinone derivatives were proven to be topoisomerase I and II inhibitors [11,12]. Furthermore, 1,4-naphthoquinone derivatives were previously proposed to display antimalarial activity by involving a cascade of redox reactions in the parasite [13,14].

Aminonaphthoquinone, an important class of the quinone family, has been proven to be interesting scaffold for pharmacological applications [15-21]. For instance, 5-hydroxy-3-amino-2-aceto-1,4-naphthoquinone (**1**) and 2-amino-3-chloro-1,4-naphthoquinone (**2**), as shown in Fig. 1, exhibited significant cytotoxic [15] and antimalarial [16] activities respectively. The extended studies to structural variations of the naphthoquinones revealed that the presence of amino or chloro substituents on the 1,4-naphthoquinone would contribute to their redox potentials [17-21]. Enhancing of biological potency was observed when amino group was inserted at 2- and/or 3- positions [17]. Phenylaminonaphthoquinones showed superior anticancer activity than that of alkylamino counterparts, and the incorporation of acetyl group on the phenylamino part led to improvement of their cytotoxic potencies [17]. Furthermore, insertion of sulfonamide moiety to phenylamino-1,4-naphthoquinone affording PI-083 (**3**, Fig. 1) that was capable of inhibition of cell proliferation, and inducing apoptosis with selective for malignant over normal cells [22].

To find novel lead candidates as promising anticancer and antimalarial agents based on the attractive phenotypes, thus, target 1,4-naphthoquinone-sulfonamide derivatives (Fig. 2) were rationally designed as follows:

(i) use 2-chloro-3-anilino-1,4-naphthoquinone as a core structure;

(ii) vary the position of sulfonyl group on aniline ring (3- or 4-position); and

(iii) vary the type of *N*-substituent of sulfonamide (opened chain alkylphenyl group, opened chain alkylpyridyl group or restricted isoquinoline ring).

A variety of expected 1,4-naphthoquinone derivatives were synthesized and evaluated for their *in vitro* antiproliferative activity against four cancer cells and normal cell line as well as antimalarial activity toward *Plasmodium faciparum*. To provide insights into the effect of sulfonamide substituents on the quinone ring in their biological activities, quantitative structure-activity relationships (QSAR) of the synthesized and structurally modified compounds were investigated.

2. Results and discussion

2.1 Chemistry

The preparation of aminobenzenesulfonamides **20**-**31** as starting materials for the synthesis of phenylaminonaphthoquinone is illustrated in Scheme 1. Initially, condensation of various primary amines (**4**-**7**) with either 3- or 4-nitrobenzenesulfonyl chloride yielded the corresponding phenethyl sulfonamides (**8**-**15**). Consequently, *N*-sulfonyl-1,2,3,4-tetrahydroisoquinolines (**16**-**19**) were readily obtained using the Pictet-Spengler reaction by treatment of nitrobenzenesulfonamides **(12**-**15)** with paraformaldehyde in refluxing formic acid. Reduction of the nitro derivatives (**8**-**11**) was carried out by catalytic hydrogenation using palladium on charcoal whereas the reduction of nitro analogs (**12**-**19**) was performed using stannous chloride to give the corresponding aminobenzenesulfonamides (**20**-**31**). With the amino derivatives (**20**-**31**) on hands, a series of desired naphthoquinones (**33**-**44**) were then synthesized by nucleophilic substitution of 2,3-dichloro-1,4-naphthoquinone **32** with the appropriate aminobenzenesulfonamide derivatives **20**-**31** in refluxing ethanol as shown in Scheme 2. However, reaction of 2,3-dichloro-1,4-naphthoquinone **32** with amines in the presenc of bases (KOH or Et_3N) and surfactant (LD or SDS) in aqueous medium have been recently reported.[23] The obtained compounds (**33**-**44**; Fig. 3) are categorized as *para*-isomer (amino and sulfonyl groups at 1,4-position of benzene ring, **33**-**38**) and *meta*-isomer (amino and sulfonyl groups at 1,3-position of benzene ring, **39**-**44**). *N*-substituents of these sulfonamides are opened chain alkylpyridines (**33**, **36**, **39** and **42**), alkylphenyls (**33**-**34**, **40**-**41**) and closed chain or restricted isoquinolines **37**-**38** and **43**-**44**).

Structures of the desired naphthoquinone **33**-**44** were confirmed based on their HRMS and NMR spectra. ^{1}H NMR spectra showed the presence of NH proton as a singlet at δ

around 9.5-9.6 ppm indicating that the nucleophilic displacement of the phenylamino derivative occurred at a chloro group of 2,3-dichloro-1,4-naphthoquinone. In addition, ^{13}C NMR spectra displayed a characteristic signal of two carbonyl groups (C=O) at chemical shift in the range of 177-181 ppm.

2.2 Biological activities

2.2.1 Cytotoxic activity

In assessing the cytotoxicity, the series of 1,4-naphthoquinones (**33-44**) were examined against four human cancer cell lines including HuCCA-1 (cholangiocarcinoma), HepG2 (hepatocellular carcinoma), A549 (lung carcinoma) and MOLT-3 (lymphoblastic leukemia) cell lines as summarized in Table 1.

2,3-Dichloro-1,4-naphthoquinone **32** was reported to exert cytotoxic activity against HuCCA-1, HepG2, A549 and MOLT-3 cells with IC_{50} values 19.20, 65.19, 45.37 and 13.04 μM, respectively [16]. Distinctively, replacement of the chloro atom of compound **32** with various aminobenzenesulfonamide moieties afforded the compounds with improved their inhibitory potencies. It was observed that all the tested naphthoquinone derivatives displayed a broad spectrum of cytotoxic activities, in which their inhibition potencies depended on the type of cancer cells.

Most naphthoquinones exhibited cytotoxic activities with comparable IC_{50} values lesser than 10 μM against HuCCA-1 cell line, except for the restricted isoquinolines **37** (IC_{50} = 57.77 μM) and **44** (IC_{50} = 26.42 μM). Apparently, the opened chain pyridine analog **42** was shown to be the most potent compound with IC_{50} 3.66 μM; however the *meta*-compound **42** displayed 9-folds lower potency than the control drug doxorubicin. Additionally, the compound **42** was also shown to be the most potent compound against A549 cell line (IC_{50} = 2.3 μM). The effects of chemical structures, *meta*- and *para*- isomers, and substituents towards bioactivities of the compounds are discussed (section 2.3).

Interestingly, most 1,4-naphthoquinones (*para*-analogs, **33-36** and *meta*-analogs, **38-43**) showed higher anticancer activity against HepG2 cell than that of the etoposide. Among these compounds, the analog **36** was shown to be the most potent compound (IC_{50} = 3.30 μM). Reducing the alkyl chain length of pyridine analog **33** led to 3-folds and 5-folds improved inhibition potencies as seen in the analog **36** against HepG2 and A-549 cells, respectively. However those results could not be observed in *meta*-analogs (**39** vs **42**). Obviously, in

MOLT-3 cell line, most compounds exerted comparable cytotoxic activities with IC_{50} lesser than 5 μM, in which the pyridine analogs (**33** and **36**) have shown to be the most potent compounds with identical IC_{50} value of 1.37 μM.

It was observed that naphthoquinones bearing opened chain sulfonamides exhibited higher cytotoxicity (all tested cells) than the analogs containing cyclic sulfonamide as seen for **34** vs **37**, **35** vs **38** (except for MOLT-3 cell) and **41** vs **44** (except for MOLT-3 cell). At this point, it seemed reasonable that NH group of the sulfonamide can act as a hydrogen bond donor which might play a crucial role for cytotoxic activity.

These naphthoquinones (**33-44**) were also tested against the noncancerous (Vero) cell line obtained from African green monkey kidney (Table 1). Comparison of the IC_{50} values measured in cancer cells versus that obtained in normal cells, the isoquinolines (**37**, **38**, **43** and **44**) had no selectivity. Most of the *meta* derivatives seem to be more cytotoxic to normal cell than that of the corresponding *para*-analogs. Notably, the opened chain compounds **33** and **34** were found to be the most promising compounds showing a broad spectrum cytotoxic activity with the best safety index. Both compounds displayed cytotoxicities against the Vero cell line with IC_{50} values of 99.89 and >107.08 μM, respectively.

2.2.2 Antimalarial activity

Antimalarial activity of the quinone-sulfonamides (**33-44**) was evaluated against *P. falciparum* (K1, multidrug resistant strain) as shown in Table 1. The synthesized quinones with opened chain sulfonamides (**35**, **40** and **41**) and restricted-ring sulfonamides (**37-38** and **43-44**) showed significant antimalarial activity with IC_{50} values in the range of 2.80-14.74 μM. Dimethoxy group insertion on the benzene ring in *para* analogs **34** and **37** created the corresponding compounds **35** and **38** with enhanced antimalarial activity; however the reduced activity was observed for *meta* analogs (**40** vs **41** and **43** vs **44**). Replacement of alkyl benzene with alkyl pyridine in *para* analogs (**34** vs **33**, **36**) could not improve the antimalarial potency while the reduced activity was observed for *meta* analogs (**40** vs **39**, **41**). Improving of the potency was observed when the opened chain of *para* analogs **34** and **35** was cyclized to the respective restricted analogs **37** and **38** in which the analog **38** was shown to be the most potent compound (IC_{50} = 2.80 μM). These may be attributed to the lipophilicity of dimethoxyphenyl and the restricted appropriate tetrahydroisoquinoline

sulfonamide which may be required for enhancing the absorption of the compounds into the cells.

2.3. QSAR analysis

Chemical structures of the tested 1,4-naphthoquinones **33-44** (Fig. 3) along with their experimental activity (pIC_{50}) were used for performing QSAR study. The chemical structures were geometrically optimized and their physicochemical descriptors were calculated using Gaussian 09 [24] and Dragon software (version 5.5) [25] to obtain 13 quantum chemical and 3224 molecular descriptors, respectively. Correlation-based feature selection was employed to initially select a set of correlated descriptors for further selection process. Pearson's correlation coefficient (r) between descriptor values and bioactivities were calculated and descriptors having $|r| \geq 0.5$ was retained and further subjected to stepwise multiple linear regression (MLR) as implemented in SPSS statistics 18.0 or attribute elevator CfsSubsetEval as implemented in the Waikato Environment for Knowledge Analysis (WEKA) version 3.4.5 [26] to obtain a sets of 9 important descriptors in which their definitions and their calculated descriptor values are shown in Table 2 and Supplementary Table S1, respectively. The multivariate analysis was performed by (WEKA) version 3.4.5 [26] using multiple linear regression (MLR) algorithm. Five QSAR models were constructed and their predictive performance are summarized in Table 3.

The constructed models provided correlation coefficient (R_{cv}) and root mean square error ($RMSE_{cv}$) values in range of 0.5647 – 0.9317 and 0.1231 – 0.2825, respectively. The A549 model provided the best performance as represented by its highest R_{cv} and its lowest $RMSE_{cv}$ values. The experimental and predicted activities (pIC_{50} values) of the tested compounds **33-44** against four cancer cell lines and *P. falciparum* are presented in Supplementary Table S2 and Fig. 7.

HuCCA-1 cell line:

$$pIC_{50} = 34.1344(X1A) + 23.1368(Gm) + 9.4788(G2u) - 21.1565 \qquad Eq.\ 1$$

The QSAR model revealed that connectivity (X1A) and symmetry (Gm and G2u) of the compound influenced anticancer activity against HuCCA-1 cell line, Eq. 1. The connectivity indices descriptor, X1A, was noted as the most influential descriptor as

represented by its highest regression coefficient. The molecular connectivity indices represent the molecular area which is accessible from outside molecule and are successfully used for describing physicochemical properties of the molecules and their intermolecular interactions [27]. Positive regression coefficients in the QSAR equation indicated that high values of X1A, Gm and G2u are required for potent activity against HuCCA-1 cell line.

HepG2 cell line:

$$pIC_{50} = -0.097(RDF105m) - 0.2179 \qquad \textit{Eq. 2}$$

According to QSAR equation, a mass-weighted RDF descriptor (RDF105m) was noted as an influential descriptor for anticancer activity against HepG2 cell line, Eq. 2.The negative regression coefficient indicated low value of RDF105m is required for potent activity against HepG2 cell line.

A549 cell line:

$$pIC_{50} = -0.0949(RDF105m) + 0.6903(Mor12u) + 0.366 \qquad \textit{Eq. 3}$$

The RDF105m descriptor was also found to influence anticancer activity against A549 cell line (Eq. 3). In addition, a 3D-MoRSE descriptor, Mor12u, was noted as the most important descriptor as shown by its high regression coefficient (Eq. 3). The negative and positive regression coefficient values of RDF105m an Mor12u indicated the low RDF105m value together with the high Mor12u value are essential for the compound to exhibit potent activity against A549 cell line.

MOLT-3 cell line:

$$pIC_{50} = 10.9192(G2u) + 0.0185(G(N..Cl)) - 2.5605 \qquad \textit{Eq. 4}$$

In addition to the G2u descriptor, a geometrical distances between nitrogen (N) atom and chlorine (Cl) atom, represented by G(N..Cl) descriptor, was found to influence anticancer activity against MOLT-3 cell line. Positive regression coefficients presented in the QSAR equation (Eq. 4) indicated that high values of both descriptors are required for high pIC_{50} value.

Antimalarial:

$$pIC_{50} = -1.6078(Mor22v) + 0.1457(B05[N-O]) + 1.2647(Mor24u) - 1.4305 \quad Eq.\ 5$$

3D-MoRSE descriptors (i.e., Mor22v and Mor24u) and the presence/absence of N-O at topological distance 5 were noted as important descriptors governing antimalarial activity. A van der Waals volume descriptor (Mor22v) was found to be the most influential descriptor as indicated by its highest regression coefficient in the QSAR model, Eq. 5. The QSAR equation revealed that low value of Mor22v along with high values of Mor24u and B05[N-O] are essential for potent activity.

2.4. Prediction of structurally modified compounds using the constructed QSAR models

The predicted pIC_{50} values of structurally modified compounds (**34a-34d**, **36a-36k**, **40a-40d**, and **42a-42k**, Figs. 4-6) were computed using the QSAR equations in which important descriptor values were assigned as independent (*X*) variables to calculated activities (dependent variable, *Y*). Predicted activities of structurally modified compounds are summarized in Supplementary Table S3.

2.5. Understanding structure-activity relationships

Understanding structure-activity relationships (SAR) is useful for the search of potential compounds to be further developed [28,29]. QSAR modelling has been successfully employed for understanding SAR of various classes of compounds and bioactivities [17, 30-36]. In this study, a comprehensive analysis of relationships between identified important descriptor values and pIC_{50} value of the individual compound in the QSAR equations was performed to gain insights into the SAR. The analyzed results of tested compounds (**33-44**, Fig. 3) and structurally modified compounds (**34a-34d**, **36a-36k**, **40a-40d**, and **42a-42k**, Figs. 4-6) are summarized in Tables S4–S6. The SAR analysis revealed that closed/opened chain structure, *para*-/*meta*- position of amino and sulfonyl groups on the benzene ring, length of the carbon chain linker as well as type of substituted ring and certain moieties may affect activities of the compounds.

In overview, contrast effects of structural variations were observed between *para*- (**33**–**38**) and *meta*- (**39-44**) series of the tested compounds (Supplementary Table S4). In particular, N-atom of sulfonamide group substituted with benzene ring provided compound with more potent anticancer activity than the pyridine ring for the *para*-compounds (**34** > **33**)

except for MOLT-3 cell while the pyridine substitution was found to be more effective for *meta*-compounds (**39** > **40**). The addition of dimethoxy (diOMe) moieties was noted to improve activity of the *para*-compounds against malarial (**38** > **37**) and cancer cell lines (**35 > 34** and **38 > 37**), except for HuCCA-1 and A549 cell lines (**34** > **35**). For the *meta*-compounds, diOMe groups were observed to ameliorate (**41** > **40**) and aggravate (**43** > **44**) anticancer activities against all cancer cell lines (except for MOLT-3), and antimalarial activities (**40** > **41**).

The structural modifications can cause an alteration, either increase or decrease, of descriptor values thereby influence activities of the compounds. Herein, QSAR equations along with descriptor values were used to reveal the relationships between these interactive factors. The effects of chemical structure on descriptor values are summarized in Supplementary Table S7. Detailed discussion of each cell line/activity is provided in Supplementary data. In brief, the closed/opened chain structure influenced anticancer activity against A549 and HepG2 cell lines, whereas the para-/meta-structure dominated the activity towards HuCCA-1 cell line. Position of aminopyridine and aminoquinoline as well as length of alkyl chain linker were shown to be crucial factors for anticancer activity against MOLT-3 cell line. Particular moieties i.e., diOMe, CF_3, and pyrrole ring were noted for their roles in antimalarial activity.

A series of potential compounds exhibiting the most potent experimental and predicted activities are summarized in Fig. 8. Two isomeric pyridine derivatives with 1C length linker, compounds **36** and **42**, were found to be the most potent anticancer agents. The *para*-compound **36** was the most active compound against HepG2 and MOLT-3 cell lines, whereas the *meta*-compound **42** was noted for HuCCA-1 and A549 cell lines. Various types of substituted rings on sulfonamide group were seen for the most potent modified compounds against each cell lines or *P. falciparum.* It should not be overlooked that the potent anticancer activity against A549 and HepG2 cell lines were observed from a set of 5-menbered ring derivatives (thiophene **42e** and furan **42f**, respectively). Particularly, the positive pIC_{50} values of **42e** were predicted against A549 cell line. The chloro group was suggested to be a crucial moiety governing the potent anticancer activity against MOLT-3 cell line. Likewise, the diOMe substituents (**38**) were noted for antimalarial activity. The results suggested that *meta*- and *para*- isomers, types of substituted ring, length of alkyl chain linker and particular

moieties of the compounds are essential factors influencing anticancer activities against distinct cell line, and antimalarial activity.

3. Conclusions

A novel series of quinones (**33-44**) have been achieved by nucleophilic displacement of 2,3-dichloro-1,4-naphthoquinone **32** with appropriate aminobenzenesulfonamide derivatives **20**-**31**. Most of the naphthoquinones bearing opened chain sulfonamides (**33-36**, **39** and **41-42**) exhibited higher anticancer activity than the cyclic sulfonamides, in which the analog **34** displayed the best safety index. Apparently, the opened chain analogs **36** (*para*-isomer) and **42** (*meta*-isomer) were shown to be the most potent compounds against HepG2 and MOLT-3; and HuCCA-1 and A549 cells, respectively. The *para*-isomer of restricted sulfonamide with diOMe groups (**38**) exerted the most potent antimalarial activity. The QSAR analysis revealed a set of important descriptors which influence the activity of the compound against particular cell lines. The predictions of structurally modified compounds indicated that certain chemical features (i.e, *meta-/para-* and opened/closed chain structures) and particular substituents (i.e., OMe, Cl and length of alkyl linker) are essential for potent activities. Finally, a set of promising compounds against cancer and malarial cell lines were highlighted for guiding the design, synthesis and development of naphthoquinone-based anticancer and antimalarial agents.

4. Experimental section

4.1 Chemistry

Column chromatography was carried out using silica gel 60 (70–230 mesh ASTM). Analytical thin-layer chromatography (TLC) was performed using silica gel 60 F254 aluminum sheets. ^{1}H- and ^{13}C- NMR spectra were recorded on a Bruker AVANCE 300 NMR spectrometer (operating at 300 MHz for ^{1}H and 75 MHz for ^{13}C). The following standard abbreviations were used for signal multiplicities: singlet (s), doublet (d), triplet (t), quartet (q), multiplet (m), and broad (br). Mass spectra were recorded on a Bruker Daltonics (microTOF). IR spectra were obtained using a universal attenuated total reflectance attached on a Perkin–Elmer Spectrum One spectrometer or on a FT-IR Spectrum BX (Perkin Elmer) in KBr. Melting points were determined using a Griffin melting point apparatus and were uncorrected.

*4.2 General Procedure for the synthesis of benzenesulfonamides (**8-15**)*

A solution of the corresponding amine (10 mmol) in dichloromethane (50 mL) was added dropwise to a stirred mixture of benzenesulfonyl chloride (10 mmol) and sodium carbonate (Na_2CO_3, 14 mmol) in dichloromethane (20 mL). The reaction mixture was stirred at room temperature overnight, and added distilled water (20 mL). The organic phase was separated and the aqueous phase was extracted with dichloromethane (2 × 30 mL). The organic extracts were combined and washed with water (30 mL). The organic layer was dried over anhydrous sodium sulfate (anh. Na_2SO_4), filtered and evaporated to dryness under reduced pressure. The crude product was further purified either by recrystalization or column chromatography.

^{1}H NMR of 4-nitro-*N*-(pyridin-2-ylmethyl)benzenesulfonamide (**9**) [37], 4-nitro-*N*-phenethylbenzenesulfonamide (**12**) [38], *N*-(3,4-dimethoxyphenethyl)-4-nitrobenzenesulfonamide (**13**) [38], 3-nitro-*N*-phenethylbenzenesulfonamide (**14**) [39] and *N*-(3,4-dimethoxyphenethyl)-3-nitrobenzenesulfonamide (**15**) [39] were consistent with that reported in the literature.

*4.2.1 4-nitro-N-(2-(pyridin-2-yl)ethyl)benzenesulfonamide (**8**)*

From 2-pyridylethylamine **4** and 4-nitrobenzenesulfonyl chloride. Pale yellow solid. Yield: 88%. mp 147-148 ^{o}C. R_f 0.33 (30% acetone:hexane). IR (UATR) cm^{-1}: 3280. ^{1}H NMR (300 MHz, $CDCl_3$) δ 2.98 (t, J = 5.8 Hz, 2H, PyCH_2), 3.44 (t, J = 5.8 Hz, 2H, CH_2NH), 6.76 (br s, 1H, N*H*), 7.10 (d, J = 7.7 Hz, 1H, Py*H*), 7.18 (dd, J = 7.1, 5.1 Hz, 1H, Py*H*), 7.61 (dt, J = 7.7, 1.7 Hz, 1H, Py*H*), 8.05 (d, J = 7.6 Hz, 2H, Ar*H*), 8.33 (d, J = 7.6 Hz, 2H, Ar*H*), 8.47 (d, J = 4.4 Hz, 1H, Py*H*). ^{13}C NMR (75 MHz, $CDCl_3$): δ 35.6, 42.3, 122.0, 123.5, 124.3 (2), 128.2 (2), 136.9, 146.3, 149.0, 149.9, 158.8. HRMS-TOF: m/z $[M+H]^+$ 308.0701 (Calcd for $C_{13}H_{14}N_3O_4S$: 308.0700).

*4.2.2 3-nitro-N-(2-(pyridin-2-yl)ethyl)benzenesulfonamide (**10**)*

From 2-pyridylethylamine **4** and 3-nitrobenzenesulfonyl chloride. Light brown solid. Yield: 80%. mp 119-120 ^{o}C. R_f 0.38 (30% acetone:hexane). IR (KBr) cm^{-1}: 3451. ^{1}H NMR (300 MHz, $CDCl_3$) δ 2.99 (t, J = 6.1 Hz, 2H, PyCH_2), 3.44 (br q, 2H, CH_2NH), 6.79 (br s, 1H, N*H*), 7.09 (d, J = 7.7 Hz, 1H, Py*H*), 7.16 (dd, J = 6.9, 5.0 Hz, 1H, Py*H*), 7.61 (dt, J = 7.7, 1.8 Hz, 1H, Py*H*), 7.72 (t, J = 8.0 Hz, 1H, Ar*H*), 8.20 (dt, J = 87.7, 1.5 Hz, 1H, Ar*H*), 8.40 (d, J = 8.0 Hz, 1H, Ar*H*), 8.48 (d, J = 4.9 Hz, 1H, Py*H*), 8.69 (t, J = 1.9 Hz, 1H, Ar*H*). ^{13}C NMR

(75 MHz, $CDCl_3$): δ 35.6, 42.3, 122.0, 122.2, 123.5, 126.8, 130.3, 132.6, 136.9, 142.6, 148.3, 149.0, 158.7. HRMS-TOF: m/z $[M+Na]^+$ 330.0516 (Calcd for $C_{13}H_{13}N_3NaO_4S$: 330.0519).

*4.2.3 3-nitro-N-(pyridin-2-ylmethyl)benzenesulfonamide (**11**)*

From picolylamine **7** and 3-nitrobenzenesulfonyl chloride. Pale yellow solid. Yield: 81%. mp 130-131 ^oC. R_f 0.38 (30% acetone:hexane). IR (UATR) cm^{-1}: 3285. ^1H NMR (300 MHz, $CDCl_3$) δ 4.33 (d, J = 1.8 Hz, 2H, PyCH_2), 6.32 (br s, 1H, N*H*), 7.07-7.17 (m, 2H, Py*H*), 7.53-7.67 (m, 2H, Ar*H* and Py*H*), 8.15 (d, J = 7.8 Hz, 1H, Ar*H*), 8.31 (d, J = 7.8 Hz, 1H, Ar*H*), 8.39 (d, J = 4.4 Hz, 1H, Py*H*), 8.61 (s, 1H, Ar*H*). ^{13}C NMR (75 MHz, $CDCl_3$): δ 47.3, 122.0, 122.4, 122.9, 126.8, 130.2, 132.6, 136.9, 142.3, 148.2, 149.1, 153.9 HRMS-TOF: m/z $[M+Na]^+$ 316.0353 (Calcd for $C_{12}H_{11}N_3NaO_4S$: 316.0363).

*4.3 General procedure for the synthesis of 1,2,3,4-tetrahydro-2-((nitrophenyl)sulfonyl)-isoquinolines (**16-19**)*

A mixture of nitrobenzenesulfonamide (0.67 mmol) and paraformaldehyde (0.72 mmol) in formic acid (15 mL) was refluxed for 2 h, and then allowed to cool to room temperature. The reaction mixture was added to 30 mL of water, and the product was extracted with CH_2Cl_2 (2 × 30 mL). Combined extracts were washed with saturated aqueous $NaHCO_3$, dried (anh. Na_2SO_4) and evaporated to dryness under reduced pressure. The crude product was recrystallized from methanol.

^1H NMR of 2-((4-nitrophenyl)sulfonyl)-1,2,3,4-tetrahydroisoquinoline (**16**) [40], 6,7-dimethoxy-2-((4-nitrophenyl)sulfonyl)-1,2,3,4-tetrahydroisoquinoline (**17**) [41], 2-((3-nitrophenyl)sulfonyl)-1,2,3,4-tetrahydroisoquinoline (**18**) [42] and 6,7-dimethoxy-2-((3-nitrophenyl)sulfonyl)-1,2,3,4-tetrahydroisoquinoline (**19**) [39] were consistent with that reported in the literature.

*4.4 General procedure for the synthesis of aminobenzenesulfonamides (**20-23**)*

A mixture of nitrobenzenesulfonamide (4 mmol) and 10% Pd-C (0.02 g) in absolute ethanol (20 mL) was stirred at room temperature under a hydrogen atmosphere until completion of the reaction as monitored by TLC. The catalyst was removed by filtration and the filtrate was concentrated under reduced pressure. The residue was purified using silica gel column chromatography.

*4.4.1 4-amino-N-(2-(pyridin-2-yl)ethyl)benzenesulfonamide (**20**)*

From 4-nitro-*N*-(2-(pyridin-2-yl)ethyl)benzenesulfonamide (**8**). Yellow solid. Yield: 43%. mp 132 ^{o}C (d). R_f 0.15 (30% acetone:hexane). IR (KBr) cm^{-1}: 3418, 3335, 3214. ^{1}H NMR (300 MHz, DMSO-d$_6$) δ 2.79 (t, J = 7.7 Hz, 2H, PyCH_2), 2.99 (t, J = 7.7 Hz, 2H, CH_2NH), 5.91 (s, 2H, NH_2), 6.58 (d, J = 8.6 Hz, 2H, ArH), 7.15-7.22 (m, 3H, NHSO$_2$ and PyH), 7.39 (d, J = 8.6 Hz, 2H, ArH), 7.66 (t, J = 7.7 Hz, 1H, PyH), 8.43 (d, J = 3.9 Hz, 1H, PyH). ^{13}C NMR (75 MHz, DMSO-d$_6$): δ 37.7, 42.8, 113.2 (2), 122.0, 123.7, 125.7, 128.9 (2), 137.0, 149.5, 152.9, 159.0. HRMS-TOF: m/z [M+H]$^+$ 278.0973 (Calcd for $C_{13}H_{16}N_3O_2S$: 278.0963).

*4.4.2 4-amino-N-(pyridin-2-ylmethyl)benzenesulfonamide (**21**)*

From 4-nitro-*N*-(pyridin-2-ylmethyl)benzenesulfonamide (**9**). Yellow solid. Yield: 52%. mp 142-143 ^{o}C. R_f 0.16 (30% acetone:hexane). IR (UATR) cm^{-1}: 3468, 3374, 3243. ^{1}H NMR (300 MHz, DMSO-d$_6$) δ 3.97 (d, J = 6.4 Hz, 2H, PyCH_2), 5.93 (s, 2H, NH_2), 6.60 (d, J = 8.7 Hz, 2H, ArH), 7.24 (dd, J = 6.5, 4.8 Hz, 1H, PyH), 7.37 (d, J = 7.9 Hz, 1H, PyH), 7.43 (d, J = 8.7 Hz, 2H, ArH), 7.69-7.77 (m, 2H, NHSO$_2$ and PyH), 8.44 (d, J = 4.8 Hz, 1H, PyH). ^{13}C NMR (75 MHz, DMSO-d$_6$): δ 48.4, 113.1 (2), 122.0, 122.7, 125.8, 129.0 (2), 137.1, 149.1, 153.0, 158.1. HRMS-TOF: m/z [M+Na]$^+$ 286.0633 (Calcd for $C_{12}H_{13}N_3NaO_2S$: 286.0621).

*4.4.3 3-amino-N-(2-(pyridin-2-yl)ethyl)benzenesulfonamide (**22**)*

From 3-nitro-*N*-(2-(pyridin-2-yl)ethyl)benzenesulfonamide (**10**). Yellow solid. Yield: 48%. mp 133-134 ^{o}C. R_f 0.28 (30% acetone:hexane). IR (UATR) cm^{-1}: 3458, 3374, 3246. ^{1}H NMR (300 MHz, DMSO-d$_6$) δ 2.83 (t, J = 7.7 Hz, 2H, PyCH_2), 3.08 (t, 2H, CH_2NH), 5.56 (s, 2H, NH_2), 6.74 (d, J = 8.0 Hz, 1H, ArH), 6.86 (d, J = 7.7 Hz, 1H, ArH), 6.97 (s, 1H, ArH), 7.14-7.24 (m, 3H, ArH and PyH), 7.50 (br s, 1H, NHSO$_2$), 7.67 (t, J = 7.6 Hz, 1H, PyH), 8.45 (d, J = 4.4 Hz, 1H, PyH). ^{13}C NMR (75 MHz, DMSO-d$_6$): δ 37.8, 42.8, 111.6, 113.6, 117.6, 122.1, 123.7, 130.0, 137.0, 141.2, 149.5, 149.8, 158.8. HRMS-TOF: m/z [M+Na]$^+$ 300.0781 (Calcd for $C_{13}H_{15}N_3NaO_2S$: 300.0777).

*4.4.4 3-amino-N-(pyridin-2-ylmethyl)benzenesulfonamide (**23**)*

From 3-nitro-*N*-(pyridin-2-ylmethyl)benzenesulfonamide (**11**). Yellow solid. Yield: 55%. mp 110-111 ^{o}C. R_f 0.29 (30% acetone:hexane). IR (KBr) cm^{-1}: 3456, 3363, 3236. ^{1}H NMR (300 MHz, DMSO-d$_6$) δ 4.03 (d, J = 6.3 Hz, 2H, PyCH_2), 5.56 (s, 2H, NH_2), 6.75 (d, J = 8.0 Hz, 1H, ArH), 6.90 (d, J = 7.7 Hz, 1H, ArH), 7.00 (s, 1H, ArH), 7.18 (t, J = 7.8 Hz, 1H, ArH), 7.25 (dd, J = 7.5, 4.8 Hz, 1H, PyH), 7.38 (d, J = 7.7 Hz, 1H, PyH), 7.75 (t, J = 7.7 Hz, 1H, PyH), 8.05 (t, J = 6.2 Hz, 1H, NHSO$_2$), 8.44 (d, J = 4.7 Hz, 1H, PyH). ^{13}C NMR (75 MHz,

DMSO-d_6): δ 48.4, 111.6, 113.7, 117.7, 121.9, 122.8, 130.0, 137.2, 141.3, 149.1, 149.8, 157.9. HRMS-TOF: m/z $[M+Na]^+$ 286.0632 (Calcd for $C_{12}H_{13}N_3NaO_2S$: 286.0621).

*4.5 General procedure for the synthesis of aminobenzenesulfonamides (**24-31**)*

A mixture of nitrobenzenesulfonamide (4 mmol) and $SnCl_2{\cdot}2H_2O$ (20 mmol) in absolute ethanol (20 mL) was stirred under reflux until completion of the reaction as monitored by TLC until completion of the reaction as monitored by TLC, then concentrated under reduced pressure. Water (20 mL) was added and extracted with EtOAc (3 × 20 mL). The organic extracts were combined and washed with water (20 mL) and brine (20 mL). The organic layer was dried over anh. Na_2SO_4, filtered and concentrated. The crude product was purified using silica gel column chromatography.

^{1}H NMR of 4-amino-*N*-phenethylbenzenesulfonamide (**24**) [43], 4-amino-*N*-(3,4-dimethoxyphenethyl)benzenesulfonamide (**25**) [43], 3-amino-N-phenethylbenzenesulfonamide (**26**) [44], 4-((3,4-dihydroisoquinolin-2(1*H*)-yl)sulfonyl)aniline (**28**) [45], 4-((6,7-dimethoxy-3,4-dihydroisoquinolin-2(1*H*)-yl)sulfonyl)aniline (**29**) [45] and 3-((3,4-dihydroisoquinolin-2(1*H*)-yl)sulfonyl)aniline (**30**) [42] and 3-((6,7-dimethoxy-3,4-dihydroisoquinolin-2(1*H*)-yl)sulfonyl)aniline (**31**) [39] were consistent with that reported in the literature.

*4.5.1 3-amino-N-(3,4-dimethoxyphenethyl)benzenesulfonamide (**27**)*

From *N*-(3,4-dimethoxyphenethyl)-3-nitrobenzenesulfonamide (**15**). Yellow solid. Yield: 80%. mp 89-90 ^{o}C. R_f 0.30 (30% acetone:hexane). IR (UATR) cm^{-1}: 3467, 3372, 3259. ^{1}H NMR (300 MHz, $CDCl_3$) δ 2.69 (t, *J* = 6.8 Hz, 2H, ArC*H*$_2$), 3.17 (q, *J* = 6.8 Hz, 2H, C*H*$_2$NH), 3.80, 3.83 (2s, 6H, 2 × OC*H*$_3$), 4.40 (t, *J* = 6.0 Hz, 1H, N*H*), 6.56 (d, *J* = 1.8 Hz, 1H, Ar*H*), 6.61 (dd, *J* = 8.1, 1.8 Hz, 1H, Ar*H*), 6.75 (d, *J* = 8.1 Hz, 1H, Ar*H*), 6.80 (dd, *J* = 8.0, 1.6 Hz, 1H, Ar*H*), 7.02 (t, *J* = 1.8 Hz, 1H, Ar*H*), 7.10 (d, *J* = 7.7 Hz, 1H, Ar*H*), 7.22 (t, *J* = 7.9 Hz, 1H, Ar*H*),. ^{13}C NMR (75 MHz, DMSO-d_6) δ 35.3, 44.4, 55.9 (2), 111.4, 111.8, 112.7, 116.6, 118.8, 120.8, 130.0, 130.1, 140.5, 147.2, 147.9, 149.1. HRMS-TOF: m/z [M + Na]$^+$ 359.1027 (Calcd for $C_{16}H_{20}N_2NaO_4S$: 359.1036).

*4.6 General procedure for the synthesis of naphthoquinones (**33-44**)*

A mixture of the appropriate amine (5 mmol) and 2,3-dichloronaphthoquinone **32** (5 mmol) in absolute ethanol (20 mL) was stirred under reflux until completion of the reaction as monitored by TLC, and then concentrated under reduced pressure. Water (20 mL) was added

and extracted with EtOAc (3 × 20 mL). The organic layer was dried over anh. Na_2SO_4, filtered and concentrated under reduced pressure. The crude product was purified using silica gel column chromatography to afford the pure product.

*4.6.1 4-((3-chloro-1,4-dioxo-1,4-dihydronaphthalen-2-yl)amino)-N-(2-(pyridin-2-yl)ethyl)benzenesulfonamide (**33**)*

From 4-amino-*N*-(2-(pyridin-2-yl)ethyl)benzenesulfonamide (**20**). Red solid. Yield: 20%. mp 202-203 ^{o}C. R_f 0.21 (30% acetone:hexane). IR (UATR) cm^{-1}: 3254, 1672, 1593. ^{1}H NMR (300 MHz, DMSO-d$_6$) δ 2.82 (t, J = 7.4 Hz, 2H, PyCH_2), 3.10 (q, J = 6.9 Hz, 2H, CH_2NH), 7.17-7.25 (m, 4H, ArH_2 and PyH_2), 7.59-7.70 (m, 4H, ArH_2, PyH and NHSO$_2$), 7.82 (dt, J = 7.4, 1.3 Hz, 1H, NTQH), 7.85 (dt, J = 7.4, 1.3 Hz, 1H, NTQH), 8.04 (d, J = 7.3 Hz, 2H, NTQH), 8.44 (d, J = 4.5 Hz, 1H, PyH), 9.53 (s, 1H, NH). ^{13}C NMR (75 MHz, DMSO-d$_6$): δ 37.7, 42.8, 118.9, 122.1, 122.9 (2), 123.7, 126.7, 127.1, 127.2 (2), 131.0, 132.2, 134.0, 134.9, 135.2, 136.9, 143.2, 143.4, 149.5, 158.8, 177.4, 180.4. HRMS-TOF: m/z [M+H]$^+$ 468.0777 (Calcd for $C_{23}H_{19}ClN_3O_4S$: 468.0779).

*4.6.2 4-((3-chloro-1,4-dioxo-1,4-dihydronaphthalen-2-yl)amino)-N-phenethylbenzenesulfonamide (**34**)*

From 4-amino-*N*-phenethylbenzenesulfonamide (**24**). Red solid. Yield: 45%. mp 181-182 ^{o}C. R_f 0.31 (30% acetone:hexane). IR (KBr) cm^{-1}: 3275, 1674, 1591. ^{1}H NMR (300 MHz, DMSO-d$_6$) δ 2.66 (t, J = 7.8 Hz, 2H, ArCH_2), 2.96 (q, J = 6.3 Hz, 2H, CH_2NH), 7.15 (d, J = 8.6 Hz, 2H, ArH), 7.17-7.30 (m, 5H, ArH), 7.63 (t, J = 5.8 Hz, 1H, NHSO$_2$), 7.69 (d, J = 8.6 Hz, 2H, ArH), 7.83 (t, J = 7.4 Hz, 1H, NTQH), 7.88 (t, J = 7.4 Hz, 1H, NTQH), 8.05 (d, J = 7.4 Hz, 2H, NTQH), 9.56 (s, 1H, NH). ^{13}C NMR (75 MHz, DMSO-d$_6$): δ 35.7, 44.6, 118.9, 122.9 (2), 126.7 (2), 127.1, 127.2 (2), 128.8 (2), 129.1 (2), 130.9, 132.2, 134.0, 134.9, 135.2, 139.2, 143.2, 143.3, 177.5, 180.4. HRMS-TOF: m/z [M+H]$^+$ 467.0821 (Calcd for $C_{24}H_{20}ClN_2O_4S$: 467.0827).

*4.6.3 4-((3-chloro-1,4-dioxo-1,4-dihydronaphthalen-2-yl)amino)-N-(3,4-dimethoxyphenethyl)benzenesulfonamide (**35**)*

From 4-amino-*N*-(3,4-dimethoxyphenethyl)benzenesulfonamide (**25**). Red solid. Yield: 55%. mp 191-192 ^{o}C. R_f 0.21 (30% acetone:hexane). IR (UATR) cm^{-1}: 3261, 1671, 1591. ^{1}H NMR (300 MHz, DMSO-d$_6$) δ 2.57 (t, J = 7.8 Hz, 2H, ArCH_2), 2.94 (q, J = 6.3 Hz, 2H, CH_2NH), 3.68, 3.70 (2s, 6H, 2 × OCH_3), 6.63 (dd, J = 8.2, 1.8 Hz, 1H, ArH), 6.72 (d, J = 1.8 Hz, 1H, ArH), 6.81 (d, J = 8.2 Hz, 1H, ArH), 7.22 (d, J = 8.6 Hz, 2H, ArH), 7.57 (t, J = 5.7 Hz, 1H,

N*H*SO_2), 7.67 (d, *J* = 8.6 Hz, 2H, Ar*H*), 7.82 (t, *J* = 7.6 Hz, 1H, NTQ*H*), 7.87 (t, *J* = 7.6 Hz, 1H, NTQ*H*), 8.04 (d, *J* = 7.6 Hz, 2H, NTQ*H*), 9.53 (s, 1H, N*H*). ^{13}C NMR (75 MHz, DMSO-d_6): δ 34.8, 44.2, 55.4, 55.5, 112.0, 112.6, 118.2, 120.4, 122.4 (2), 126.2, 126.5, 126.7 (2), 130.5, 131.1, 131.8, 133.4, 134.5, 134.7, 142.8, 143.1, 147.3, 148.6, 176.8, 179.9. HRMS-TOF: m/z $[M+H]^+$ 527.1036 (Calcd for $C_{26}H_{24}ClN_2O_6S$: 527.1038).

*4.6.4 4-((3-chloro-1,4-dioxo-1,4-dihydronaphthalen-2-yl)amino)-N-(pyridin-2-ylmethyl)benzenesulfonamide (**36**)*

From 4-amino-*N*-(pyridin-2-ylmethyl)benzenesulfonamide (**21**). Red-brown solid. Yield: 31%. mp 225-226 ^{o}C. R_f 0.38 (30% acetone:hexane). IR (UATR) cm^{-1}: 3261, 1675, 1591. ^{1}H NMR (300 MHz, DMSO-d_6) δ 4.10 (d, *J* = 6.2 Hz, 2H, PyCH_2), 7.17-7.28 (m, 3H, ArH_2 and Py*H*), 7.36 (d, *J* = 7.8 Hz, 1H, Py*H*), 7.65-7.77 (m, 3H, ArH_2 and Py*H*), 7.84 (t, *J* = 7.4 Hz, 1H, NTQ*H*), 7.89 (t, *J* = 7.4 Hz, 1H, NTQ*H*), 8.06 (d, *J* = 7.4 Hz, 2H, NTQ*H*), 8.19 (t, *J* = 6.2 Hz, 1H, N*H*SO_2), 8.44 (d, *J* = 4.3 Hz, 1H, Py*H*), 9.56 (s, 1H, N*H*). ^{13}C NMR (75 MHz, DMSO-d_6): δ 48.4, 119.0, 122.0, 122.8 (2), 122.9, 126.7, 127.1, 127.2 (2), 131.0, 132.2, 134.0, 135.0, 135.2, 137.2, 143.1, 143.3, 149.2, 157.7, 177.5, 180.4. HRMS-TOF: m/z $[M+Na]^+$ 476.0448 (Calcd for $C_{22}H_{16}ClN_3NaO_4S$: 476.0442).

*4.6.5 2-chloro-3-((4-((3,4-dihydroisoquinolin-2(1H)-yl)sulfonyl)phenyl)amino)naphthalene-1,4-dione (**37**)*

From 4-((3,4-dihydroisoquinolin-2(1*H*)-yl)sulfonyl)aniline (**28**). Red solid. Yield: 38%. mp 179-180 ^{o}C. R_f 0.36 (30% acetone:hexane). IR (KBr) cm^{-1}: 3275, 1674, 1591. ^{1}H NMR (300 MHz, DMSO-d_6) δ 2.84 (t, *J* = 7.8 Hz, 2H, C4-IQ*H*), 3.31 (t, *J* = 6.3 Hz, 2H, C3-Iq*H*), 4.21 (s, 2H, C1-IQ*H*), 7.07-7.18 (m, 4H, IQ*H*), 7.25 (d, *J* = 8.7 Hz, 2H, Ar*H*), 7.72 (d, *J* = 8.7 Hz, 2H, Ar*H*), 7.83 (t, *J* = 7.4 Hz, 1H, NTQ*H*), 7.88 (t, *J* = 7.4 Hz, 1H, NTQ*H*), 8.05 (d, *J* = 7.4 Hz, 2H, NTQ*H*), 9.59 (s, 1H, N*H*). ^{13}C NMR (75 MHz, DMSO-d_6): δ 28.3, 44.0, 47.7, 119.7, 122.7 (2), 126.6, 126.7, 126.9, 127.0, 127.1, 128.1 (2), 129.1, 130.0, 130.1, 131.0, 132.1, 133.5, 134.0, 135.2, 143.0, 144.1, 177.5, 180.3. HRMS-TOF: m/z $[M+H]^+$ 479.0829 (Calcd for $C_{25}H_{20}ClN_2O_4S$: 479.0827).

*4.6.6 2-chloro-3-((4-((6,7-dimethoxy-3,4-dihydroisoquinolin-2(1H)-yl)sulfonyl)phenyl)amino)naphthalene-1,4-dione (**38**)*

From 4-((6,7-dimethoxy-3,4-dihydroisoquinolin-2(1*H*)-yl)sulfonyl)aniline (**29**). Red solid. Yield: 41%. mp 161-162 ^{o}C. R_f 0.29 (30% acetone:hexane). IR (KBr) cm^{-1}: 3313, 1671, 1594. ^{1}H NMR (300 MHz, DMSO-d_6) δ 2.75 (br t, *J* = 5.1 Hz, 2H, C4-IQ*H*), 3.31 (t, *J* = 5.2

Hz, 2H, C3-Iq*H*), 3.68 (s, 6H, 2 × OCH_3), 4.11 (s, 2H, C1-IQ*H*), 6.66, 6.76 (2s, 2H, IQ*H*), 7.25 (d, *J* = 8.6 Hz, 2H, Ar*H*), 7.70 (d, *J* = 8.6 Hz, 2H, Ar*H*), 7.83 (t, *J* = 7.3 Hz, 1H, NTQ*H*), 7.88 (t, *J* = 7.3 Hz, 1H, NTQ*H*), 8.05 (d, *J* = 7.3 Hz, 2H, NTQ*H*), 9.59 (s, 1H, N*H*). ^{13}C NMR (75 MHz, DMSO-d_6): δ 27.8, 44.2, 47.5, 55.9 (2), 110.2, 112.2, 119.6, 122.7 (2), 123.7, 125.2, 126.7, 127.1, 128.1 (2), 130.1, 131.0, 132.2, 134.0, 135.2, 143.1, 144.1, 147.8, 148.0, 177.5, 180.3. HRMS-TOF: m/z $[M+Na]^+$ 561.0859 (Calcd for $C_{27}H_{23}ClN_2NaO_6S$: 561.0863).

*4.6.7 3-((3-chloro-1,4-dioxo-1,4-dihydronaphthalen-2-yl)amino)-N-(2-(pyridin-2-yl)ethyl)benzenesulfonamide (**39**)*

From 3-amino-*N*-(2-(pyridin-2-yl)ethyl)benzenesulfonamide (**22**). Red solid. Yield: 22%. mp 172-173 ^{o}C. R_f 0.21 (30% acetone:hexane). IR (KBr) cm^{-1}: 3291, 1668, 1588. ^{1}H NMR (300 MHz, DMSO-d_6) δ 2.85 (t, *J* = 7.4 Hz, 2H, PyCH_2), 2.96 (q, *J* = 6.9 Hz, 2H, CH_2NH), 7.18-7.24 (m, 2H, Py*H*), 7.34-7.40 (m, 1H, Ar*H*), 7.47-7.55 (m, 3H, Ar*H*), 7.68 (dt, *J* = 7.7, 1.7 Hz, 1H, Py*H*), 7.75 (t, *J* = 5.7 Hz, 1H, N*H*SO_2), 7.81 (dt, *J* = 7.4, 1.1 Hz, 1H, NTQ*H*), 7.88 (dt, *J* = 7.4, 1.1 Hz, 1H, NTQ*H*), 8.02 (dd, *J* = 7.4, 1.1 Hz, 1H, NTQ*H*), 8.05 (dd, *J* = 7.4, 1.1 Hz, 1H, NTQ*H*), 8.45 (d, *J* = 4.5 Hz, 1H, Py*H*), 9.52 (s, 1H, N*H*), ^{13}C NMR (75 MHz, DMSO-d_6): δ 37.8, 42.8, 116.8, 121.6, 122.1, 122.2, 123.7, 126.6, 127.0, 127.3, 129.3, 130.9, 132.3, 133.8, 135.2, 136.9, 140.3, 140.7, 143.5, 149.5, 158.7, 177.3, 180.3. HRMS-TOF: m/z $[M+H]^+$ 468.0768 (Calcd for $C_{23}H_{19}ClN_3O_4S$: 468.0779).

*4.6.8 3-((3-chloro-1,4-dioxo-1,4-dihydronaphthalen-2-yl)amino)-N-phenethylbenzenesulfonamide (**40**)*

From 3-amino-*N*-phenethylbenzenesulfonamide (**26**). Red solid. Yield: 41%. mp 161-462 ^{o}C. R_f 0.36 (30% acetone:hexane). IR (UATR) cm^{-1}: 3289, 1673, 1592. ^{1}H NMR (300 MHz, DMSO-d_6) δ 2.66 (t, *J* = 7.8 Hz, 2H, ArCH_2), 2.96 (q, *J* = 6.3 Hz, 2H, CH_2NH), 7.13-7.31 (m, 5H, Ar*H*), 7.34-7.39 (m, 1H, Ar*H*), 7.48-7.55 (m, 3H, Ar*H*), 7.75 (t, *J* = 5.7 Hz, 1H, N*H*SO_2), 7.81 (t, *J* = 7.5 Hz, 1H, NTQ*H*), 7.88 (t, *J* = 7.5 Hz, 1H, NTQ*H*), 8.01 (d, *J* = 7.5 Hz, 1H, NTQ*H*), 8.05 (d, *J* = 7.5 Hz, 1H, NTQ*H*), 9.52 (s, 1H, N*H*). ^{13}C NMR (75 MHz, DMSO-d_6): δ 35.7, 44.5, 116.8, 121.6, 122.2, 126.6, 126.7, 127.0, 127.3, 128.8 (2), 129.1 (2), 129.4, 130.9, 132.3, 133.9, 135.2, 139.1, 140.3, 140.7, 143.5, 177.3, 180.3. HRMS-TOF: m/z $[M+Na]^+$ 489.0652 (Calcd for $C_{24}H_{19}ClN_2NaO_4S$: 489.0646).

*4.6.9 3-((3-chloro-1,4-dioxo-1,4-dihydronaphthalen-2-yl)amino)-N-(3,4-dimethoxyphenethyl)benzenesulfonamide (**41**)*

From 3-amino-*N*-(3,4-dimethoxyphenethyl)benzenesulfonamide (**27**). Red solid. Yield: 49%. mp 163-164 ^{o}C. R_f 0.33 (30% acetone:hexane). IR (UATR) cm^{-1}: 3291, 1674, 1592. ^{1}H NMR (300 MHz, DMSO-d$_6$) δ 2.60 (t, J = 5.7 Hz, 2H, ArCH_2), 2.95 (q, J = 5.7 Hz, 2H, CH_2NH), 3.69, 3.70 (2s, 6H, 2 × OCH$_3$), 6.64 (dd, J = 8.2, 1.8 Hz, 1H, Ar*H*), 6.74 (d, J = 1.8 Hz, 1H, Ar*H*), 6.82 (d, J = 8.2 Hz, 1H, Ar*H*), 7.33-7.38 (m, 1H, Ar*H*), 7.46-7.55 (m, 3H, Ar*H*), 7.69 (t, J = 5.7 Hz, 1H, N*H*SO$_2$), 7.79 (t, J = 7.6 Hz, 1H, NTQ*H*), 7.87 (t, J = 7.6 Hz, 1H, NTQ*H*), 7.99 (d, J = 7.6 Hz, 1H, NTQ*H*), 8.04 (d, J = 7.6 Hz, 1H, NTQ*H*), 9.49 (s, 1H, N*H*). ^{13}C NMR (75 MHz, DMSO-d$_6$): δ 35.4, 44.7, 55.9, 56.0, 112.4, 113.1, 121.0 (2), 121.6, 122.2, 126.6, 127.0, 127.3, 129.3, 130.9, 131.6, 132.3, 133.8, 135.2, 140.4, 140.8, 143.6, 147.8, 149.1, 177.3, 180.3. HRMS-TOF: m/z [M+H]$^+$ 527.1053 (Calcd for $C_{26}H_{24}ClN_2O_6S$: 527.1038).

*4.6.10 3-((3-chloro-1,4-dioxo-1,4-dihydronaphthalen-2-yl)amino)-N-(pyridin-2-ylmethyl)benzenesulfonamide (**42**)*

From 3-amino-*N*-(pyridin-2-ylmethyl)benzenesulfonamide (**23**). Red-brown solid. Yield: 28%. mp 180-181 ^{o}C. R_f 0.30 (30% acetone:hexane). IR (UATR) cm^{-1}: 3209, 1680, 1593. ^{1}H NMR (300 MHz, DMSO-d$_6$) δ 4.11 (d, J = 7.4 Hz, 2H, PyCH_2), 7.21-7.28 (m, 1H, Py*H*), 7.31-7.40 (m, 2H, Ar*H* and Py*H*), 7.45-7.58 (m, 3H, Ar*H*), 7.74 (t, J = 7.7 Hz, 1H, Py*H*), 7.82 (t, J = 7.3 Hz, 1H, NTQ*H*), 7.88 (t, J = 7.3 Hz, 1H, NTQ*H*), 8.05 (d, J = 7.3 Hz, 2H, NTQ*H*), 8.29 (t, J = 6.3 Hz, 1H, N*H*SO$_2$), 8.44 (d, J = 4.7 Hz, 1H, Py*H*), 9.50 (s, 1H, N*H*). ^{13}C NMR (75 MHz, DMSO-d$_6$): δ 48.4, 116.8, 121.6, 122.0, 122.1, 122.9, 126.6, 127.1, 127.3, 129.3, 130.9, 132.3, 133.9, 135.2, 137.2, 140.2, 140.8, 143.5, 149.2, 157.7, 177.3, 180.4. HRMS-TOF: m/z [M+Na]$^+$ 476.0443 (Calcd for $C_{22}H_{16}ClN_3NaO_4S$: 476.0442).

*4.6.11 2-chloro-3-((3-((3,4-dihydroisoquinolin-2(1H)-yl)sulfonyl)phenyl)amino)naphthalene-1,4-dione (**43**)*

From 3-((3,4-dihydroisoquinolin-2(1*H*)-yl)sulfonyl)aniline (**30**). Red solid. Yield: 32%. mp 224-225 ^{o}C. R_f 0.51 (30% acetone:hexane). IR (KBr) cm^{-1}: 3286, 1671, 1591. ^{1}H NMR (300 MHz, DMSO-d$_6$) δ 2.87 (t, J = 7.8 Hz, 2H, C4-IQ*H*), 3.29 (t, J = 6.3 Hz, 2H, C3-Iq*H*), 4.22 (s, 2H, C1-IQ*H*), 7.15-7.29 (m, 4H, IQ*H*), 7.39-7.44 (m, 1H, Ar*H*), 7.51-7.60 (m, 3H, Ar*H*), 7.82 (dt, J = 7.3, 1.3 Hz, 1H, NTQ*H*), 7.88 (dt, J = 7.3, 1.3 Hz, 1H, NTQ*H*), 8.02 (dd, J = 7.3, 1.3 Hz, 1H, NTQ*H*), 8.06 (dd, J = 7.3, 1.3 Hz, 1H, NTQ*H*), 9.52 (s, 1H, N*H*). ^{13}C NMR (75 MHz, DMSO-d$_6$): δ 28.5, 44.1, 47.7, 117.0, 122.3, 123.0, 126.6, 126.8, 127.0, 127.2,

127.5, 128.1, 129.2, 129.5, 131.0, 132.0, 132.3, 133.5, 133.9, 135.2, 136.3, 140.7, 143.6, 177.4, 180.3. HRMS-TOF: m/z $[M+H]^+$ 479.0842 (Calcd for $C_{25}H_{20}ClN_2O_4S$: 479.0827).

*4.6.12 2-chloro-3-((3-((6,7-dimethoxy-3,4-dihydroisoquinolin-2(1H)-yl)sulfonyl)phenyl)amino)naphthalene-1,4-dione (**44**)*

From 3-((6,7-dimethoxy-3,4-dihydroisoquinolin-2(1H)-yl)sulfonyl)aniline (**31**). Red solid. Yield: 39%. mp 199-200 ^oC. R_f 0.38 (30% acetone:hexane). IR (UATR) cm^{-1}: 3297, 1672, 1592. ^1H NMR (300 MHz, DMSO-d_6) δ 2.77 (t, J = 7.8 Hz, 2H, C4-IQ*H*), 3.26 (t, J = 6.3 Hz, 2H, C3-Iq*H*), 3.69 (s, 6H, 2 × OCH_3), 4.12 (s, 2H, C1-IQ*H*), 6.69, 6.72 (2s, 2H, C5-IQ*H* and C8-IQ*H*), 7.38-7.44 (m, 1H, Ar*H*), 7.48-7.60 (m, 3H, Ar*H*), 7.82 (dt, J = 7.4, 1.4 Hz, 1H, NTQ*H*), 7.88 (dt, J = 7.4, 1.4 Hz, 1H, NTQ*H*), 8.02 (dd, J = 7.4, 1.4 Hz, 1H, NTQ*H*), 8.05 (dd, J = 7.4, 1.4 Hz, 1H, NTQ*H*), 9.52 (s, 1H, N*H*). ^{13}C NMR (75 MHz, DMSO-d_6): δ 28.1, 44.2, 47.4, 55.9 (2), 110.2, 112.3, 116.9, 122.3, 123.1, 123.6, 125.2, 126.6, 127.0, 128.2, 129.5, 130.9, 132.3, 133.9, 135.2, 136.2, 140.6, 143.6, 147.8, 148.0, 177.4, 180.3. HRMS-TOF: m/z $[M+Na]^+$ 561.0862 (Calcd for $C_{27}H_{23}ClN_2NaO_6S$: 561.0858).

4.7 Cytotoxic assay: cancer cell lines

The cells suspended in the corresponding culture medium were inoculated in 96-well microtiter plates (Corning Inc., NY, USA) at a density of 10,000-20,000 cells per well, and incubated for 24 h at 37 ^oC in a humidified atmosphere with 95% air and 5% CO_2. An equal volume of additional medium containing either the serial dilutions of the test compounds, positive control (etoposide and/or doxorubicin), or negative control (DMSO) was added to the desired final concentrations, and the microtiter plates were further incubated for an additional 48 h. The number of surviving cells in each well was determined using MTT assay [46,47] (for adherent cells: HuCCA-1, HepG2, and A549 cells) and XTT assay [48] (for suspended cells: MOLT-3 cells). The IC_{50} value is defined as the drug (or compound) concentration that inhibits cell growth by 50% (relative to negative control).

4.8 Antimalarial assay: Radioisotope techniques

P.falciparum (K1, multidrug resistant strain) was cultivated *in vitro* conditions, according to Trager & Jensen (1976) [49], in RPMI 1640 medium containing 20 mM HEPES (*N*-2-hydroxyethylpiperazine-*N*'-2-ethanesulfonic acid), 32 mM $NaHCO_3$ and 10% heat activated human serum with 3% erythrocytes, in humidified 37^oC incubator with 3% CO_2.

The culture was passaged with fresh mixture of erythrocytes and medium every day to maintain cell growth. Quantitative assessment of antimalarial activity in vitro was determined by microculture radioisotope techniques based upon the methods described by Desjardins et al. (1979) [50]. Briefly, a mixture of 200 μL of 1.5% erythrocytes with 1% parasitemia at the early ring stage was pre-exposed to 25 μL of the medium containing a test sample dissolved in 1% DMSO (0.1% final concentration) for 24 h. Subsequently, 25 μL of [^{3}H] hypoxanthine (Amersham, USA) in culture medium (0.5 μCi) was added to each well and the plates were incubated for an additional 24 h. Levels of incorporated radioactive labeled hypoxanthine, indicating parasite growth, were determined using the Top Count microplate scintillation counter (Packard, USA). The percentage of parasite growth was calculated using the signal count per minute of treated (CPMT) and untreated conditions (CPMU) as shown by the following equation;

$$\% \text{ parasite growth} = \text{CPMT/CPMU} \times 100 \qquad \textit{Eq. 6}$$

4.9 Cytotoxicity assay: primate cell line (Vero)

The cytotoxicity assay was performed using the Green Fluorescent Protein (GFP) detection method [51]. The GFP-expressing Vero cell line was generated in-house by stably transfecting the African green monkey kidney cell line (Vero, ATCC CCL-81), with pEGFP-N1 plasmid (Clontech). The cell line was maintained in a minimal essential medium supplemented with 10% heat-inactivated fetal bovine serum, 2 mM L-glutamine, 1 mM sodium pyruvate, 1.5 g/L sodium bicarbonate and 0.8 mg/mL geneticin, at 37 °C in a humidified incubator with 5% CO_2. The assay was carried out by adding 45 μL of cell suspension at 3.3×10^4 cells/mL to each well of 384-well plates containing 5 μL of test compounds previously diluted in 0.5% DMSO, and then incubated for 4 days at 37 ^{o}C incubator with 5% CO_2. Fluorescence signals were measured using SpectraMax M5 microplate reader (Molecular Devices, USA) in the bottom reading mode with excitation and emission wavelengths of 485 and 535 nm, respectively. Fluorescence signal at day 4 was subtracted from background fluorescence at day 0. IC_{50} values were derived from dose-response curves, using 6 concentrations of 3-fold serially diluted samples, by the SOFTMax Pro software (Molecular device). Ellipticine and 0.5% DMSO were used as a positive and a negative controls, respectively.

4.10 QSAR analysis

Conceptually, the chemical structures of the tested compounds (**33-44**, Fig. 3) together with their experimental activities (IC_{50} values) were used as data sets for construction of five QSAR models. The additional set of 30 structurally modified compounds (**34a-34d**, **36a-36k**, **40a-40d**, and **42a-42k**, Figs. 4-6) was virtually constructed, and their activities were predicted using the constructed QSAR models.

4.10.1 Data set

Chemical structures of the tested compounds (**33-44)** along with their IC_{50} values were used as data sets for QSAR analysis. Regarding anticancer activity against 4 cancer cell lines and antimalarial activity of the investigated compounds, data sets were arranged as 5 data sets in which QSAR models were separately developed. To obtain distribution of data points, IC_{50} values of the tested compounds **33-44** were converted to pIC_{50} values by taking the negative logarithm to the base of 10 (-log IC_{50}). Experimentally inactive compounds were excluded from the data set.

4.10.2 Molecular structure optimization and descriptor calculation

Chemical structures of 12 tested (**33-44**, Fig. 3) and 30 structurally modified (**34a-34d**, **36a-36k**, **40a-40d**, and **42a-42k**, Figs. 4-6) compounds were drawn using the GaussView software [52] and were subjected to geometrical optimization to obtain the low-energy conformers. Initially, all structures were geometrically optimized using Gaussian 09 [24] at the semi-empirical Austin Model 1 (AM1) level. Subsequently, density functional theory (DFT) calculation was performed using the Becke's three-parameter hybrid method with the Lee-Yang-Parr correlation functional (B3LYP) together with the LANL2DZ ECP basis set. The optimized structures were consequently used as an input for extracting descriptor values. A set of 13 quantum chemical descriptors i.e., mean absolute atomic charge (Q_m), total energy (E_{total}), total dipole moment (μ), highest occupied molecular orbital energy (E_{HOMO}), lowest unoccupied molecular orbital energy (E_{LUMO}), energy difference of HOMO and LUMO ($HOMO\text{-}LUMO_{Gap}$), electron affinity (EA), ionization potential (IP), Mulliken electronegativity (χ), hardness (η), softness (S), electrophilic index (ω_i) and electrophilicity (ω) were extracted using an in-house developed script. The optimized structures were further used for calculation of an additional set of 3,224 molecular descriptors using Dragon software (version 5.5) [25]. Dragon descriptors comprised of 22 classes including Constitutional

descriptors, Topological descriptors, Walk and path counts, Connectivity indices, Information indices, 2D autocorrelation, Edge adjacency indices, Burden eigenvalues, Topological charge indices, Eigenvalue-based indices, Randic molecular profiles, Geometrical descriptors, RDF descriptors, 3D-MoRSE descriptors, WHIM descriptors, GETAWAY descriptors, Functional group counts, Atom-centred fragments, Charge descriptors, Molecular properties, 2D binary fingerprints and 2D frequency fingerprints.

4.10.3 Descriptor selection

Feature selection was performed to select a set of informative descriptors from the whole set of descriptors obtained from the calculation. Correlation-based feature selection was employed for initial selection. The pair-correlation of each descriptor value and bioactivity (pIC_5) was calculated and the Pearson's correlation coefficient (r) value of 0.5 were used as the cut-off value in which descriptors with $|r| < 0.5$ were considered as low correlated descriptors and were excluded while descriptors with $|r| \geq 0.5$ were used for further selection using stepwise multiple linear regression (MLR) as implemented in the SPSS statistics 18.0 software or subjected to the attribute evaluator CfsSubsetEval using the BestFirst search method as implemented in Waikato Environment for Knowledge Analysis (WEKA) version 3.4.5 [26]. Finally, a set of important descriptors were obtained for multivariate analysis.

4.10.4 Multivariate analysis

Multivariate analysis was performed by Waikato Environment for Knowledge Analysis (WEKA) version 3.4.5 [26] using multiple linear regression (MLR) algorithm where the selected descriptors and pIC_{50} values were assigned as independent variables (X) and dependent variable (Y), respectively. The MLR models were constructed according to the following equation.

$$Y = B_0 + \sum B_n X_n \qquad \textit{Eq. 7}$$

where Y is the pIC_{50} values of compounds, B_0 is the intercept and B_n are the regression coefficient of descriptors X_n.

4.10.5 Data sampling

Leave-one-out cross validation (LOO-CV) was used for splitting the data set into a training set and a testing set. Principally, one sample was left out as the testing set while the

remaining *N*-1 samples were used as the training set. This procedure was continued until every sample in the data set was used as the testing set to predict *Y* variable (activity).

4.10.6 Evaluating the performance of QSAR models

The performance of constructed QSAR models was evaluated using two statistical parameters. The correlation coefficient (*R*) indicated the predictive performance, and the root mean square error (RMSE) represented predictive error of the models.

4.10.7 Prediction of structurally modified compounds using the constructed QSAR models

The important descriptor values of the structurally modified compounds (**34a**-**34d**, **36a-36k**, **40a-40d**, and **42a-42k**, Figs. 4-6) were obtained from the calculation as described previously. The QSAR equations were used to predict activities of these modified compounds in which important descriptor values of each modified compound were assigned in the equation for computing its predicted activity (predicted pIC_{50} value).

Acknowledgments

This project was financially supported from Srinakharinwirot University under the Government Budget. R.P. is grateful for the Thailand Research Fund (MRG5680001). Great supports from the Office of Higher Education Commission and Mahidol University under the National Research Universities Initiative are appreciated. We are also indebted to Chulabhorn Research Institute for recording mass spectra and bioactivity testing.

References

[1] N. El-Najjar, H. Gali-Muhtasib, R.A. Ketola, P. Vuorela, A. Urtti, H. Vuorela, The chemical and biological activities of quinones: overview and implications in analytical detection, Phytochem. Rev. 10 (2011) 353-370.

[2] S.N. Sunassee, M.T. Davies-Coleman, Cytotoxic and antioxidant marine prenylated quinones and hydroquinones, Nat. Prod. Rep. 29 (2012) 513-535.

[3] E.J.S. Salustiano, C.D. Netto, R.F. Fernandes, A.J.M. da Silva, T.S. Bacelar, C.P. Castro, C.D. Buarque, R.C. Maia, V.M. Rumjanek, P.R.R. Costa, Comparison of the cytotoxic effect of lapachol, *α*-lapachone and pentacyclic 1,4-naphthoquinones on human leukemic cells, Invest. New Drug 28 (2010) 139-144.

[4] K.V. Wellington, Understanding cancer and the anticancer activities of naphthoquinones-a review, RSC Adv. 5 (2015) 20309-20338.

[5] V.K. Tandon, S. Kumar, Recent development on naphthoquinone derivatives and their therapeutic applications as anticancer agents. Expert Opin. Ther. Patents 23 (2013) 1087-1108.

[6] G.L. Nixon, D.M. Moss, A.E. Shone, D.G. Lalloo, N. Fisher, P.M. O'Neill, S.A. Ward, G.A. Biagini, Antimalarial pharmacology and therapeutics of atovaquone, J. Antimicrob. Chemother. 68 (2013) 977-985.

[7] R.W. Rickards, J.M. Rothschild, A.C. Willis, N.M. De Chazal, J. Kirk, K. Kirk, K.J. Saliba, G.D. Smith, Calothrixins A and B, novel pentacyclic metabolites from *Calothrix* cyanobacteria with potent activity against malaria parasites and human cancer cells, Tetrahedron 55 (1999) 13513-13520.

[8] P.J. O'Brien, Molecular mechanisms of quinone cytotoxicity, Chem. Biol. Interact. 80 (1991) 1-41.

[9] J.L. Bolton, M.A. Trush, T.M. Penning, G. Dryhurst, T.J. Monks, Role of quinines in toxicology, Chem. Res. Toxicol. 13 (2000) 135-160.

[10] S.L. de Castro, F.S. Emery, E.N. da Silva Júnior, Synthesis of quinoidal molecules: Strategies towards bioactive compounds with an emphasis on lapachones, Eur. J. Med. Chem. 69 (2013) 678-700.

[11] D.A. Boothman, D.K. Trask, A.B. Pardee, Inhibition of potentially lethal DNA damage repair in human tumor cells by β-lapachone, an activator of topoisomerase I, Cancer Res. 49 (1989) 605-612.

[12] N. Fujii, Y. Yamashita, Y. Arima, M. Nagashima, H. Nakano, Induction of topoisomerase II-mediated DNA cleavage by the plant naphthoquinones plumbagin and shikonin. Antimicrob. Agents Chemother. 36 (1992) 2589-2594.

[13] T. Müller, L. Johann, B. Jannack, M. Brückner, D.A. Lanfranchi, H. Bauer, C. Sanchez, V. Yardley, C. Deregnaucourt, J. Schrével, M. Lanzer, R.H. Schirmer, E. Davioud-Charvet, Glutathione reductase-catalyzed cascade of redox reactions to bioactivate potent antimalarial 1,4-naphthoquinones - A new strategy to combat malarial parasites J. Am. Chem. Soc. 133 (2011) 11557-11571.

[14] D.A. Lanfranchi, E. Cesar-Rodo, B. Bertrand, H.-H. Huang, L. Day, L. Johann, M. Elhabiri, K. Becker, D.L. Williams, E. Davioud-Charvet, Synthesis and biological evaluation of 1,4-naphthoquinones and quinoline-5,8-diones as antimalarial and schistosomicidal agents, Org. Biomol. Chem. 10 (2012) 6375-6387.

[15] N. Soonthornchareonnon, K. Suwanborirux, R. Bavovada, C. Patarapanich, J.M. Cassady, New cytotoxic 1-azaanthraquinones and 3-aminonaphthoquinone from the stem bark of *Goniothalamus marcanii*, J. Nat. Prod. 62 (1999) 1390-1394.

[16] G.J. Kapadia, M.A. Azuine, V. Balasubramanian, R. Sridhar, Aminonaphthoquinones - A novel class of compounds with potent antimalarial activity against *Plasmodium falciparum*, Pharmacol. Res. 43 (2001) 363-367.

[17] V. Prachayasittikul, R. Pingaew, A. Worachartcheewan, C. Nantasenamat, S. Prachayasittikul, S. Ruchirawat, V. Prachayasittikul, Synthesis, anticancer activity and QSAR study of 1,4-naphthoquinone derivatives, Eur. J. Med. Chem. 84 (2014) 247-263.

[18] J. Benites, J.A. Valderrama, K. Bettega, R.C. Pedrosa, P.B. Calderon, J. Verrax, Biological evaluation of donor-acceptor aminonaphthoquinones as antitumor agents, Eur. J. Med. Chem. 45 (2010) 6052-6057.

[19] I. Sieveking, P. Thomas, J.C. Estévez, N. Quiñones, M.A. Cuéllar, J. Villena, C. Espinosa-Bustos, A. Fierro, R.A. Tapia, J.D. Maya, R. López-Muñoz, B.K. Cassels, R.J. Estévez, C.O. Salas, 2-Phenylaminonaphthoquinones and related compounds: Synthesis, trypanocidal and cytotoxic activities. Bioorg. Med. Chem. 22 (2014) 4609-4620.

[20] V.K. Tandon, H.K. Maurya, N.N. Mishra, P.K. Shukla, Design, synthesis and biological evaluation of novel nitrogen and sulfur containing hetero-1,4-naphthoquinones as potent antifungal and antibacterial agents, Eur. J. Med. Chem. 44 (2009) 3130-3137.

[21] D. Bhasin, S.N. Chettiar, J.P. Etter, M. Mok, P.K. Li, Anticancer activity and SAR studies of substituted 1,4-naphthoquinones, Bioorg. Med. Chem. 21 (2013) 4662-4669.

[22] A. Kazi, H. Lawrence, W.C. Guida, M.L. McLaughlin, G.M. Springett, N. Berndt, R.M.L.Yip, S.M. Sebti, Discovery of a novel proteasome inhibitor selective for cancer cells over non-transformed cells, Cell Cycle 8 (2009) 1940-1951.

[23] V.K. Tandon, H.K. Maurya, S. Kumar, A. Rashid, D. Panda, Synthesis and evaluation of 2-heteroaryl and 2,3-diheteroaryl-1,4-naphthoquinones that potently induce apoptosis in cancer cells, RSC Adv. 4 (2014) 12441-12447.

[24] M.J. Frisch, G.W. Trucks, H.B. Schlegel, G.E. Scuseria, M.A. Robb, J.R. Cheeseman, G. Scalmani, V. Barone, B. Mennucci, G.A. Petersson, H. Nakatsuji, M. Caricato, X. Li, H.P. Hratchian, A.F. Izmaylov, J. Bloino, G. Zheng, J.L. Sonnenberg, M. Hada, M. Ehara, K. Toyota, R. Fukuda, J. Hasegawa, M. Ishida, T. Nakajima, Y. Honda, O. Kitao, H. Nakai, T. Vreven, J.A.M. Jr., J.E. Peralta, F. Ogliaro, M. Bearpark, J.J. Heyd, E.

Brothers, K.N. Kudin, V.N. Staroverov, R. Kobayashi, J. Normand, K. Raghavachari, A. Rendell, J.C. Burant, S.S. Iyengar, J. Tomasi, M. Cossi, N. Rega, J.M. Millam, M. Klene, J.E. Knox, J.B. Cross, V. Bakken, C. Adamo, J. Jaramillo, R. Gomperts, R.E. Stratmann, O. Yazyev, A.J. Austin, R. Cammi, C. Pomelli, J.W. Ochterski, R.L. Martin, K. Morokuma, V.G. Zakrzewski, G.A. Voth, P. Salvador, J.J. Dannenberg, S. Dapprich, A.D. Daniels, Ö. Farkas, J.B. Foresman, J.V. Ortiz, J. Cioslowski, D.J. Fox, Gaussian Inc., Wallingford CT, 2009.

[25] Talete, Dragon for Windows (Software for Molecular Descriptor Calculations), Version 5.5, Milan, Italy, 2007.

[26] I.H. Witten, E. Frank, M.A. Hall, Data mining: practical machine learning tools and techniques, second ed., Morgan Kaufmann, San Francisco, 2011.

[27] E. Estrada, Physicochemical interpretation of molecular connectivity indices, J. Phys. Chem. A. 106 (2002) 9085-9091.

[28] J.P. Hughes, S. Rees, S.B. Kalindjian, K.L. Philpott, Principles of early drug discovery, Br. J. Pharmacol. 162 (2011) 1239-1249.

[29] J.E.S. Wikberg, M. Eklund, E.L. Willighagen, O. Spijuth, M. Lapins, O. Engkvist, J. Alvarsson, Drug discovery and development, in: J.E.S. Wikberg (Eds.), Introduction of Pharmaceutical Bioinformatics, Oakleaf Academic Publishing House, Stockholm, 2011, pp. 27-39.

[30] S. Singh, Computational design and chemometric QSAR modeling of Plasmodium falciparum carbonic anhydrase inhibitors, Bioorg. Med. Chem. Lett. 25 (2015) 133-141.

[31] A. Worachartcheewan, C. Nantasenamat, W. Owasirikul, T. Monnor, O. Naruepantawart, S. Janyapaisarn, S. Prachayasittikul, V. Prachayasittikul, Insights into antioxidant activity of 1-adamantylthiopyridine analogs using multiple linear regression, Eur. J. Med. Chem. 73 (2014) 258-264.

[32] C. Nantasenamat, T. Monnor, A. Worachartcheewan, P. Mandi, C. Isarankura-Na-Ayudhya, V. Prachayasittikul, Predictive QSAR modeling of aldose reductase inhibitors using Monte Carlo feature selection, Eur. J. Med. Chem. 76 (2014) 352-359.

[33] S. Nandi, M. Bagchi, QSAR modeling of 4-anilinofuro[2,3-*b*]quinolines: an approach to anticancer drug design, Med. Chem. Res. 23 (2014) 1672-1682.

[34] A. Worachartcheewan, C. Nantasenamat, C. Isarankura-Na-Ayudhya, V. Prachayasittikul, QSAR study of amidino bis-benzimidazole derivatives as potent anti-malarial agents against *Plasmodium falciparum*, Chem. Pap. 67 (2013) 1462-1473.

[35] S. Paula, E. Hofmann, J. Burden, D.T. Stanton, Novel phenolic inhibitors of the sarco/endoplasmic reticulum calcium ATPase: identification and characterization by quantitative structure–activity relationship modeling and virtual screening, J. Enzyme Inhib. Med. Chem. 30 (2014) 1-8.

[36] J.B. Veselinović, A.A. Toropov, A.P. Toropova, G.M. Nikolić, A.M. Veselinović, Monte Carlo Method-Based QSAR Modeling of Penicillins Binding to Human Serum Proteins, Arch. Pharm. 348 (2015) 62-67.

[37] K. Komatsu, K. Kikuchi, H. Kojima, Y. Urano, T. Nagano, Selective zinc sensor molecules with various affinities for Zn^{2+}, revealing dynamics and regional distribution of synaptically released Zn^{2+} in hippocampal slices, J. Am. Chem. Soc. 127 (2005) 10197-10204.

[38] R. Pingaew, S. Prachayasittikul, S. Ruchirawat, V. Prachayasittikul, Synthesis and cytotoxicity of novel *N*-sulfonyl-1,2,3,4-tetrahydroisoquinoline thiosemicarbazone derivatives, Med. Chem. Res. 22 (2013) 267–277.

[39] R. Pingaew, V. Prachayasittikul, P. Mandi, C. Nantasenamat, S. Prachayasittikul, S. Ruchirawat, V. Prachayasittikul, Synthesis and molecular docking of 1,2,3-triazole-based sulfonamides as aromatase inhibitors, Bioorg. Med. Chem. 23 (2015) 3472-3480.

[40] S.P. Miller, Y.-L. Zhong, Z. Liu, M. Simeone, N. Yasuda, J. Limanto, Z. Chen, J. Lynch, V. Capodanno, Practical and cost-effective manufacturing route for the synthesis of a *β*-lactamase inhibitor, Org. Lett. 16 (2014) 174-177.

[41] R. Pingaew, S. Prachayasittikul, S. Ruchirawat, V. Prachayasittikul, Tungstophosphoric acid catalyzed synthesis of *N*-sulfonyl-1,2,3,4-tetrahydroisoquinoline analogs, Chin. Chem. Lett. 24 (2013) 941–944.

[42] S.M.F. Jamieson, D.G. Brooke, D. Heinrich, G.J. Atwell, S. Silva, E.J. Hamilton, A.P. Turnbull, L.J.M. Rigoreau, E. Trivier, C. Soudy, S.S. Samlal, P.J. Owen, E. Schroeder, T. Raynham, J.U. Flanagan, W.A. Denny, 3-(3,4-dihydroisoquinolin-2(1H)-ylsulfonyl)benzoic acids: Highly potent and selective inhibitors of the type 5 17-β-hydroxysteroid dehydrogenase AKR1C3, J. Med. Chem. 55 (2012) 7746-7758.

[43] R. Pingaew, S. Prachayasittikul, S. Ruchirawat, V. Prachayasittikul, Synthesis and cytotoxicity of novel 4-(4-(substituted)-1H-1,2,3-triazol-1- yl)-N-phenethylbenzenesulfonamides, Med. Chem. Res. 23 (2014) 1768-1780.

[44] M. Schlitzer, M. Böhm, I. Sattler, H.M. Dahse, Design, synthesis and early structure-activity relationship of farnesyltransferase inhibitors which mimic both the peptidic and the prenylic substrate, Bioorg. Med. Chem. 8 (2000) 1991-2006.

[45] R. Pingaew, P. Mandi, C. Nantasenamat, S. Prachayasittikul, S. Ruchirawat, V. Prachayasittikul, Design, synthesis and molecular docking studies of novel N-benzenesulfonyl-1,2,3,4-tetrahydroisoquinoline-based triazoles with potential anticancer activity, Eur. J. Med. Chem. 81 (2014) 192-203.

[46] J. Carmichael, W.G. DeGraff, A.F. Gazdar, J.D. Minna, J.B. Mitchell, Evaluation of a tetrazolium-based semiautomated colorimetrie assay: assessment of radiosensitivity, Cancer Res. 47 (1987) 943–946.

[47] T. Mosmann, Rapid colorimetric assay for cellular growth and survival: application to proliferation and cytotoxicity assays, J. Immunol. Methods 65 (1983) 55–63.

[48] A. Doyle, J.B. Griffiths, Mammalian cell culture: essential techniques, John Wiley & Sons, Chichester, UK, 1997.

[49] W. Trager, J.B. Jensen, Human malaria parasites in continuous culture. Science 193 (1976) 673-675.

[50] R.E. Desjardins, C.J. Canfield, J.D. Haynes, J.D. Chulay, Quantitative assessment of antimalarial activity *in vitro* by a semiautomated microdilution technique. Antimicrob. Agents Chemother. 16 (1979) 710-718.

[51] L. Hunt, M. Jordan, M. De Jesus, F.M. Wurm, GFP-expressing mammalian cells for fast, sensitive, noninvasive cell growth assessment in a kinetic mode. Biotechnol. Bioeng. 65 (1999) 201–205.

[52] I.I.R. Dennington, T. Keith, J. Millam, K. Eppinnett, W.L. Hovell, R. Gilliland, GaussView, Version 3.09 [Computer Software]. Semichem Shawnee Mission, KS, USA, 2003.

Figure Legends

Fig. 1. Representative structures of bioactive 1,4-naphthoquinones **1-3**

Fig. 2. Designed 1,4-naphthoquinone-based sulfonamides

Scheme 1. Synthesis of aminobenzenesulfonamides **20-31**

Scheme 2. Synthesis of 1,4-naphthoquinone-based sulfonamides **33-44** through nucleophilic displacement

Fig. 3. Chemical structures of the tested compounds **33-44**

Fig. 4. Chemical structures of structurally modified compounds series **34** and **40**

Fig. 5. Chemical structures of structurally modified compounds series **36**

Fig. 6. Chemical structures of structurally modified compounds series **42**

Fig. 7. Plots of experimental versus predicted pIC_{50} values of cytotoxic activities against four cell lines (A: HuCCA-1, B: HepG2, C: A549, D: MOLT-3) and antimalarial activity (E) generated by QSAR models (training set: compounds are represented by closed circle and regression line is shown as a solid line, leave-one-out validated testing set: compounds are represented by opened hex and regression line is shown as a dotted line)

Fig. 8. Summary of potential anticancer and antimalarial agents

Table 1

Cytotoxic and antimalarial activities (IC_{50}, μM) of compounds (**33 - 44**).

Compound	Cancer cell lines[a]				Antimalarial	Vero cell line[b]
	HuCCA-1	**HepG2**	**A549**	**MOLT-3**		
33	5.88 ± 0.09	10.32 ± 0.58	31.37 ± 0.42	1.37 ± 0.09 [d]	Inactive	99.89
34	4.93 ± 0.71	6.27 ± 0.51	11.24 ± 1.06	2.18 ± 0.31	Inactive	>107.08[c]
35	5.50 ± 0.14	6.07 ± 0.69	13.00 ± 1.63	2.05 ± 0.21	9.96	21.10
36	5.00 ± 0.21	3.30 ± 0.40 [d]	5.88 ± 0.04	1.37 ± 0.14 [d]	Inactive	10.84
37	57.77 ± 0.11	36.87 ± 2.52	48.44 ± 1.69	8.56 ± 0.71	14.74	20.27
38	5.21 ± 0.13	14.38 ± 3.18	20.24 ± 0.45	1.73 ± 0.28	2.80 [d]	0.944
39	5.77 ± 0.46	5.13 ± 0.85	3.93 ± 1.05	2.20 ± 0.03	Inactive	20.20
40	9.47 ± 0.13	12.85 ± 1.32	31.05 ± 3.54	3.30 ± 0.38	6.30	3.85
41	8.50 ± 0.52	9.49 ± 0.92	27.15 ± 2.74	4.95 ± 0.60	10.08	3.76
42	3.66 ± 0.37 [d]	4.56 ± 0.85	2.31 ± 0.07 [d]	2.38 ± 0.21	Inactive	2.82
43	6.08 ± 0.01	10.96 ± 1.06	21.92 ± 0.31	1.92 ± 0.33	7.27	4.20
44	26.42 ± 1.10	43.28 ± 7.67	63.08 ± 5.66	2.34 ± 0.21	8.79	11.21
Etoposide[e]	ND	33.98 ± 0.01	ND	0.041 ± 0.003	ND	ND
Doxorubicin[e]	0.42 ± 0.02	0.57 ± 0.05	0.37 ± 0.02	ND	ND	ND
Mefloquine[e]	ND	ND	ND	ND	0.0269	ND
Dihydroartemisinine[e]	ND	ND	ND	ND	1.42[f]	ND
Ellipticine[e]	ND	ND	ND	ND	ND	4.05

[a] Cancer cell lines comprise the following: HuCCA-1 human cholangiocarcinoma cancer cell line, HepG2 human hepatocellular carcinoma cell line, A549 human lung carcinoma cell line, MOLT-3 human lymphoblastic leukemia cell line
[b] Vero cell line was African green monkey kidney cell line
[c] IC_{50} > 107.08 μM denoted as non-cytotoxic.
[d] The compound exhibited the most potent activity.
[e] Etoposide, doxorubicin, mefloquine, dihydroartemisinine and ellipticine were used as reference drugs.
[f] IC_{50} is shown as nM.
ND = not determined

Table 2

Definition of descriptors using for development of QSAR models.

Descriptor	Type	Definition
X1A	Connectivity indices	Average connectivity index of order 1
Gm	WHIM descriptors	Total symmetry index / weighted by mass
G2u	WHIM descriptors	2nd component symmetry directional WHIM index / unweighted
RDF105m	RDF descriptors	Radial Distribution Function - 105 / weighted by mass
Mor12u	3D-MoRSE descriptors	Signal 12 / unweighted
G(N..Cl)	3D Atom Pairs	Sum of geometrical distances between N..Cl
Mor22v	3D-MoRSE descriptors	Signal 22 / weighted by van der Waals volume
B05[N-O]	2D Atom Pairs	Presence/absence of N - O at topological distance 5
Mor24u	3D-MoRSE descriptors	Signal 24 / unweighted

Table 3

Summary of QSAR equations and their predictive performances in predicting cytotoxic and antimalarial activities of 1,4-naphthoquinones derivatives (**33 - 44**).

Model	Equation	N	R_{Tr}	$RMSE_{Tr}$	R_{CV}	$RMSE_{CV}$
HuCCA-1	pIC_{50} = 34.1344(*X1A*) + 23.1368(*Gm*) + 9.4788(*G2u*) - 21.1565	12	0.8130	0.1936	0.5647	0.2825
HepG2	pIC_{50} = -0.097(*RDF105m*) - 0.2179	12	0.8730	0.1596	0.8249	0.1855
A549	pIC_{50} = -0.0949(*RDF105m*) + 0.6903(*Mor12u*) + 0.366	12	0.9506	0.1310	0.9317	0.1534
MOLT-3	pIC_{50} = 10.9192(*G2u*) + 0.0185(*G(N..Cl)*) - 2.5605	12	0.8119	0.1281	0.6277	0.1740
Antimalarial	pIC_{50} = -1.6078(*Mor22v*) + 0.1457(*B05[N-O]*) + 1.2647(*Mor24u*) - 1.4305	7	0.9650	0.0552	0.8147	0.1231

pIC_{50} is the concentration of compound required for 50% inhibition of cell growth.

N is a number of data set.

R_{Tr} is a correlation coefficient of the training set.

$RMSE_{Tr}$ is a root mean square error of the training set.

R_{CV} is a correlation coefficient of leave-one-out cross validation (LOO-CV) of the testing set.

$RMSE_{CV}$ is a root mean square error LOO-CV of the testing set.

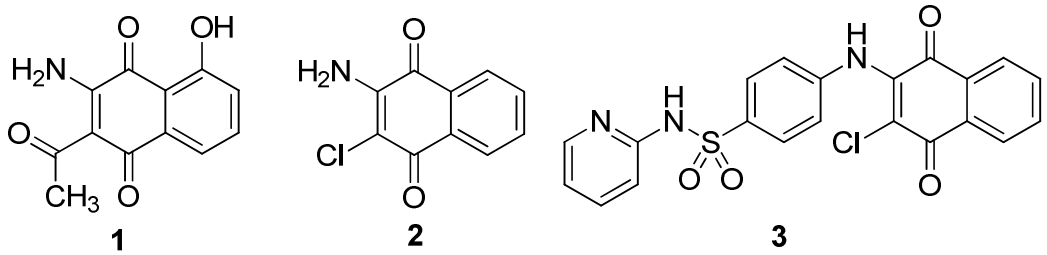

Fig. 1.

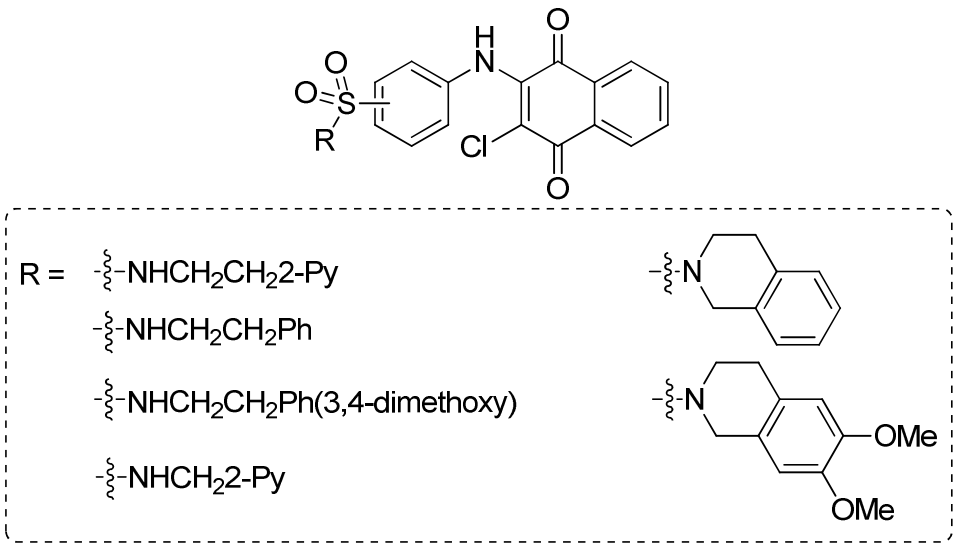
H
N
O
O
O
S
R
Cl
O
R =
NHCH2CH2 2-Py
NHCH2CH2Ph
NHCH2CH2Ph(3,4-dimethoxy)
NHCH2 2-Py
N
N
OMe
OMe

Fig. 2.

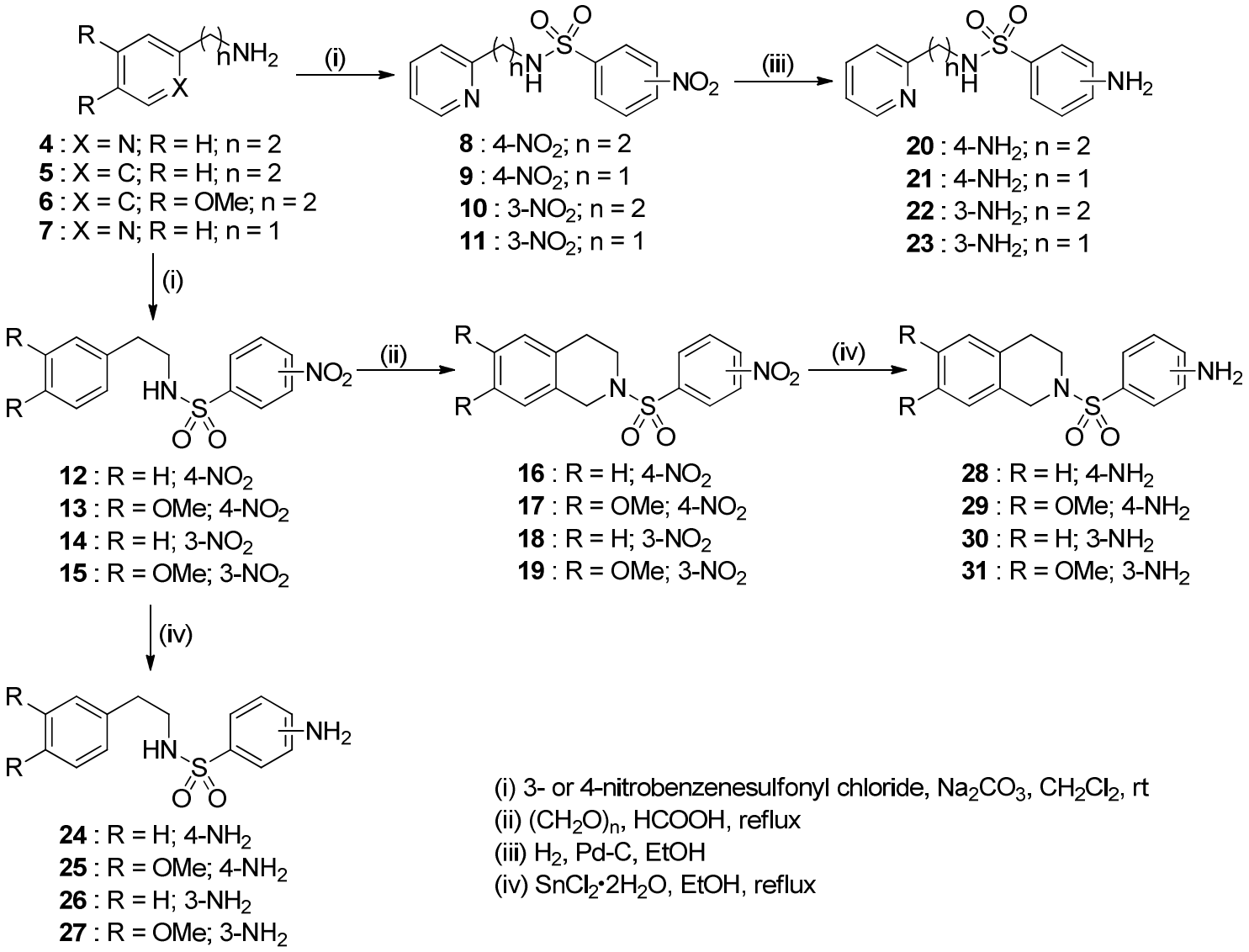

4 : X = N; R = H; n = 2
5 : X = C; R = H; n = 2
6 : X = C; R = OMe; n = 2
7 : X = N; R = H; n = 1

8 : 4-NO_2; n = 2
9 : 4-NO_2; n = 1
10 : 3-NO_2; n = 2
11 : 3-NO_2; n = 1

20 : 4-NH_2; n = 2
21 : 4-NH_2; n = 1
22 : 3-NH_2; n = 2
23 : 3-NH_2; n = 1

12 : R = H; 4-NO_2
13 : R = OMe; 4-NO_2
14 : R = H; 3-NO_2
15 : R = OMe; 3-NO_2

16 : R = H; 4-NO_2
17 : R = OMe; 4-NO_2
18 : R = H; 3-NO_2
19 : R = OMe; 3-NO_2

28 : R = H; 4-NH_2
29 : R = OMe; 4-NH_2
30 : R = H; 3-NH_2
31 : R = OMe; 3-NH_2

24 : R = H; 4-NH_2
25 : R = OMe; 4-NH_2
26 : R = H; 3-NH_2
27 : R = OMe; 3-NH_2

Scheme 1.

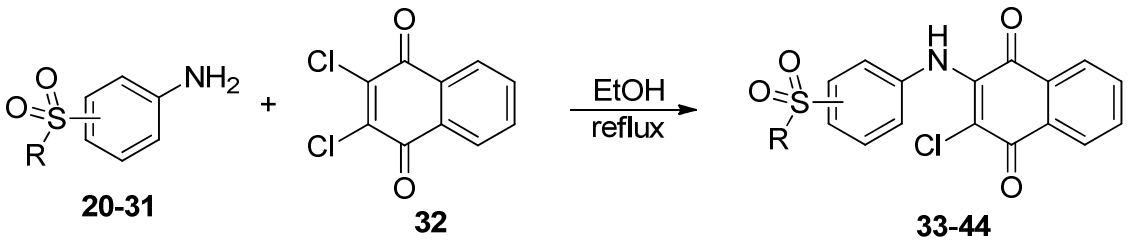

Scheme 2.

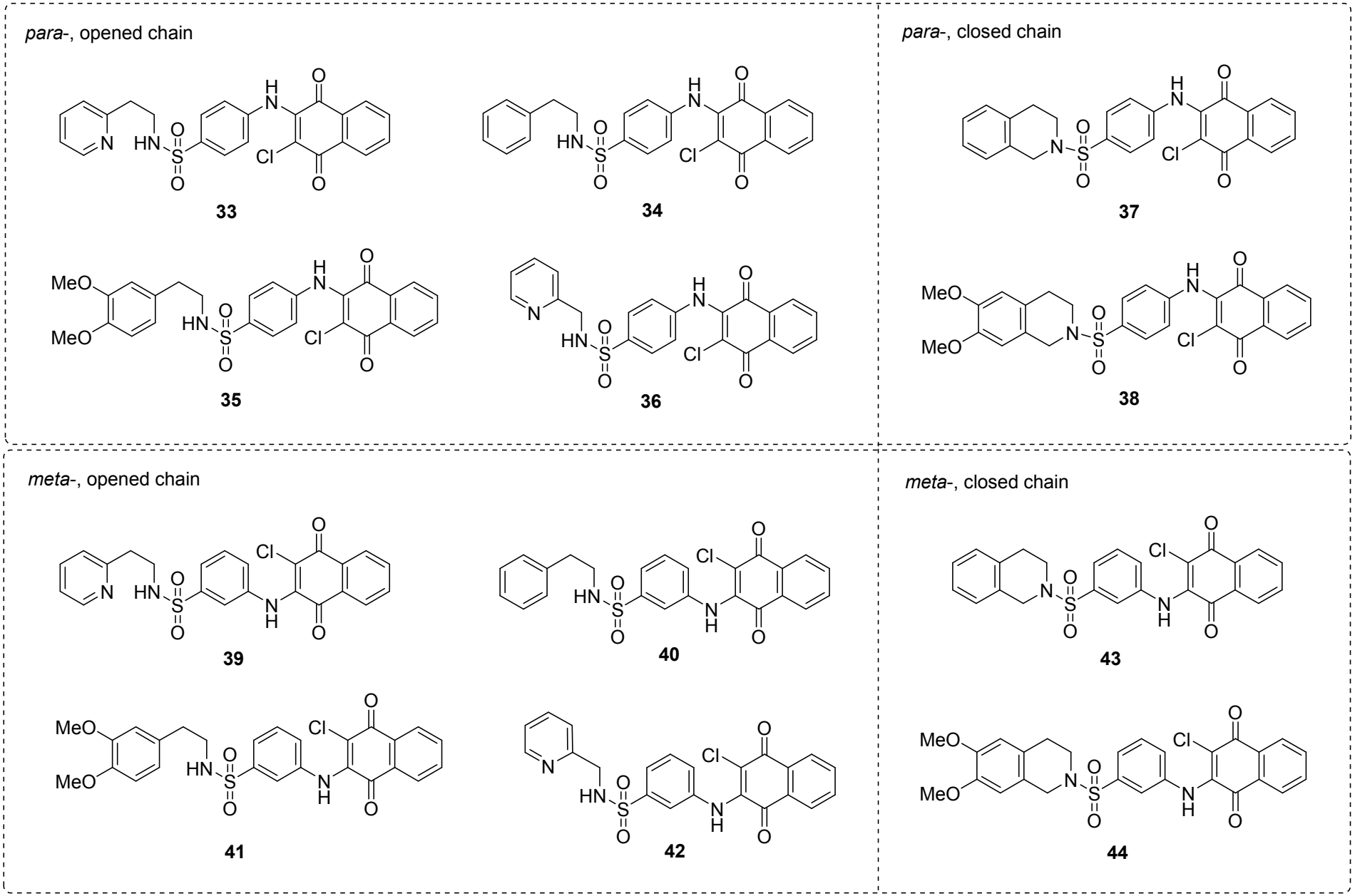
para-, opened chain
33
34
35
36
para-, closed chain
37
38
meta-, opened chain
39
40
41
42
meta-, closed chain
43
44

Fig. 3.

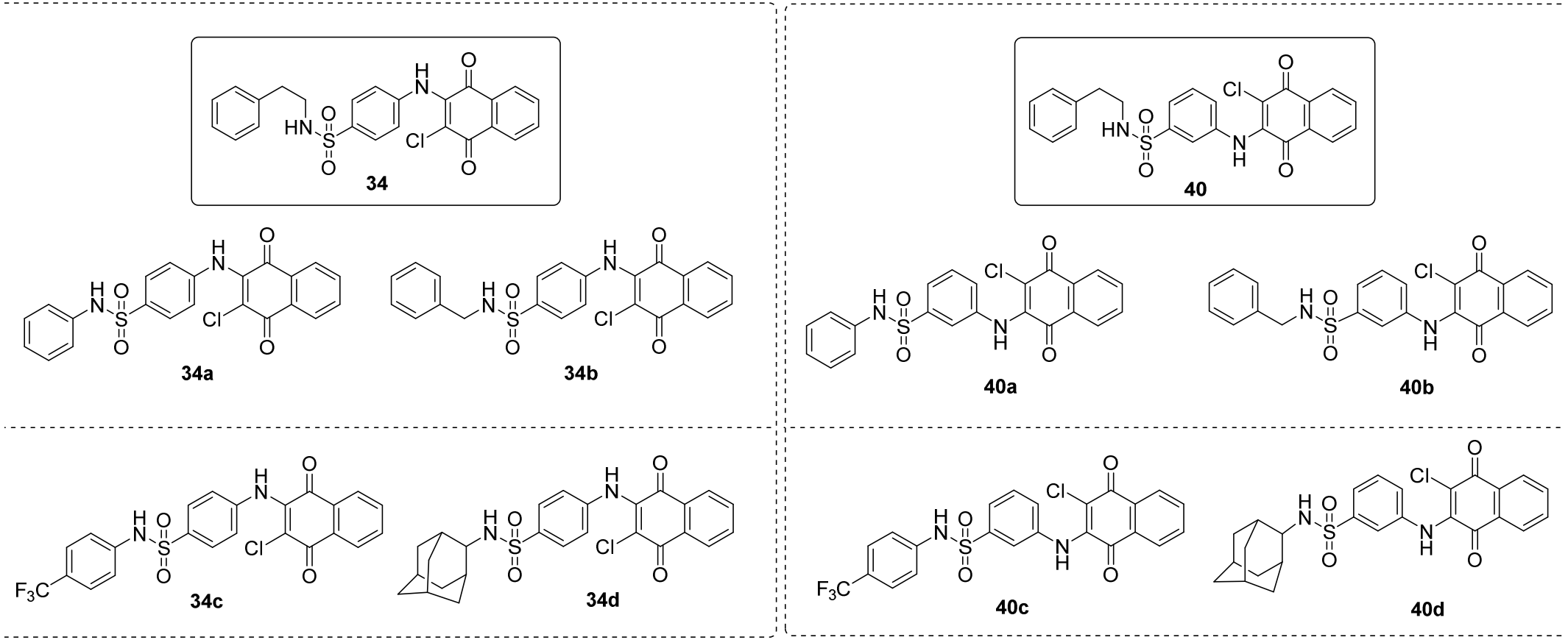

Fig. 4.

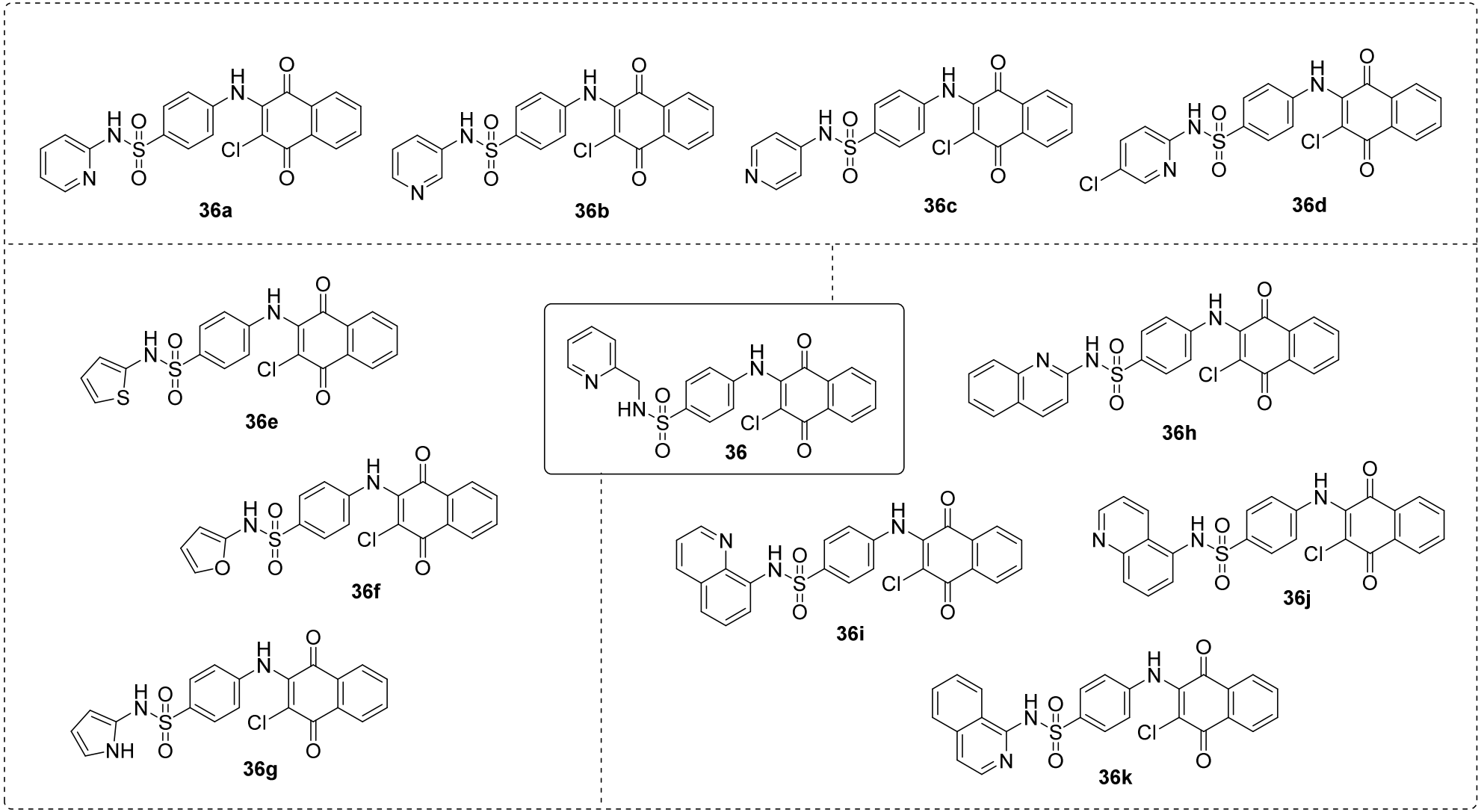

Fig. 5.

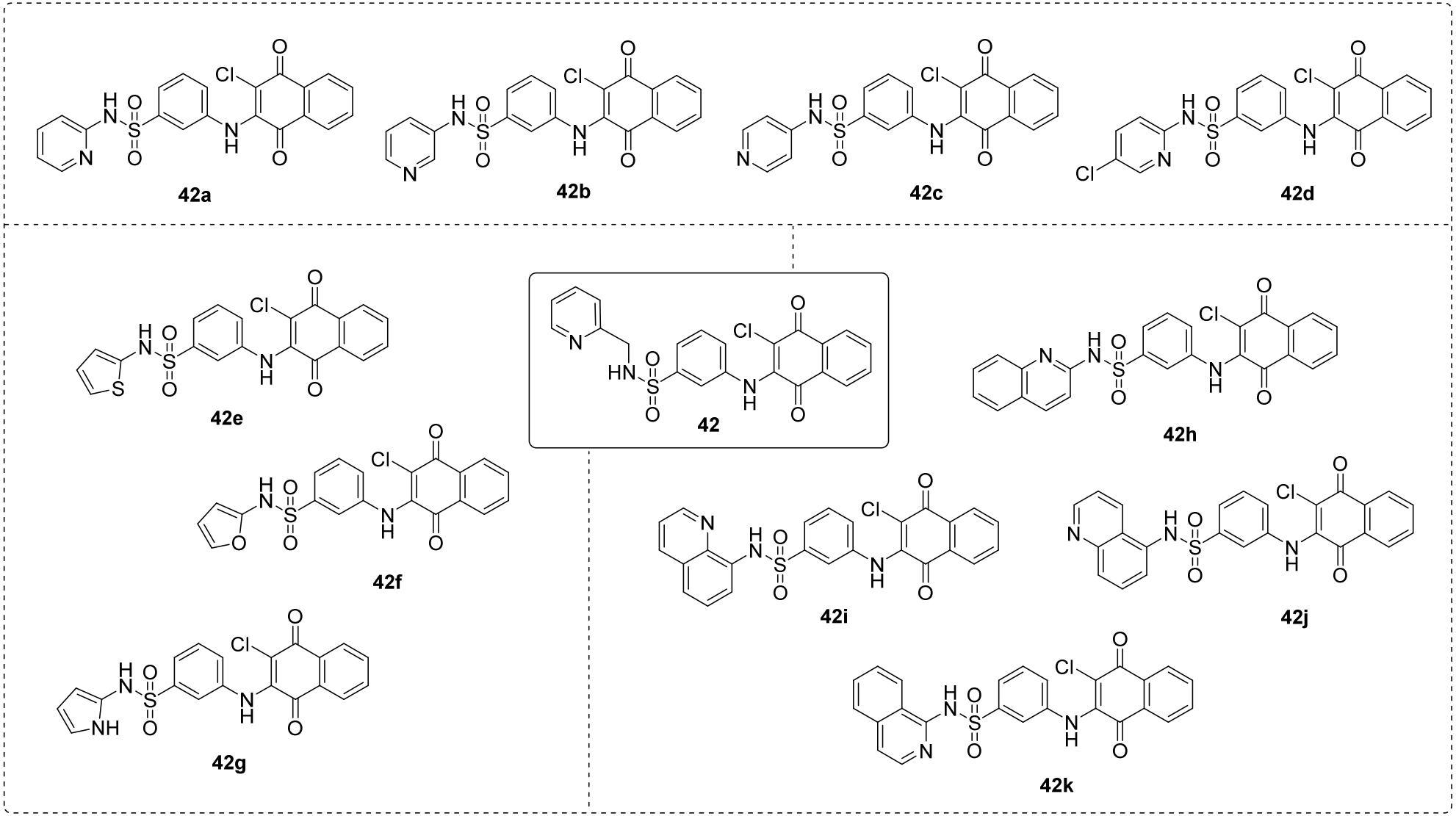

Fig. 6.

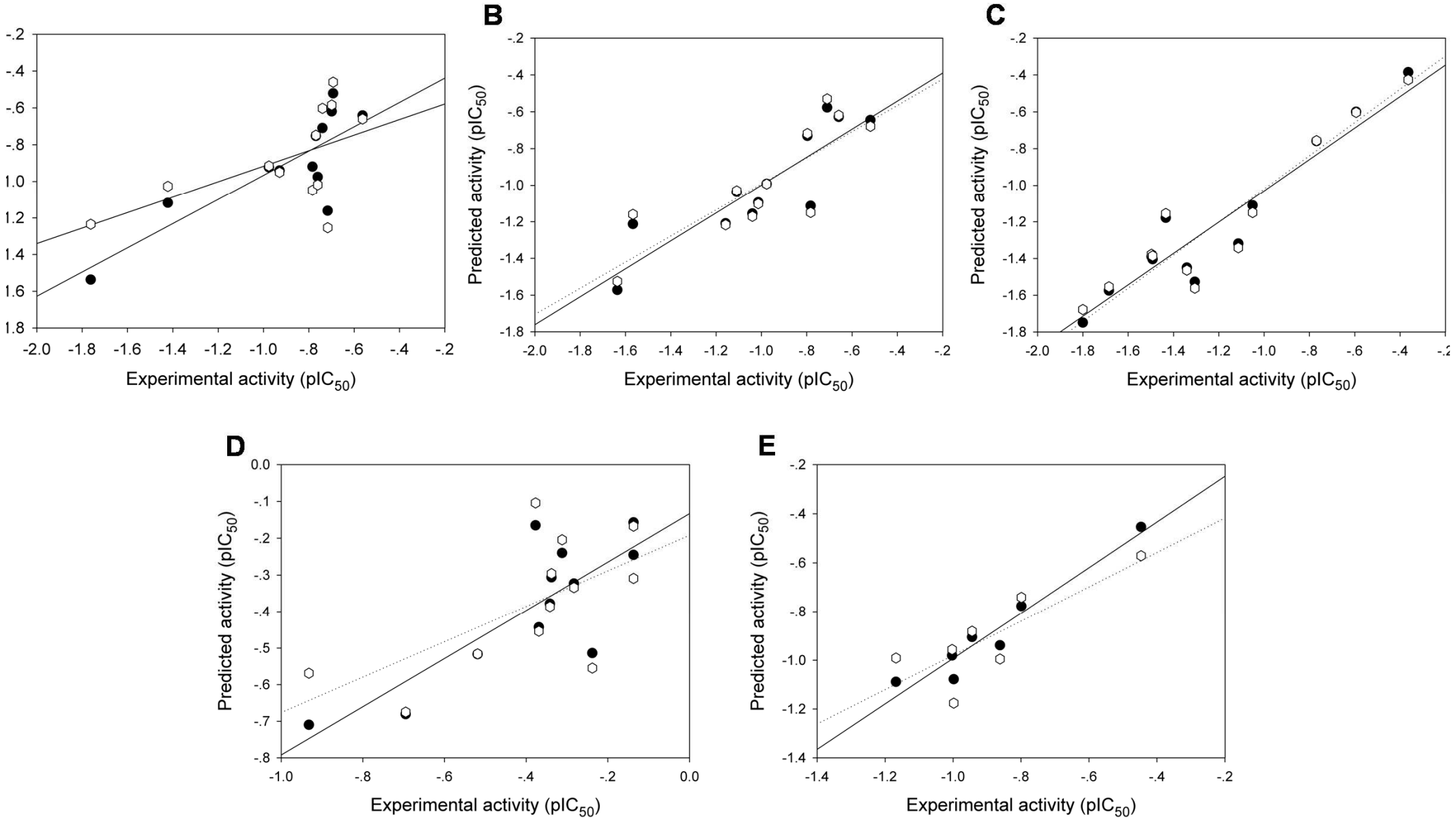
B
C
D
E
Predicted activity (pIC50)
Experimental activity (pIC50)

Fig. 7.

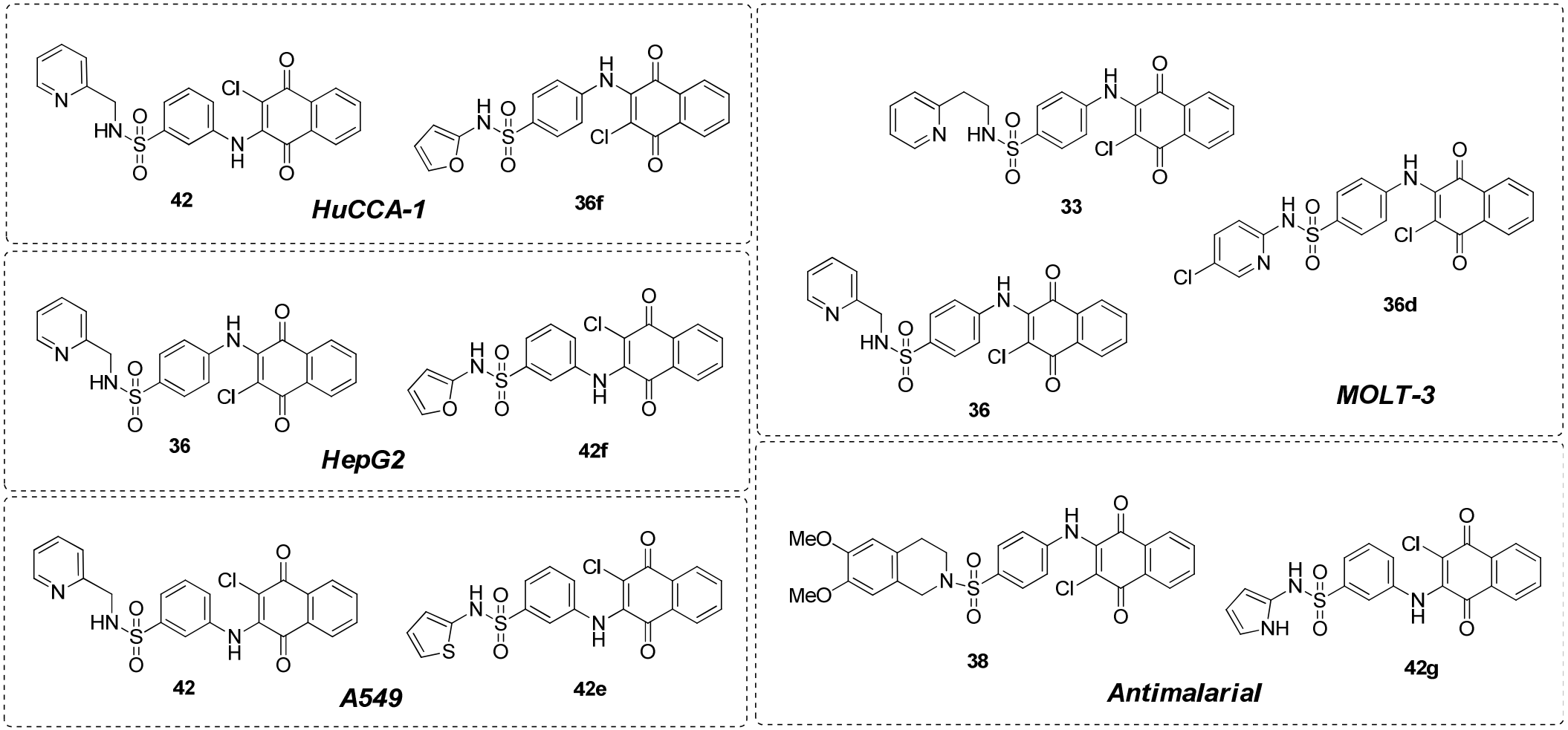
42
HuCCA-1
36f
36
HepG2
42f
42
A549
42e
33
36d
36
MOLT-3
38
Antimalarial
42g

Fig. 8.

- ▶Novel quinone-sulfonamides (**33**-**44**) were synthesized.
- ▶All quinones displayed a broad spectrum of cytotoxic activities.
- ▶The quinone **34** was the most potent cytotoxic compound without affecting normal cell.
- ▶Most quinones exerted higher anticancer activity against HepG2 cells than etoposide.
- ▶QSAR was performed to reveal important chemical features governing the activities.

Novel 1,4-naphthoquinone-based sulfonamides: synthesis, QSAR, anticancer and antimalarial studies

Ratchanok Pingaew,* Veda Prachayasittikul, Apilak Worachartcheewan, Chanin Nantasenamat, Supaluk Prachayasittikul, Somsak Ruchirawat, Virapong Prachayasittikul*

E-mail: ratchanok@swu.ac.th (R. Pingaew)

Tel: 662-649-5000 ext 18253; Fax: 662-260-0128

E-mail: virapong.pra@mahidol.ac.th (V. Prachayasittikul)

Tel: 662-441-4376; Fax: 662-441-4380

Supplementary data

Table S1

Values of informative molecular descriptors of tested compounds (**33 - 44**) and virtually modified compounds (**34a - 34d**, **36a - 36k**, **40a - 40d**, **42a - 42k**).

Compound	X1A	Gm	G2u	RDF105m	Mor12u	G(N..Cl)	Mor22v	B05[N-O]	Mor24u
33	0.439	0.165	0.169	9.034	-1.301	25.398	-0.098	0	0.180
34	0.439	0.168	0.186	5.288	-1.411	12.093	0.015	0	0.158
35	0.442	0.153	0.192	9.242	-1.170	12.129	-0.094	0	0.159
36	0.437	0.170	0.178	4.405	-1.024	24.863	-0.003	1	0.054
37	0.429	0.154	0.149	10.263	-1.400	12.088	-0.042	0	0.217
38	0.433	0.157	0.167	10.226	-1.336	12.077	-0.262	1	0.324
39	0.439	0.157	0.165	3.707	-0.890	20.606	0.043	1	0.294
40	0.439	0.158	0.168	8.445	-1.403	11.321	-0.024	1	0.371
41	0.442	0.159	0.153	7.980	-1.140	11.300	-0.044	1	0.184
42	0.437	0.167	0.183	4.231	-0.506	21.46	0.074	1	0.146
43	0.429	0.166	0.185	9.677	-1.300	11.757	0.020	1	0.299
44	0.433	0.156	0.174	13.964	-1.143	11.766	-0.072	1	0.209
34a	0.435	0.172	0.176	3.642	-1.202	12.171	0.036	0	0.276
34b	0.437	0.178	0.152	5.997	-1.131	12.734	-0.158	0	0.175
34c	0.432	0.152	0.191	9.839	-0.855	12.156	-0.124	0	0.496
34d	0.418	0.166	0.168	11.664	-2.804	12.757	0.323	0	0.521
36a	0.435	0.173	0.177	9.576	-0.746	20.724	-0.118	0	0.269
36b	0.435	0.166	0.188	4.402	-0.701	21.273	-0.097	1	0.246
36c	0.435	0.173	0.161	4.769	-0.760	21.919	-0.154	0	0.138
36d	0.434	0.173	0.188	18.383	-0.543	40.053	-0.091	0	0.100
36e	0.433	0.172	0.180	8.465	-0.259	12.122	-0.096	0	0.135
36f	0.433	0.176	0.192	2.899	-0.951	12.135	-0.222	0	0.400
36g	0.433	0.174	0.168	4.311	-0.640	22.224	-0.113	0	0.628
36h	0.430	0.163	0.151	11.257	-0.596	20.778	-0.037	0	0.285
36i	0.430	0.177	0.169	7.782	-0.697	22.338	-0.152	1	0.397
36j	0.430	0.168	0.198	9.144	-0.953	20.422	-0.117	0	0.240
36k	0.430	0.168	0.188	9.170	-0.531	20.805	-0.103	0	0.328
40a	0.435	0.175	0.154	2.942	-0.516	12.014	-0.117	1	0.108
40b	0.437	0.172	0.181	7.740	-1.320	11.015	0.055	1	0.216
40c	0.432	0.160	0.152	3.266	-0.244	11.977	-0.097	1	0.306
40d	0.418	0.156	0.176	6.737	-2.754	11.358	0.491	1	0.377
42a	0.435	0.162	0.182	1.943	-0.523	20.083	-0.172	1	0.297
42b	0.435	0.172	0.161	3.696	-0.248	20.397	-0.107	1	0.304
42c	0.435	0.166	0.166	2.768	-0.453	22.119	-0.14	1	0.060
42d	0.434	0.177	0.166	2.100	-0.438	37.873	-0.091	1	0.128
42e	0.433	0.166	0.204	0.169	0.032	11.981	-0.124	1	0.226
42f	0.433	0.173	0.169	0.135	-0.309	11.985	-0.417	1	0.296
42g	0.433	0.159	0.156	0.267	-0.473	21.027	-0.239	1	0.599

42h	0.430	0.169	0.198	5.604	-0.364	20.710	-0.030	1	0.359
42i	0.430	0.168	0.174	5.080	-0.734	23.552	-0.082	1	0.214
42j	0.430	0.154	0.179	5.981	-0.226	23.831	-0.039	1	0.605
42k	0.430	0.160	0.169	3.738	-0.238	20.110	-0.211	1	0.361

Table S2

Experimental and predicted cytotoxic and antimalarial activities (pIC_{50}) of compounds **33 - 44**.

Compound	**HuCCA-1**		**HepG2**		**A549**		**MOLT-3**		**Antimalarial**	
	Exp.	Pred.	Exp.	Pred.	Exp.	Pred.	Exp.	Pred.	Exp.	Pred.
33	-0.769	-0.748	-1.014	-1.102	-1.497	-1.377	-0.137	-0.309	- [a]	- [a]
34	-0.693	-0.460	-0.797	-0.718	-1.051	-1.150	-0.338	-0.296	- [a]	- [a]
35	-0.740	-0.602	-0.783	-1.150	-1.114	-1.342	-0.312	-0.204	-0.998	-1.176
36	-0.699	-0.584	-0.519	-0.679	-0.769	-0.756	-0.137	-0.167	- [a]	- [a]
37	-1.762	-1.235	-1.567	-1.160	-1.685	-1.554	-0.932	-0.569	-1.168	-0.991
38	-0.717	-1.254	-1.158	-1.217	-1.306	-1.562	-0.238	-0.555	-0.447	-0.571
39	-0.761	-1.018	-0.710	-0.530	-0.594	-0.603	-0.342	-0.386	- [a]	- [a]
40	-0.976	-0.915	-1.109	-1.030	-1.492	-1.386	-0.519	-0.516	-0.799	-0.741
41	-0.929	-0.950	-0.977	-0.993	-1.434	-1.155	-0.695	-0.675	-1.003	-0.956
42	-0.563	-0.660	-0.659	-0.619	-0.364	-0.426	-0.377	-0.104	- [a]	- [a]
43	-0.784	-1.048	-1.040	-1.171	-1.341	-1.464	-0.283	-0.334	-0.862	-0.995
44	-1.422	-1.026	-1.636	-1.525	-1.800	-1.678	-0.369	-0.454	-0.944	-0.881

Exp. = experimental activity, Pred. = predicted activity. - [a] = the compound was experimentally inactive and was excluded from the data set of QSAR analysis

Table S3

Predicted cytotoxic and antimalarial activities (pIC_{50}) of modified compounds (**34a - 34d**, **36a - 36k**, **40a - 40d** and **42a -42k)** and experimental activities of reference drugs.

Compound	HuCCA-1	HepG2	A549	MOLT-3	Antimalarial
34a	-0.660	-0.571	-0.809	-0.414	-1.139
34b	-0.681	-0.799	-0.984	-0.665	-0.955
34c	-1.083	-1.172	-1.158	-0.250	-0.604
34d	-1.455	-1.349	-2.677	-0.490	-1.291
36a	-0.628	-1.147	-1.058	-0.244	-0.901
36b	-0.685	-0.645	-0.536	-0.114	-0.818
36c	-0.779	-0.680	-0.611	-0.397	-1.008
36d	-0.558	-2.001	-1.753	0.233[b]	-1.158
36e	-0.691	-1.039	-0.616	-0.371	-1.105
36f	-0.484[b]	-0.499	-0.566	-0.240	-0.568
36g	-0.758	-0.636	-0.485	-0.315	-0.455
36h	-1.276	-1.309	-1.114	-0.527	-1.011
36i	-0.782	-0.973	-0.854	-0.302	-0.538
36j	-0.715	-1.105	-1.160	-0.021	-0.939
36k	-0.810	-1.107	-0.871	-0.123	-0.850
40a	-0.799	-0.503	-0.269	-0.657	-0.960
40b	-0.545	-0.969	-1.280	-0.380	-1.100
40c	-1.268	-0.535	-0.112	-0.679	-0.742
40d	-1.611	-0.871	-2.174	-0.429	-1.597
42a	-0.835	-0.406	-0.179	-0.202	-0.633
42b	-0.802	-0.576	-0.156	-0.425	-0.728
42c	-0.894	-0.486	-0.209	-0.339	-0.984
42d	-0.673	-0.422	-0.136	-0.047	-0.977
42e	-0.602	-0.234	0.372[b]	-0.111	-0.799
42f	-0.772	-0.231[b]	0.140	-0.493	-0.240
42g	-1.219	-0.244	0.014	-0.468	-0.143[b]
42h	-0.692	-0.762	-0.417	-0.015	-0.783
42i	-0.942	-0.711	-0.623	-0.225	-0.882
42j	-1.219	-0.798	-0.358	-0.165	-0.457
42k	-1.175	-0.580	-0.153	-0.343	-0.489
Etoposide [a]	ND[c]	-1.531	ND[c]	1.387	ND[c]
Doxorubicin [a]	0.377	0.244	0.432	ND[c]	ND[c]
Mefloquine [a]	ND[c]	ND[c]	ND[c]	ND[c]	1.570
Dihydroartemisinine [a]	ND[c]	ND[c]	ND[c]	ND[c]	2.848

[a] Experimental pIC_{50} values. [b] The compound which was predicted to be the most potent compound. [c] Not tested.

Table S4

Summary of structure-activity relationships (SAR) of the tested compounds (**33 - 44**).

Activity/ cell line	**Series** (compounds)	**Closed / opened**	**Type of ring**	**Methoxy group**
HuCCA-1	*para*- (**33**-**38**)	opened > closed : **34** > **37** closed > opened[a]: **38** > **35**	benzene > pyridine: **34** > **33**	↓ activity : **34** > **35** ↑ activity : **38** > **37**
	meta- (**39**-**44**)	closed > opened : **43** > **40** opened > closed[a]: **41** > **44**	pyridine > benzene: **39** > **40**	↑ activity : **41** > **40** ↓ activity : **43** > **44**
	opened-chain (**33**-**35** & **39**-**41**)	*para* > *meta* : **34** > **40**, **35** > **41**[a] *meta* > *para* : **39** > **33**	-	*para*: ↓ activity : **34** > **35** *meta*: ↑ activity : **41** > **40**
	closed-chain (**37**-**38** & **43**-**44**)	*meta* > *para* : **43** > **37** *para* > *meta*[a] : **38** > **44**	-	*para*: ↑ activity : **38** > **37** *meta*: ↓ activity : **43** > **44**
	Length of linker (**33**, **36** and **42**)	1C > 2C : **36** > **33** *meta* > *para*[b] : **42 > 36**	-	-
HepG2	*para*- (**33**-**38**)	opened > closed : **34** > **37** opened > closed[a] :**35** > **38**	benzene > pyridine: **34** >**33**	↑ activity : **35** > **34**, **38** > **37**
	meta- (**39**-**44**)	closed > opened : **43** > **40** opened > closed[a]: **41** > **44**	pyridine > benzene: **39** > **40**	↑ activity : **41** > **40** ↓ activity : **43** > **44**
	opened-chain (**33**-**35** & **39**-**41**)	*meta* > *para* : **39** > **33** *para* > *meta* : **34** > **40**, **35** > **41**[a]	-	*para*: ↑ activity : **35** > **34** *meta*: ↑ activity : **41** > **40**
	closed-chain (**37**-**38** & **43**-**44**)	*meta* > *para* : **43** > **37** *para* > *meta*[a] : **38** > **44**	-	*para*: ↑ activity : **38** > **37** *meta*: ↓ activity : **43** > **44**
	Length of linker (**33**, **36** and **42**)	1C > 2C : **36** >**33** *para* > *meta*[b] : **36 > 42**	-	-

[a] With the presence of methoxy substitutions. [b] For 1C length linker.

Table S4

Summary of structure-activity relationships (SAR) of the tested compounds (**33 - 44**), continued.

Activity/ cell line	**Series** (compounds)	**Closed / opened**	**Type of ring**	**Methoxy group**
A549	*para*- (**33**-**38**)	opened > closed : **34** > **37** opened > closed[a]: **35** > **38**	benzene > pyridine: **34** > **33**	↓ activity : **34** > **35** ↑ activity : **38** > **37**
	meta- (**39**-**44**)	closed > opened : **43** > **40** opened > closed[a]: **41** > **44**	pyridine > benzene: **39** > **40**	↑ activity : **41** > **40** ↓ activity : **43** > **44**
	opened-chain (**33**-**35** & **39**-**41**)	*meta* > *para* : **39** > **33** *para* > *meta* : **34** > **40**, **35** > **41**[a]	-	*para* :↓ activity : **34** > **35** *meta* :↑ activity : **41** > **40**
	closed-chain (**37**-**38** & **43**-**44**)	*meta* > *para* : **43** > **37** *para* > *meta*[a] : **38** > **44**	-	*para*: ↑ activity : **38** > **37** *meta*: ↓ activity : **43** > **44**
	Length of linker (**33**, **36** and **42**)	1C > 2C : **36** >**33** *meta* > *para*[b] : **42 > 36**	-	-
MOLT-3	*para*- (**33**-**38**)	opened > closed : **34** > **37** closed > opened[a]: **38** > **35**	pyridine > benzene: **33** > **34**	↑ activity : **35** > **34**, **38** > **37**
	meta- (**39**-**44**)	closed > opened : **43** > **40** closed > opened[a]: **44** > **41**	pyridine > benzene: **39** > **40**	↓ activity : **40** > **41**, **43** > **44**
	opened-chain (**33**-**35** & **39**-**41**)	*para* > *meta* : **33** > **39**, **34** > **40**, **35** > **41**[a]	-	*para*: ↑ activity: **35** > **34** *meta*: ↓ activity : **40** > **41**
	closed-chain (**37**-**38** & **43**-**44**)	*meta* > *para* : **43** > **37** *para* > *meta*[a] : **38** > **44**	-	*para*: ↑ activity: **38** > **37** *meta*: ↓ activity : **43** > **44**
	Length of linker (**33**, **36** and **42**)	1C = 2C : **36** = **33** *para* > *meta*[b]: **36 > 42**	-	-

[a] With the presence of methoxy substitutions. [b] For 1C length linker.

Table S4

Summary of structure-activity relationships (SAR) of the tested compounds (**33 - 44**), continued.

Activity/ cell line	**Series** (compounds)	**Closed / opened**	**Type of ring**	**Methoxy group**
Antimalarial	*para*- (**33**-**38**)	closed > opened: **37** > **34** closed > opened[a]: **38** > **35**	both pyridine (**33**) and benzene (**34**) derivatives are inactive	↑ activity : **35** > **34**, **38** > **37**
	meta- (**39**-**44**)	opened > closed: **40** > **43** closed > opened[a]: **44** > **41**	benzene > pyridine : **40** > **39**	↓ activity : **40** > **41**, **43** > **44**
	opened-chain (**33**-**35** & **39**-**41**)	*meta* > *para* : **40** > **34** *meta* ≈ *para*: **39** ≈ **33** *para* > *meta*: **35** > **41**[a]	-	*para*: ↑ activity: **35** > **34** *meta*: ↓ activity : **40** > **41**
	closed-chain (**37**-**38** & **43**-**44**)	*meta* > *para* : **43** > **37** *para* > *meta*[a] : **38** > **44**	-	*para*: ↑ activity: **38** > **37** *meta*: ↓ activity : **43** > **44**
	Length of linker (**33**, **36** and **42**)	1C = 2C : **36** = **33** *meta* ≈ *para*[b]: **42** ≈ **36**	-	-

[a] With the presence of methoxy substitutions. [b] For 1C length linker.

Table S5

Summary of structure-activity relationships (SAR) of modified compounds series **34** and **40**.

Modified series	Activity / cell line	Length of linker chain	CF_3 moiety	Type of ring
34	HuCCA-1	attached > 1C > 2C : **34a** > **34b** > **34** Shorter is better	↓activity : **34a** > **34c**	benzene > adamantane : **34a** > **34d**
	HepG2	attached > 2C > 1C : **34a** > **34** > **34b**	↓activity : **34a** > **34c**	benzene > adamantane : **34a** > **34d**
	A549	attached > 1C > 2C : **34a** > **34b** > **34** Shorter is better	↓activity : **34a** > **34c**	benzene > adamantane : **34a** >> **34d**
	MOLT-3	2C > attached > 1C : **34** > **34a** > **34b**	↑activity : **34c** > **34a**	benzene > adamantane : **34a** > **34d**
	Antimalarial	1C > attached > 2C : **34b** > **34a** > **34**	↑activity : **34c** >> **34a**	benzene > adamantane : **34a** > **34d**
40	HuCCA-1	1C > attached > 2C : **40b** > **40a** > **40**	↓activity : **40a** > **40c**	benzene > adamantane : **40a** > **40d**
	HepG2	attached > 1C > 2C : **40a** > **40b** > **40** Shorter is better	↓activity : **40a** > **40c**	benzene > adamantane : **40a** > **40d**
	A549	attached > 1C > 2C : **40a** > **40b** > **40** Shorter is better	↑activity : **40c** > **40a**	benzene > adamantane : **40a** > > **40d**
	MOLT-3	1C > 2C > attached : **40b** > **40** > **40a**	↓activity : **40a** > **40c**	adamantane > benzene : **40d** > **40a**
	Antimalarial	2C > attached > 1C : **40** > **40a** > **40b**	↑activity : **40c** > **40a**	benzene > adamantane : **40a** > **40d**

Table S6

Summary of structure-activity relationships (SAR) of modified compounds series **36** and **42**.

Series	Activity / cell line	Type of ring	Cl moiety	Position of aminopyridine	Position of aminoquinoline	Notes
36	HuCCA-1	F > PD > T > PR : **36f** > **36a** > **36e** > **36g**	↑activity: **36d** > **36a**	2AP > 3AP > 4AP: **36a** > **36b** > **36c**	5AQ > 8AQ > isoQ > 2AQ: **36j** > **36i** > **36k** > **36h**	2AP > 2AQ : **36a** > **36h** All 5-menbered monocyclic rings > AQ series (except 5AQ)
	HepG2	F > PR > T > PD: **36f** > **36g** > **36e** > **36a**	↓activity: **36a** > **36d**	3AP > 4AP > 2AP: **36b** > **36c** > **36a**	8AQ > 5AQ > isoQ > 2AQ: **36i** > **36j** > **36k** > **36h**	2AP > 2AQ : **36a** > **36h** All 5-menbered monocyclic rings > AQ series (except 8AQ)
	A549	PR > F > T > PD: **36g** > **36f** > **36e** > **36a**	↓activity: **36a** > **36d**	3AP > 4AP > 2AP: **36b** > **36c** > **36a**	8AQ > isoQ > 2AQ > 5AQ: **36i** > **36k** > **36h** > **36j**	2AP > 2AQ : **36a** > **36h** All 5-menbered monocyclic rings > AQ series
	MOLT-3	F > PD > PR > T: **36f** > **36a** > **36g** > **36e**	↑activity: **36d** > **36a**	3AP > 2AP > 4AP: **36b** > **36a** > **36c**	5AQ > isoQ > 8AQ > 2AQ: **36j** > **36k** > **36i** > **36h**	2AP > 2AQ : **36a** > **36h** All AQ series (except 2AQ) > 5-menbered monocyclic rings
	Antimalarial	PR > F > PD > T: **36g** > **36f** > **36a** > **36e**	↓activity: **36a** > **36d**	3AP > 2AP > 4AP: **36b** > **36a** > **36c**	8AQ > isoQ > 5AQ > 2AQ: **36i** > **36k** > **36j** > **36h**	2AP > 2AQ : **36a** > **36h** All 5-menbered monocyclic rings (except T) > AQ series (except 2AQ and 8AQ)

AP = aminopyridine, AQ = aminoquinoline, isoQ = isoquinoline, F = furan, PD = pyridine, T = thiophene, PR = pyrrole

Table S6

Summary of structure-activity relationships (SAR) of modified compounds series **36** and **42**, continued.

Series	Activity / cell line	Type of ring	Cl moiety	Position of aminopyridine	Position of aminoquinoline	Notes
42	HuCCA-1	T > F > PD > PR : **42e** > **42f** > **42a** > **42g**	↑activity: **42d** > **42a**	3AP > 2AP > 4AP: **42b** > **42a** > **42c**	2AQ > 8AQ > isoQ > 5AQ: **42h** > **42i** > **42k** > **42j**	2AQ > 2AP : **42h** > **42a** All 5-menbered monocyclic rings > AQ series (except 2AQ)
	HepG2	F > T> PR > PD: **42f** > **42e** > **42g** > **42a**	↓activity: **42a** > **42d**	2AP > 4AP > 3AP: **42a** > **42c** > **42b**	isoQ > 8AQ > 2AQ > 5AQ: **42k** > **42i** > **42h** > **42j**	2AP > 2AQ : **42a** > **42h** All 5-menbered monocyclic rings > AQ series
	A549	T > F > PR > PD : **42e** > **42f** > **42g** > **42a**	↑activity: **42d** > **42a**	3AP > 2AP > 4AP: **42b** > **42a** > **42c**	isoQ > 5AQ > 2AQ > 8AQ: **42k** > **42j** > **42h** > **42i**	2AP > 2AQ : **42a** > **42h** All 5-menbered monocyclic rings > AQ series
	MOLT-3	T > PD > PR > F : **42e** > **42a** > **42g** > **42f**	↑activity: **42d** > **42a**	2AP > 4AP > 3AP: **42a** > **42c** > **42b**	2AQ > 5AQ > 8AQ > isoQ: **42h** > **42j** > **42i** > **42k**	2AQ > 2AP : **42h** > **42a** AQ series > 5-menbered monocyclic rings (except thiophene, **42e**)
	Antimalarial	PR > F > PD > T : **42g** > **42f** > **42a** > **42e**	↓activity: **42a** > **42d**	2AP > 3AP > 4AP: **42a** > **42b** > **42c**	5AQ > isoQ > 2AQ > 8AQ: **42j** > **42k** > **42h** > **42i**	2AP > 2AQ : **42a** > **42h** All 5-menbered monocyclic rings (except thiophene, **42e**) > AQ series

AP = aminopyridine, AQ = aminoquinoline, isoQ = isoquinoline, F = furan, PD = pyridine, T = thiophene, PR = pyrrole

Table S7

Effects of structural modifications on important descriptor values.

Activity / cell line	**closed/ opened chain**	***para-* / *meta-***	**OMe moiety**	**Length of linker**	**Types of ring**	**Cl moiety**	**CF_3 moiety**	**AP position**	**AQ position**
HuCCA-1	X1A Gm G2u	Gm G2u	X1A	Gm G2u	Gm G2u	Gm G2u	X1A Gm G2u	Gm G2u	Gm G2u
HepG2	RDF105m	RDF105m	RDF105m	RDF105m	RDF105m	RDF105m	RDF105m	RDF105m	RDF105m
A549	RDF105m	RDF105m	RDF105m Mor12u	RDF105m Mor12u	RDF105m Mor12u	RDF105m Mor12u	RDF105m Mor12u	RDF105m Mor12u	RDF105m Mor12u
MOLT-3	G2u G(N..Cl)	G2u G(N..Cl)	G2u G(N..Cl)	G2u G(N..Cl)	G2u G(N..Cl)	G(N..Cl)	G2u G(N..Cl)	G2u G(N..Cl)	G2u G(N..Cl)
Antimalarial	Mor22v Mor24u	Mor22v B05[N-O] Mor24u	Mor22v Mor24u	Mor22v Mor24u	Mor22v Mor24u	Mor22v Mor24u	Mor22v Mor24u	Mor22v Mor24u	Mor22v Mor24u

Understanding structure-activity relationships: A detailed discussion

Considering the *para*-compounds, more potent activities against four cancer cell lines were observed for the opened chain compounds than the closed chain compounds (**34 > 37**), while the opposite effect was found for antimalarial activity (**37 > 34**). Distinct effects of diOMe substituent to activities of *para*-compounds (**33-38**) were noted for particular cancer cell lines. The closed chain *para*-compound elicited more potent activities against HuCCA-1 and MOLT-3 cell lines (**38** > **35**), while the opened chain *para*-compound were observed to be more active against HepG2 and A549 cell lines (**35** > **38**). For *meta*-compounds, the closed chain compound was noted as more potent compound against all cancer cell lines (**43** > **40**). In contrast, dimethoxy derivative of the opened chain *meta*-compound exerted more potent activities than the closed chain analog (**41** > **44**), except for cytotoxic activity against MOLT-3 cell line and antimalarial activity. In addition, the length of alkyl chain linking between sulfonamide group and pyridine ring was found to influence the anticancer activities against all cancer cell lines except for MOLT-3. The compound with 1C length linker was noted for its more potent activities against HuCCA-1, HepG2 and A549 cell lines when compared to the compound with 2C length (**36** > **33**). However, the influence of the length of linker, either 1C or 2C, on anticancer activity against MOLT-3 cell line, and antimalarial activity was not observed (**36** = **33**). For compounds with 1C linker, similar effects of *meta*-/*para*- isomers were noted for HuCCA-1 and A549 cell lines in which the *meta*-compound was noted to be more potent than the *para*-compound (**42** > **36**). In contrast, the *para*-compound exhibited more potent activities against HepG2 and MOLT-3 cell lines (**36** > **42**).

Similar results were noted for structurally modified compounds in series **34** and **40** (Supplementary Table S5). The benzene substituted compounds were predicted to exhibit more potent anticancer and antimalarial activities than adamantane derivatives (**34a** > **34d** and **40a** > **40d**), except for MOLT-3 cell lines (**40d** > **40a**). Substitution of trifluoromethyl (CF_3) moiety to compounds **34** and **40** was found to improve antimalarial activity while aggravate anticancer activities. However, the improved anticancer activities against MOLT-3 and A549 cell lines were observed for compounds **34c** and **40c**, respectively. In addition, the results indicated that particular length of alkyl chain linker is required for potent activity against distinct cell lines.

Various effects of structural modifications were observed for series **36** and **42** (Supplementary Table S6). The addition of chlorine moiety can both ameliorate and aggravate activities of the compounds. Most of the 5-membered monocyclic substituted compounds (**36e - 36g** and **42e - 42g**) exhibited more potent activities than aminoquinoline (AQ) derivatives (**36h - 36k** and **42h - 42k**). However, more potent cytotoxic activities against MOLT-3 cell line were found for AQ derivatives rather than monocyclic-substituted compounds. The comparison between aminopyridine (AP) compounds (**36a** and **42a**) and AQ compounds (**36h** and **42h**) showed that the AP moiety

provided more potent activities, except for anticancer activities of compound **42h** against HuCCA-1 and MOLT-3 cell lines. Certain positions of substituted AP and AQ on N-atom of sulfonamide were found to influence activities of the compounds. Derivatives of 2AP and 3AP exhibited the most potent activities when compared to the others in the same AP series. Similarly, 5AQ, 8AQ and isoquinoline moieties were predicted as crucial substituents essential for potent activities. Concerning the types of substituted ring, the most potent compounds of the modified series **36** against particular cancer cell lines were noted to be furan (**36f**) and pyrrole (**36g**) derivatives. In addition, furan (**42f**) and thiophene (**42e**) compounds were found to be the most potent anticancer agents of the series **42**. For antimalarial activity, the pyrrole derivatives (**36g** and **42g**) were predicted as the most potent compounds.

For HuCCA-1 cell line, the position of substituents, length of alkyl linker and type of substituted ring can directly affect the symmetry of the compounds as represented by the alteration of Gm and G2u descriptor values. The alterations of these descriptor values (Table S1) were notably observed when comparing the *para*-compounds with their *meta*- derivatives (i.e., **33** & **39**, **34** & **40** and **37** & **43**) in which both isomers possess equal connectivity indices, X1A value, but have different Gm and G2u values i.e., *para* compound **33** (Gm = 0.165, G2u = 0.169) and *meta* compound **39** (Gm = 0.157, G2u = 0.165). The most potent compound (**42**, pIC_{50} = -0.563) had the highest total symmetry value (Gm = 0.167) among the *meta* compounds (**39**-**44**). In addition, the opened/closed chain structures, diOMe and CF_3 moieties altered the value of X1A descriptor which indicated their influences on the connectivity (X1A) of the compounds. A reduced X1A value was observed for the least potent compound **37** (X1A = 0.429), which is the closed chain analog of the second most potent compound **34** (X1A = 0.439). The addition of diOMe moiety was generally observed to increase X1A values of the compounds comparing to the ones without diOMe i.e., **35** (XIA = 0.442) > **34** (XIA = 0.439), **38** (XIA = 0.433) > **37** (XIA = 0.429), **41** (XIA = 0.442) > **40** (XIA = 0.439), and **44** (XIA = 0.433) > **43** (XIA = 0.429). However, this modification can possibly lead to improved and reduced activities of the compounds. On the other hand, the compounds with CF_3 moiety (**34c** and **40c**) had lower X1A values as compared to the compounds without CF_3 (**34a** and **40a**), thereby aggravated the activity (HuCCA-1) of the compounds as noted by pIC_{50} values (Table S2) i.e., **34a** (-0.660) > **34c** (-1.083) and **40a** (-0.799) > **40c** (-1.286).

For A549 cell line, the structure of closed/opened chain and *para*-/*meta*-isomers were found to mainly affect mass-descriptor, RDF105m, value (Tables S1) in which the closed chain compounds with the same isomer (*m*- or *p*- isomer) had higher RDF values than their opened chain analogs i.e., *p*-isomers **37** (RDF105m = 10.263) > **34** (RDF105m = 5.288) and *m*-isomer **43** (RDF105m = 9.677) > **40** (RDF105m = 8.445). According to the QSAR model, the high value of Mor12u but low RDF105m values are required for potent activity of the compound. This was noted for the most potent activity (A5469) of the opened chain compound **42**, which had the highest Mor12u (-0.506) but low

RDF105m (4.231) values. Other structural modifications can alter both RDF105m and Mor12u descriptor values. Improved and decreased activities can be observed when introducing CF_3 moiety to the compounds. In case of CF_3 moiety aggravates the activity, an approximately 3 folds increased of RDF105m value of trifluoromethyl compound **34c** was observed when compared to its non- CF_3 substituted analog **34a** (activity: **34a** (pIC_{50} = -0.809) > **34c** (pIC_{50} = -1.158), RDF105m: **34a** = 3.642, **34c** = 9.839). In contrast, the Mor12u value may influence the improved activity (activity: **40c** (pIC_{50} = -0.112) > **40a** (pIC_{50} = -0.269), Mor12u: **40a** = -0.516, **40c** = -0.244). Similar effects were observed for chloro substituted compounds in which the improved activity (pIC_{50}), **42d** (-0.136) > **42a** (-0.179), can be noted for the compounds with the higher Mor12u **42d** (-0.438) > **42a** (-0.523) whereas the reduced activity may be due to the 2-folds increase RDF105m value (activity: **36a** (pIC_{50} = -1.058) > **36d** (pIC_{50} = -1.753), RDF105m: **36a** = 9.576, **36d** = 18.383). Notably, modification by various types of ring resulted in the alteration of RDF105m values as observed for 5-membered ring substituted series of compounds **42** i.e., **42e** (thiophene), **42f** (furan) and **42g** (pyrrole), in which approximately 10-folds decreased RDF105m values (**42e** = 0.169, **42f** = 0.135 and **42g** = 0.267) comparing to substituted pyridine ring **42a** (RDF105m = 1.943). The markedly improved activity affording positive pIC_{50} values (**42e** = 0.372, **42f** = 0.140 and **42g** = 0.014, Table S3) were observed as compared to their six-membered ring analog, 2-aminopyridine compound **42a** (pIC_{50} = -0.179).

In HepG2 cell line, RDF105m descriptor governed the activity of compound in which the opened chain analogs (**33**-**36** and **39**-**42**) had lower RDF105m values than the closed chain. The most potent *para*-compound **36** (pIC_{50} = -0.519) possessed relatively low RDF105m value (4.405). Similarly, relatively high potency of *meta*-compound **42** (pIC_{50} = -0.659) had low value of RDF105m (4.231). Most of the structurally modified compounds had low RDF105m value but with high pIC_{50} comparing to their parent compounds (TableS1 and S3). Particularly, *meta* compounds (**42e**-**42g**) with five membered ring analogs possessed very low RDF105m (< 0.300) in which the furan **42f** had the lowest RDF105m (0.135) with the highest predicted pIC_{50} (-0.230). Similarly, thiophene (**42e**) and pyrrole (**42g**) analogs had relatively high pIC_{50} values (-0.234 and -0.244) but with remarkably low RDF105m of 0.169 and 0.267, respectively. In addition, *meta* isomer of pyridine analogs (**42a**-**42d**) also exhibited high predicted pIC_{50} values (-0.576 to -0.406) as compared to methylpyridine analog **42** (pIC_{50} = -0.659), in which their RDF105m values were well correlated with the pIC_{50} values. The results suggested that directly connected pyridine ring (**42a**-**42d**) to N-atom of aminosulfonyl group afforded high predicted pIC_{50} value comparing to the pyridine compound with CH_2 linker (**42**). Furthermore, *meta*-isomer of phenyl derivatives (**40a** and **40c**), and its analog with CH_2 linker (**40b**) as well as 1-adamantyl analog **40d** had high predicted pIC_{50} values which were correlated with their RDF105m values. Inversely, the least potent closed chain compound **44** (pIC_{50} = -1.636) had the highest RDF105m value (13.964).

For MOLT-3 cell line, compound **33** exhibited a comparable potent activity with that of compound **36** which suggested the corresponding linkers with 2C and 1C length as appropriate length. Unlike other cell lines, chlorine substitution increased G(N..Cl) descriptor values thereby improved activities of compounds **36d** (*p*-isomer) and **42d** (*m*-isomer). Considerably, the most potent one (**36d**) of structurally modified compounds possessed the highest G(N..Cl) value of 40.053 (Table S1), and was the only compound exhibiting positive pIC_{50} value (0.233, Table S3) against MOLT-3 cell. Similarly, very high G(N..Cl) value (37.873) was noted for *m*-compound (**42d**) with relatively high predicted pIC_{50} value (-0.047). In addition, positions of aminopyridine and aminoquinoline, and length of alkyl chain linker affected activity of the compounds by influencing their symmetry, as indicated by the altered G2u values. It was found that compound **36b** (3AP) with high G2u (0.188) had high predicted pIC_{50} (-0.114), while the compound **42a** (2AP) with lower G2u (0.182) possessed the lower predicted pIC_{50} (-0.202). Similar effects were noted for *p*-isomer **36j** (5AQ, G2u = 0.198, pIC_{50} = -0.021), and for *m*-isomer **42h** (2AQ, G2u = 0.198, pIC_{50} = -0.015). For five-membered ring substituted compounds, furan **36f** with high G2u (0.192) had high predicted pIC_{50} (-0.240) as well as thiophene **42e** had G2u = 0.204 and pIC_{50} = -0.111.

For antimalarial activity, structural modifications mostly affected Mor22v and Mor24u descriptors. The interactive role of these descriptors was generally observed. Particularly, markedly reduced in van der Waals volume (Mor22v) together with large increased Mor24u values were found for compounds exhibiting potent activity i.e., compounds **38** and **42g**. The addition of diOMe moiety can decrease Mor22v value indicated its effect on the van der Waal volume of the compound. Notably, the diOMe substitution caused a change from inactive compound **34** to weakly active compound **35** *via* marked reduction of Mor22v value shifting from positive to negative value (**34** = 0.015, **35** = -0.094, Table S1). It was found that introducing CF_3 moiety increases Mor24u value thereby improves activities of trifluoromethyl derivatives (**34c** and **40c**). Likewise, substitution with pyrrole ring caused the increase of Mor24u value giving rise to the mark improved activity. Greater than 2-folds increased Mor24u values were found for pyrrole analogs **36g** (Mor24u = 0.628) and **42g** (Mor24u = 0.599) as compared to their pyridine analogs **36a** (Mor24u = 0.269) and **42a** (Mor24u = 0.297). Therefore, higher activities (pIC_{50} values) were noted for **36g** (-0.455) and **42g** (-0.143) comparing to **36a** (-0.901) and **42a** (-0.633).

^{1}H and ^{13}C NMR spectra of compound **8** ($CDCl_3$)

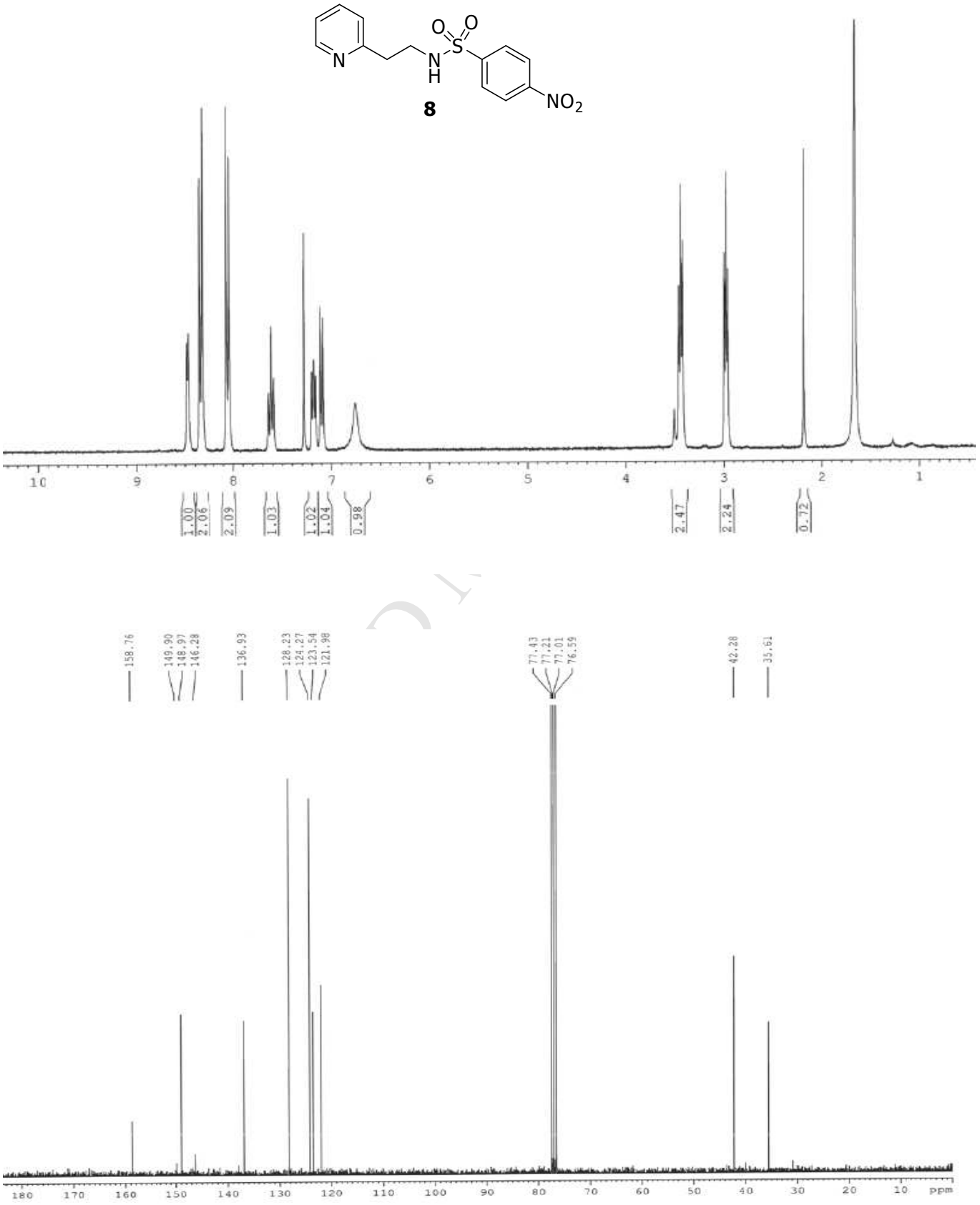

^{1}H and ^{13}C NMR spectra of compound **10** ($CDCl_3$)

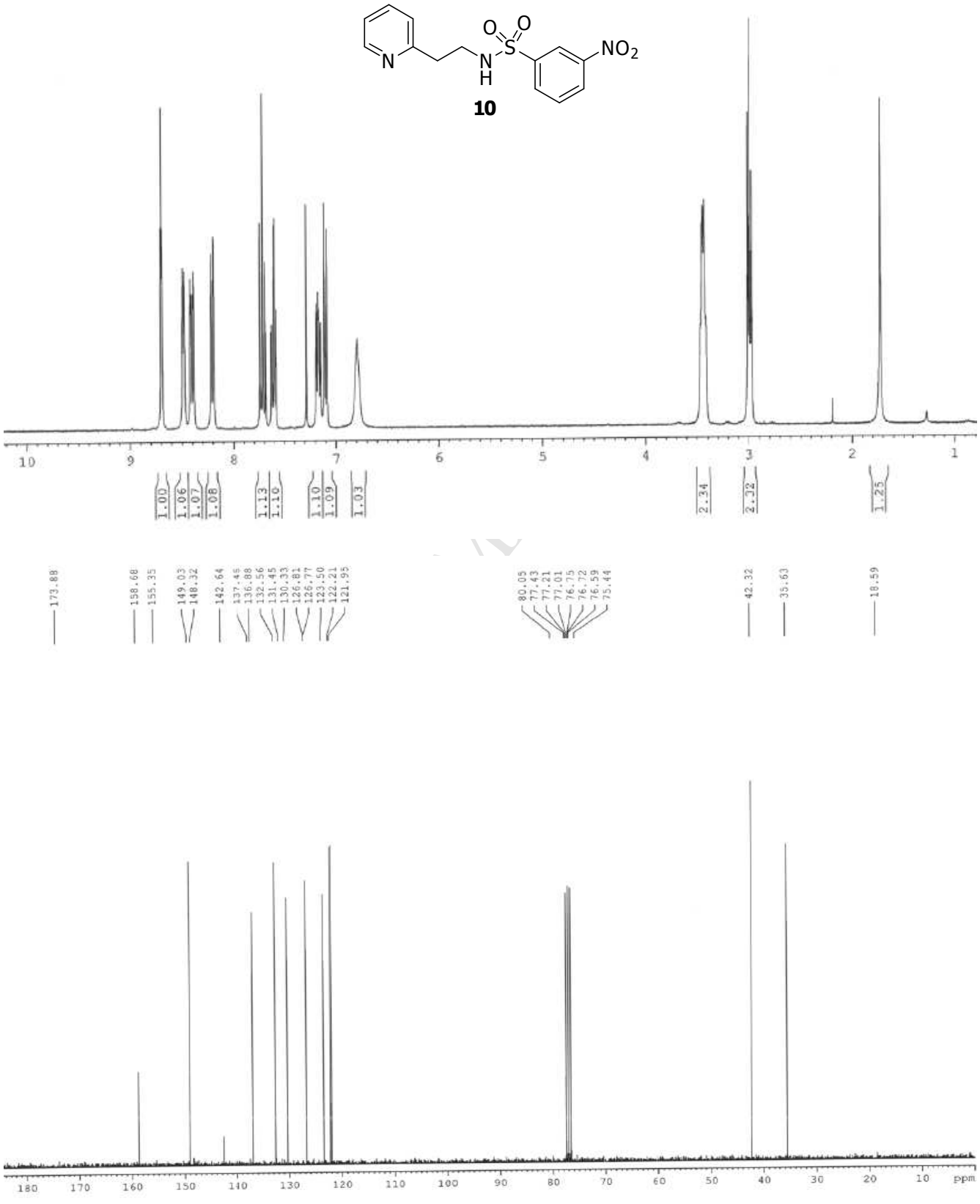

^{1}H and ^{13}C NMR spectra of compound **11** ($CDCl_3$)

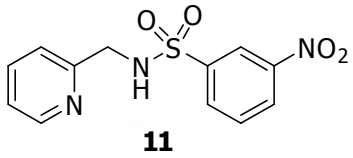

11

^{1}H and ^{13}C NMR spectra of compound **20** (DMSO-d_6)

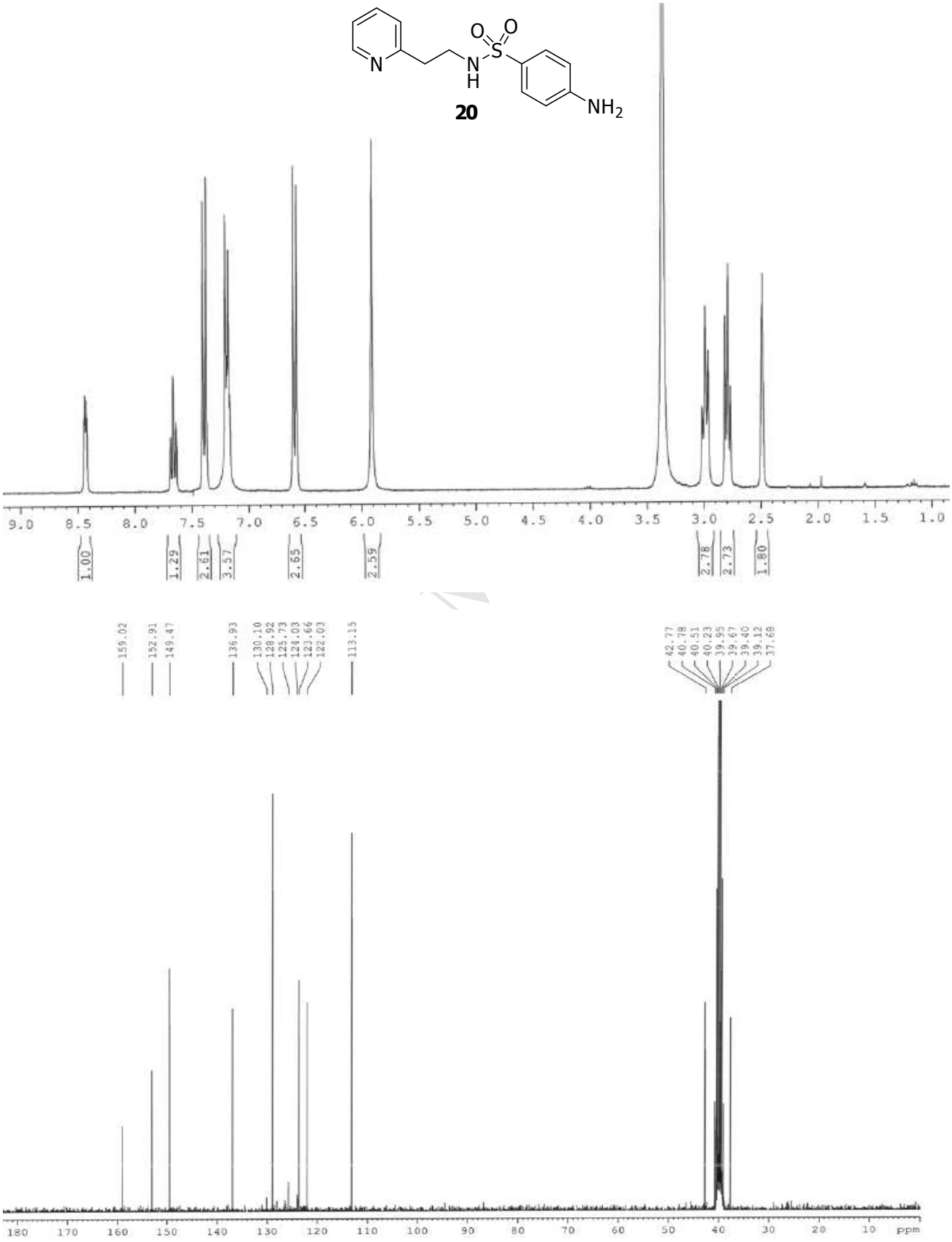

^{1}H and ^{13}C NMR spectra of compound **21** (DMSO-d_6)

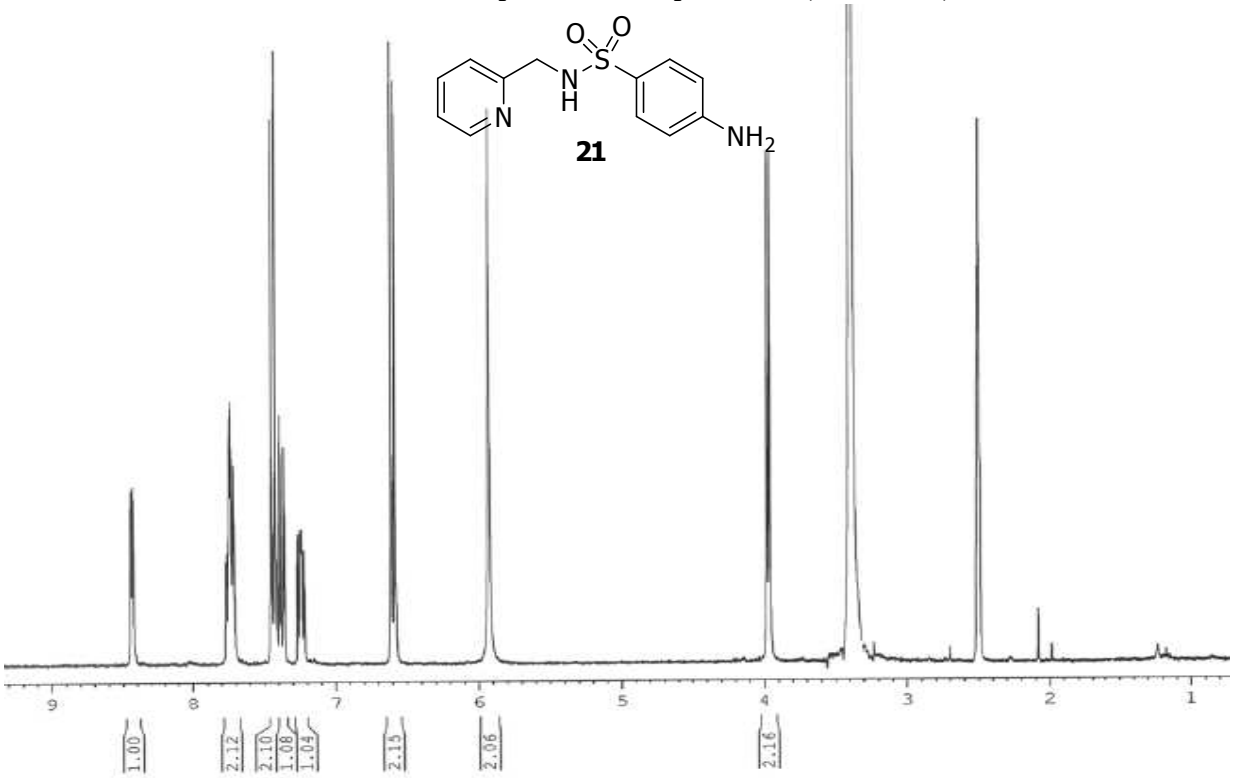

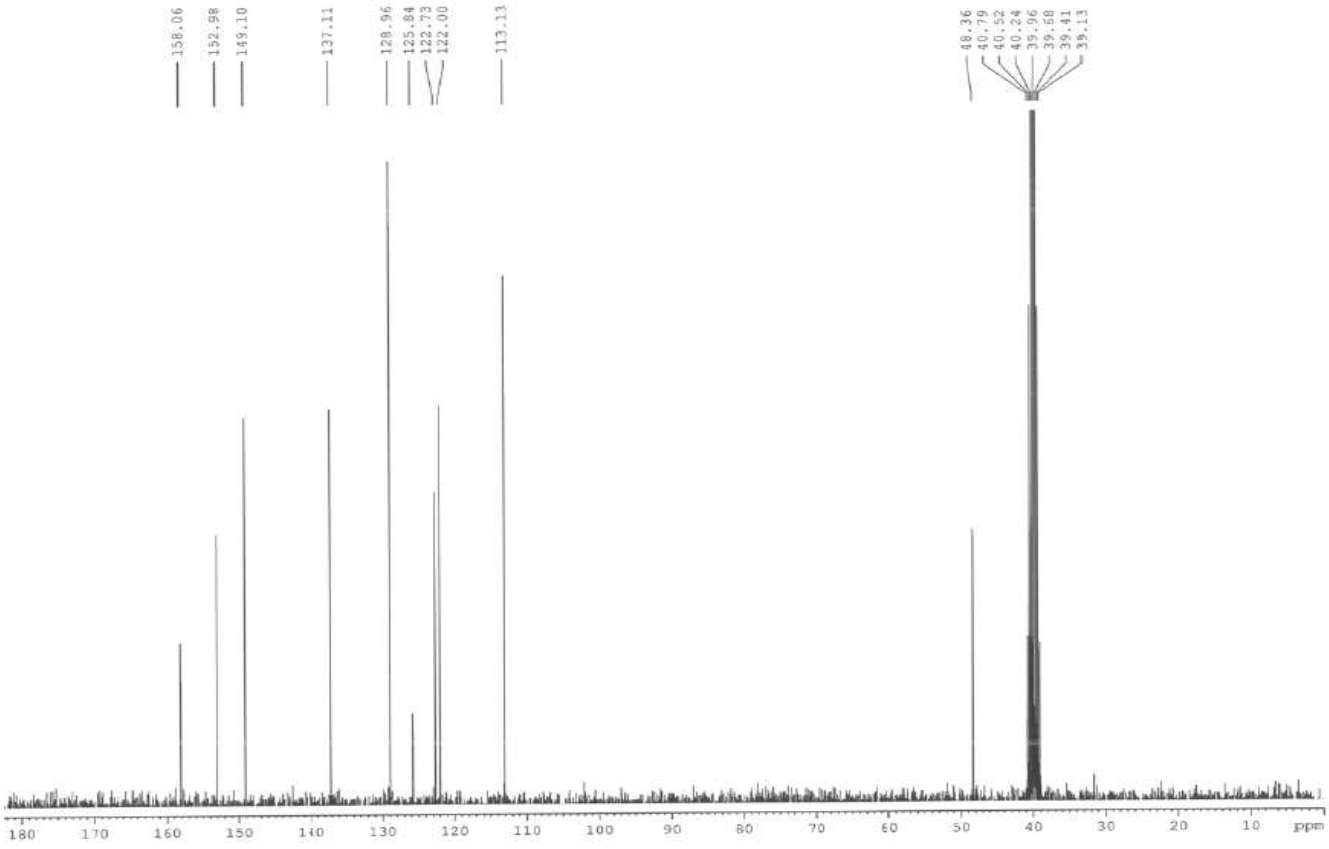

^{1}H and ^{13}C NMR spectra of compound **22** (DMSO-d_6)

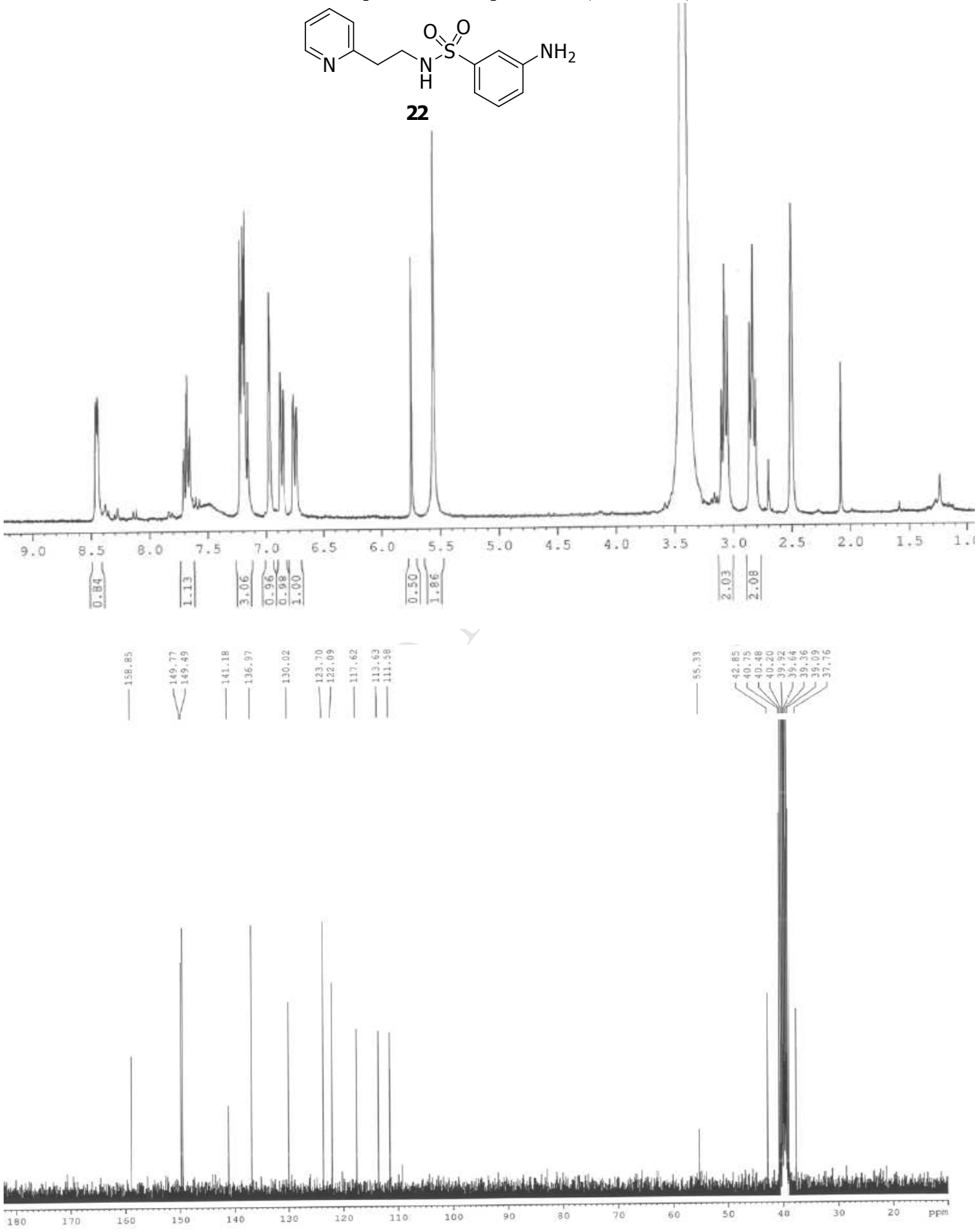

^{1}H and ^{13}C NMR spectra of compound **23** (DMSO-d_6)

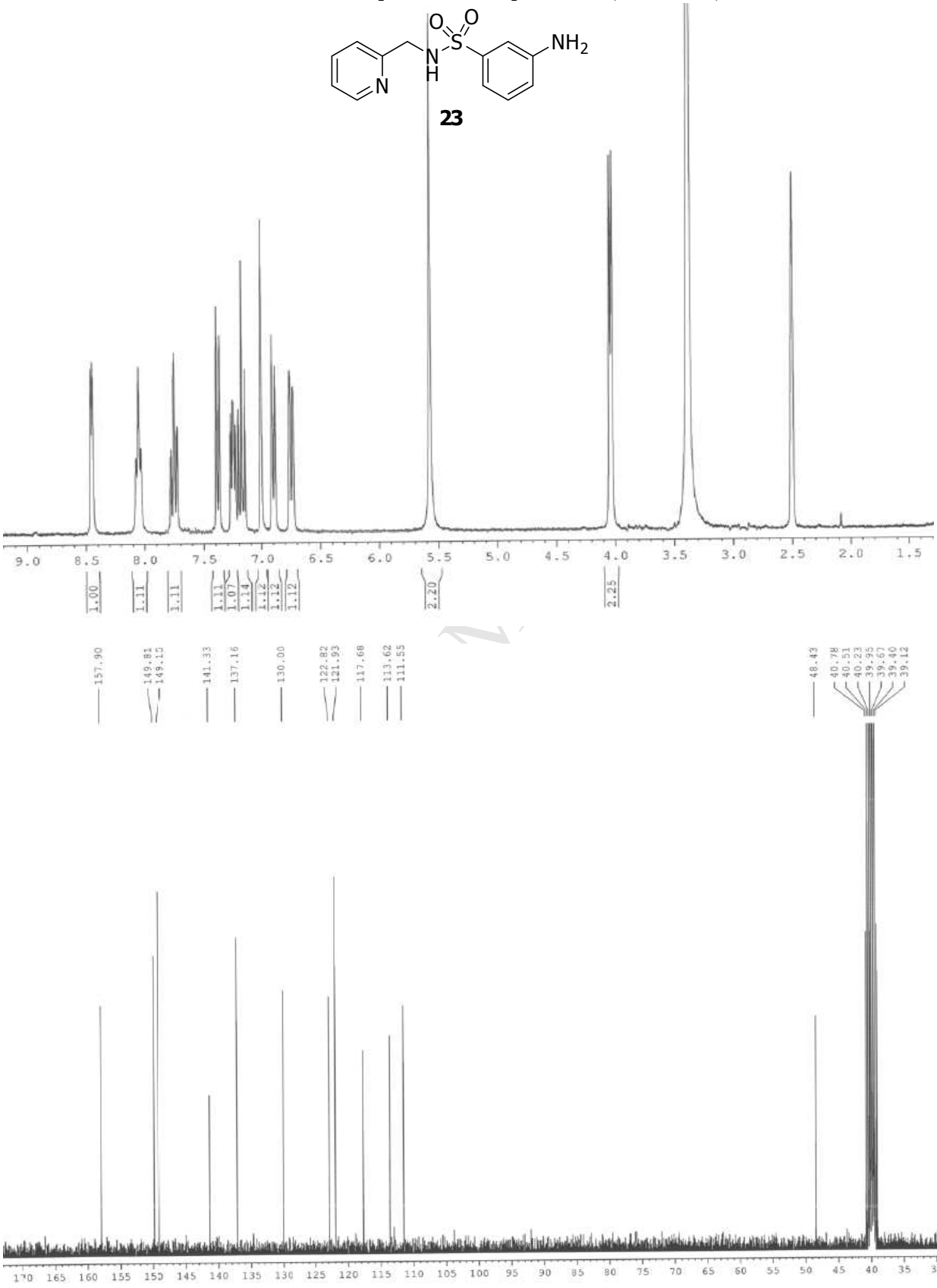

^{1}H and ^{13}C NMR spectra of compound **27** (DMSO-d_6)

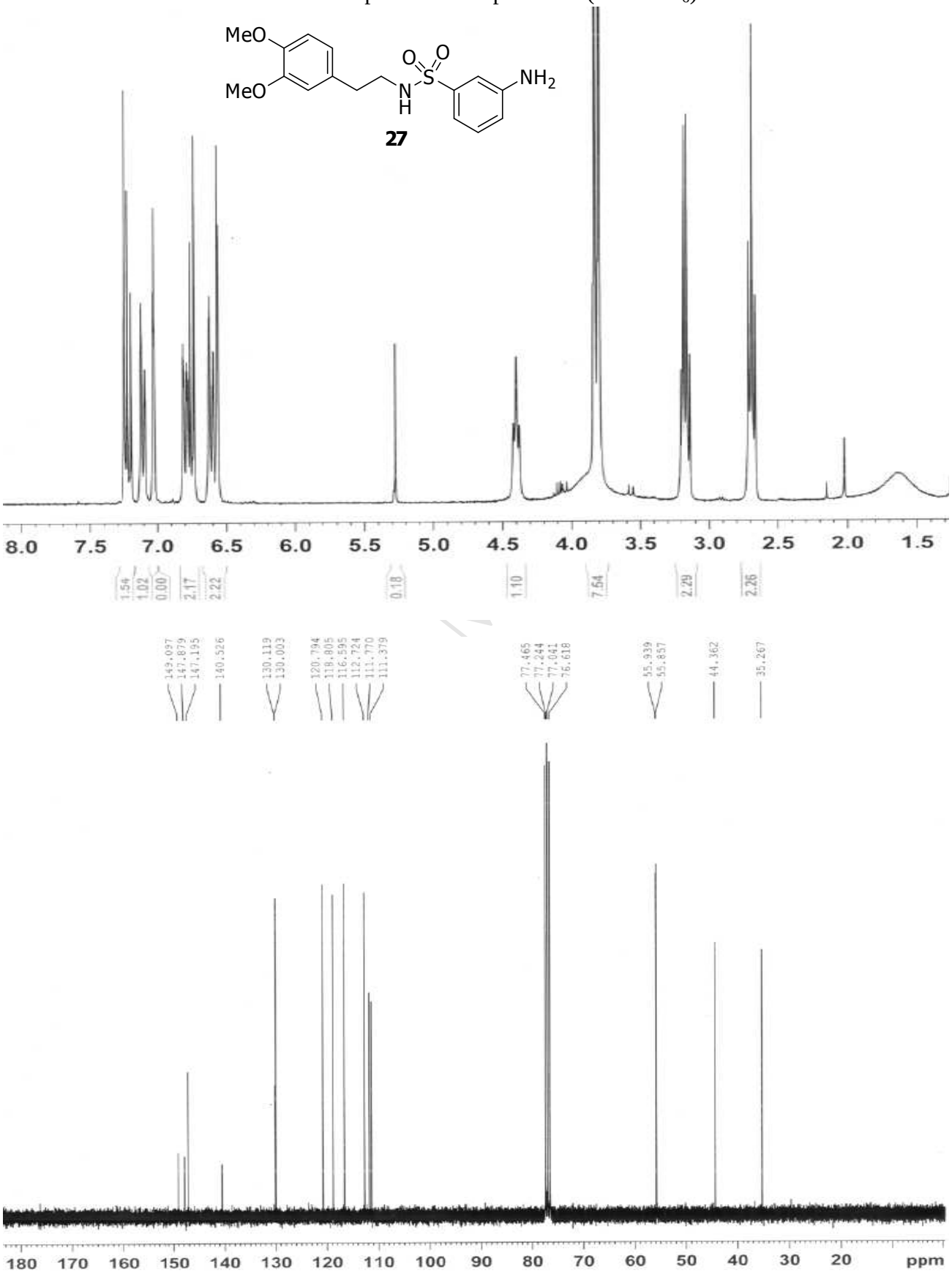

^{1}H and ^{13}C NMR spectra of compound **33** (DMSO-d_6)

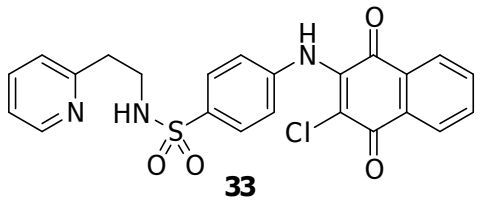

33

^{1}H and ^{13}C NMR spectra of compound **34** (DMSO-d_6)

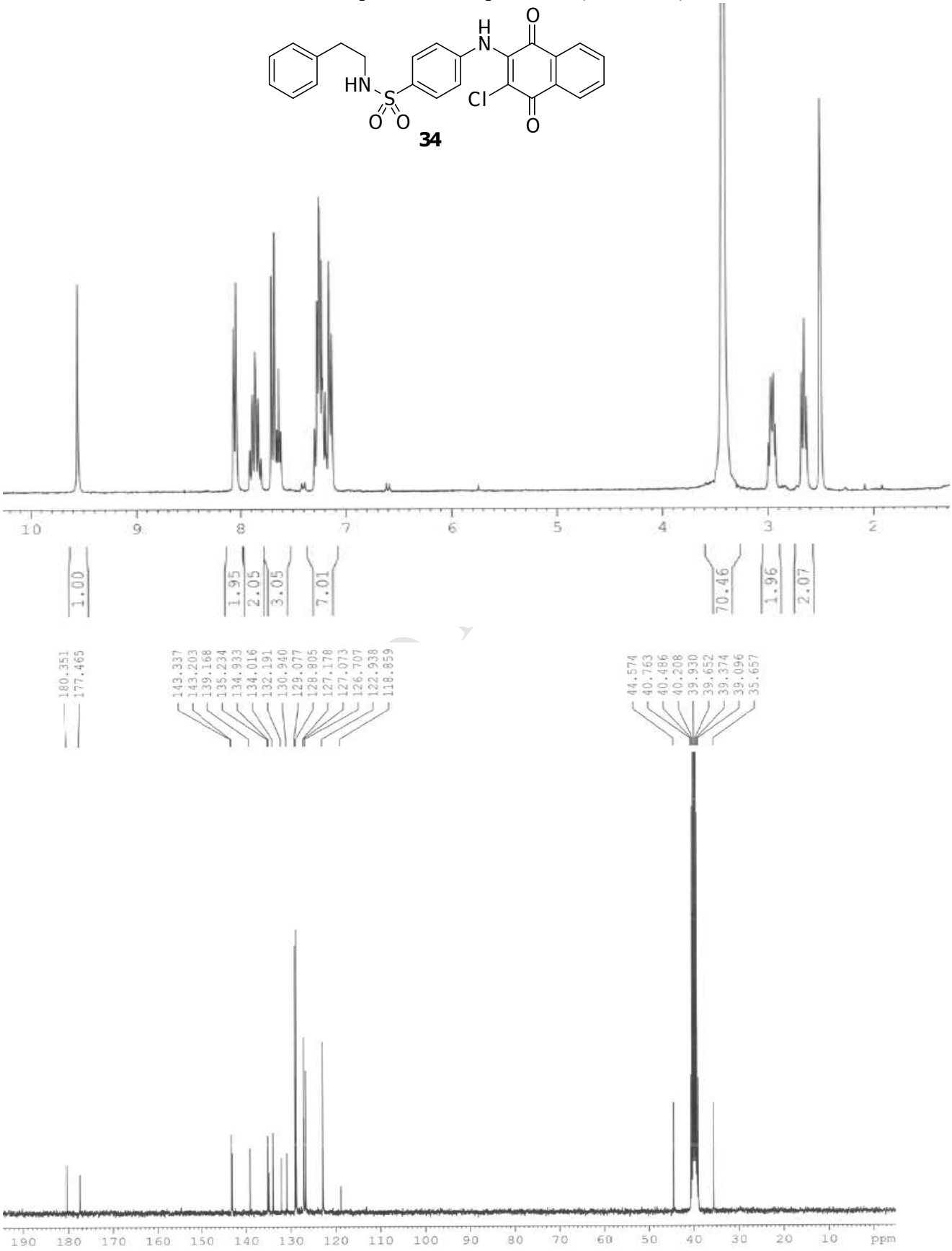

^{1}H and ^{13}C NMR spectra of compound **35** (DMSO-d_6)

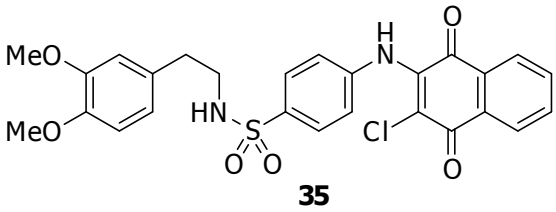

35

^{1}H and ^{13}C NMR spectra of compound **36** (DMSO-d_6)

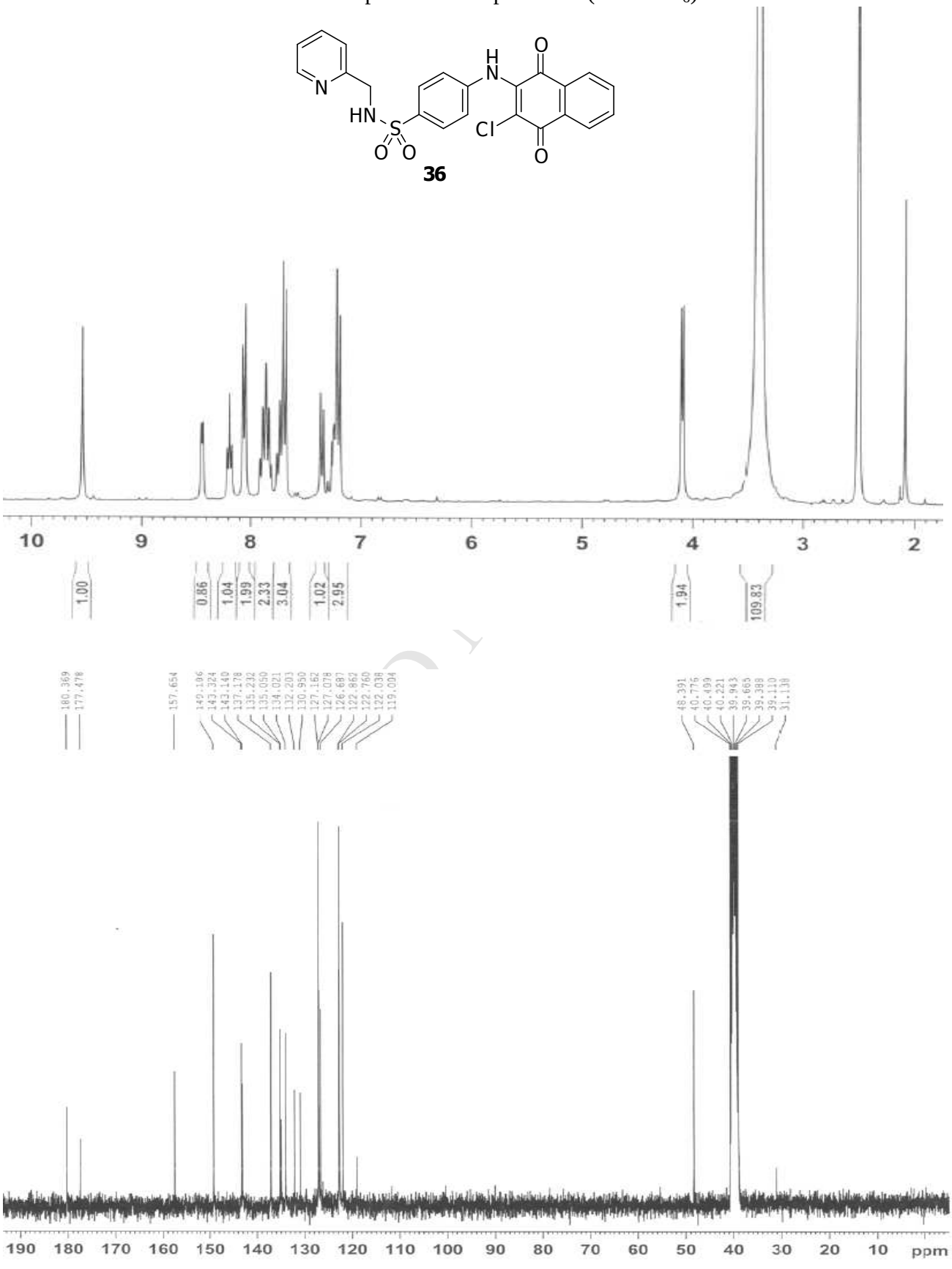

^{1}H and ^{13}C NMR spectra of compound **37** (DMSO-d_6)

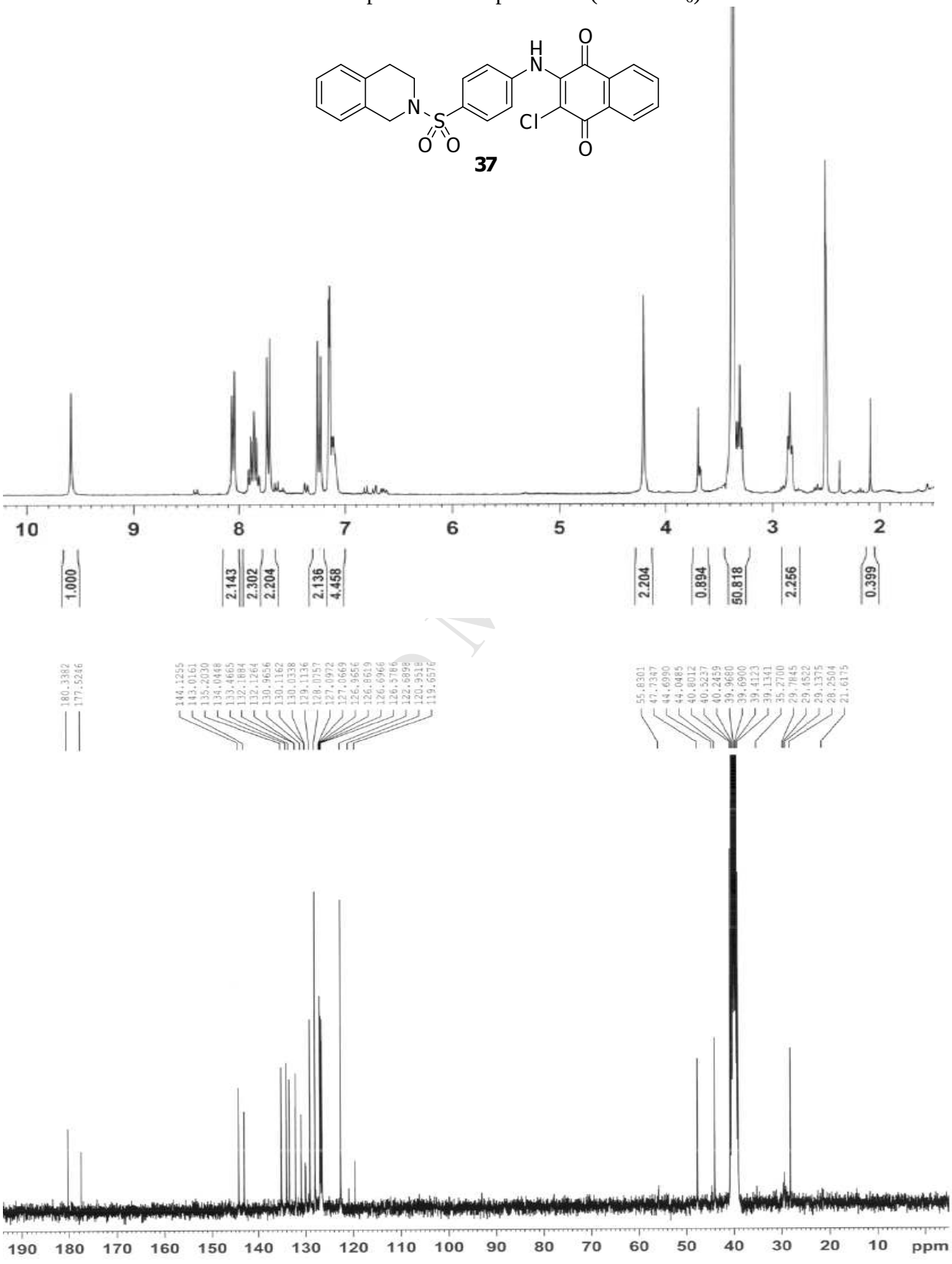

^{1}H and ^{13}C NMR spectra of compound **38** (DMSO-d_6)

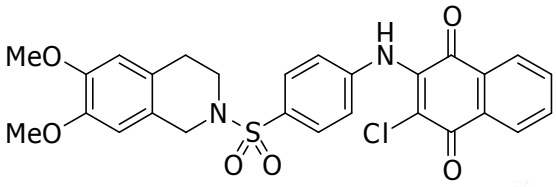

38

^{1}H and ^{13}C NMR spectra of compound **39** (DMSO-d_6)

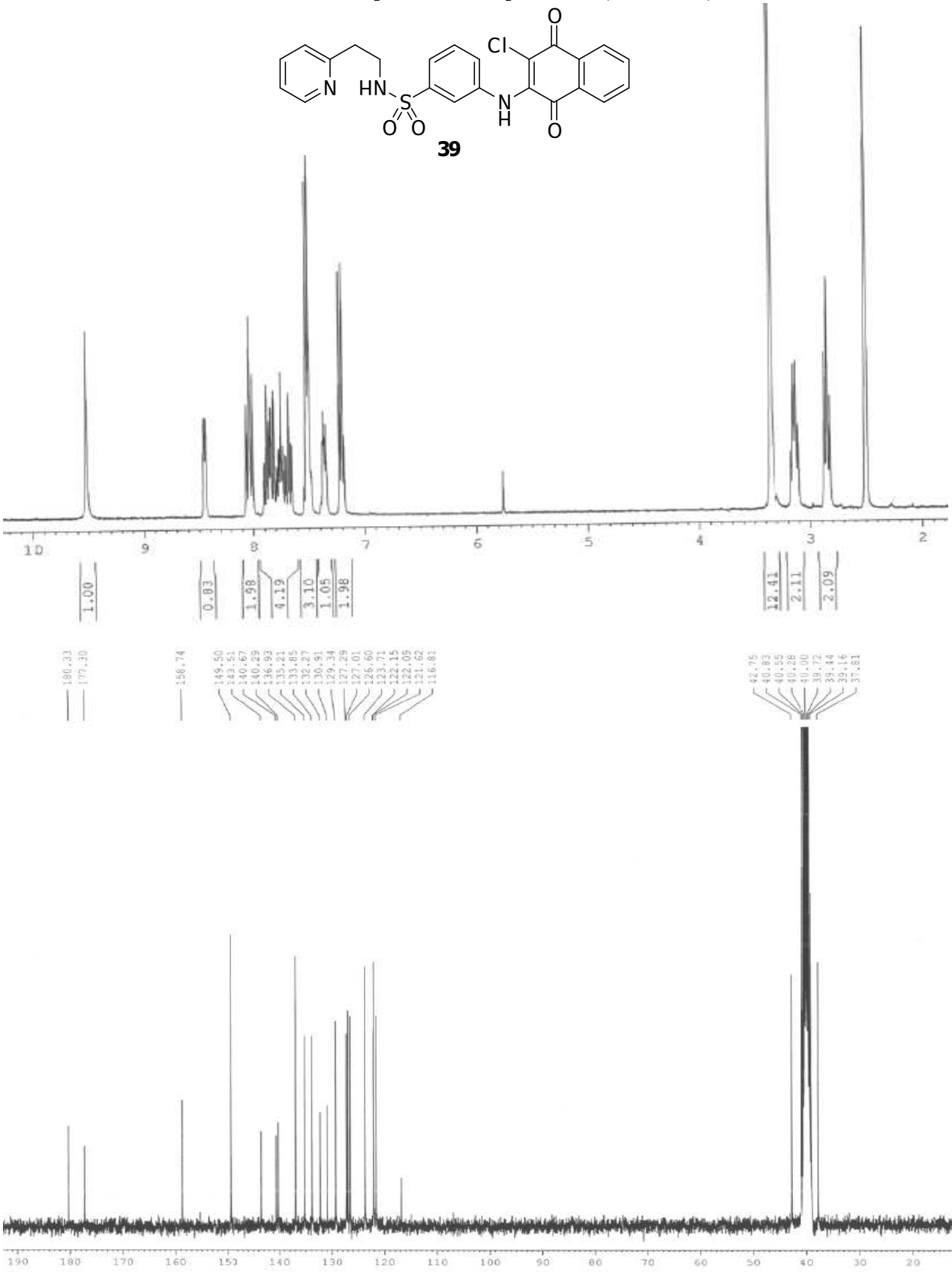

^{1}H and ^{13}C NMR spectra of compound **40** (DMSO-d_6)

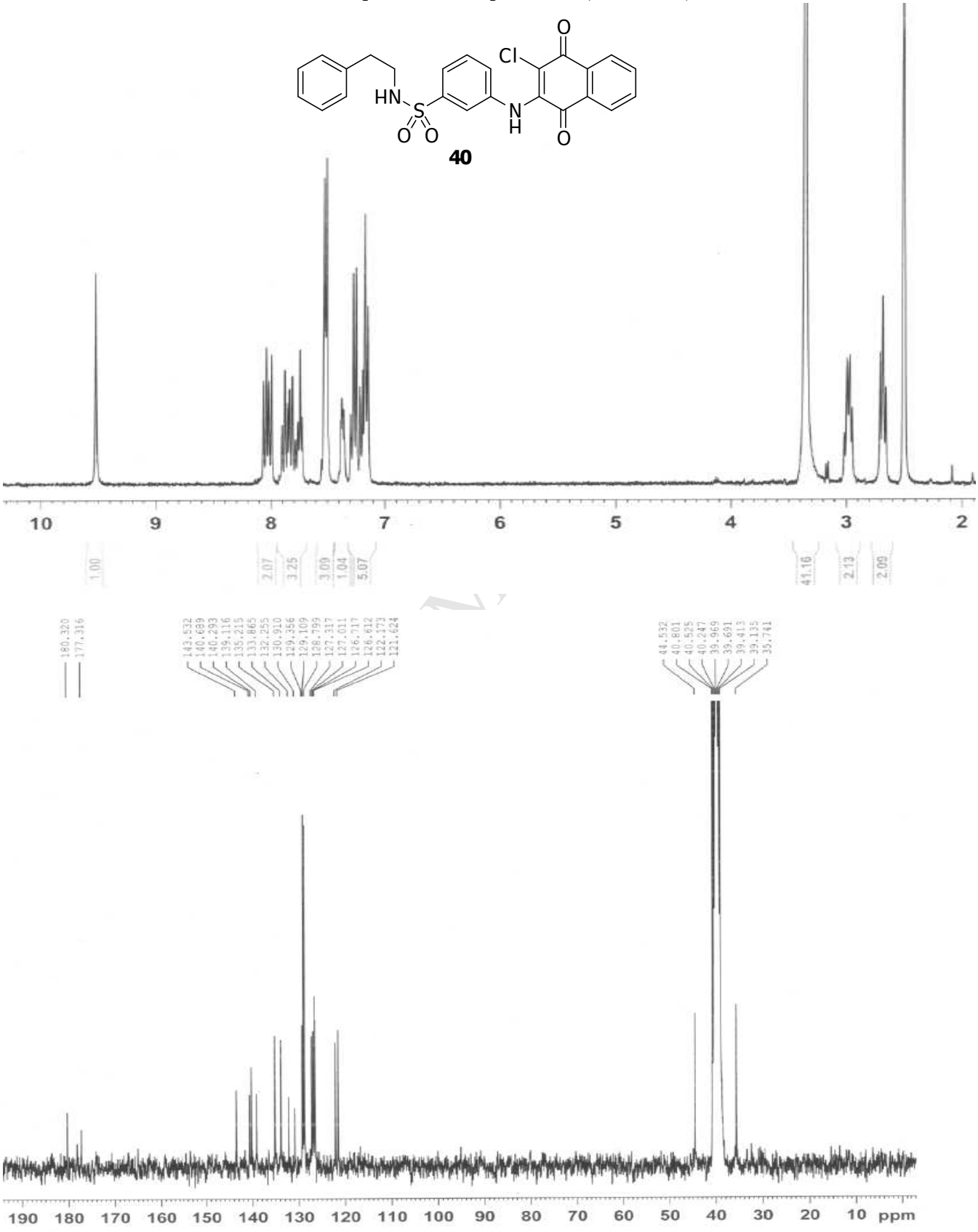

^{1}H and ^{13}C NMR spectra of compound **41** (DMSO-d_6)

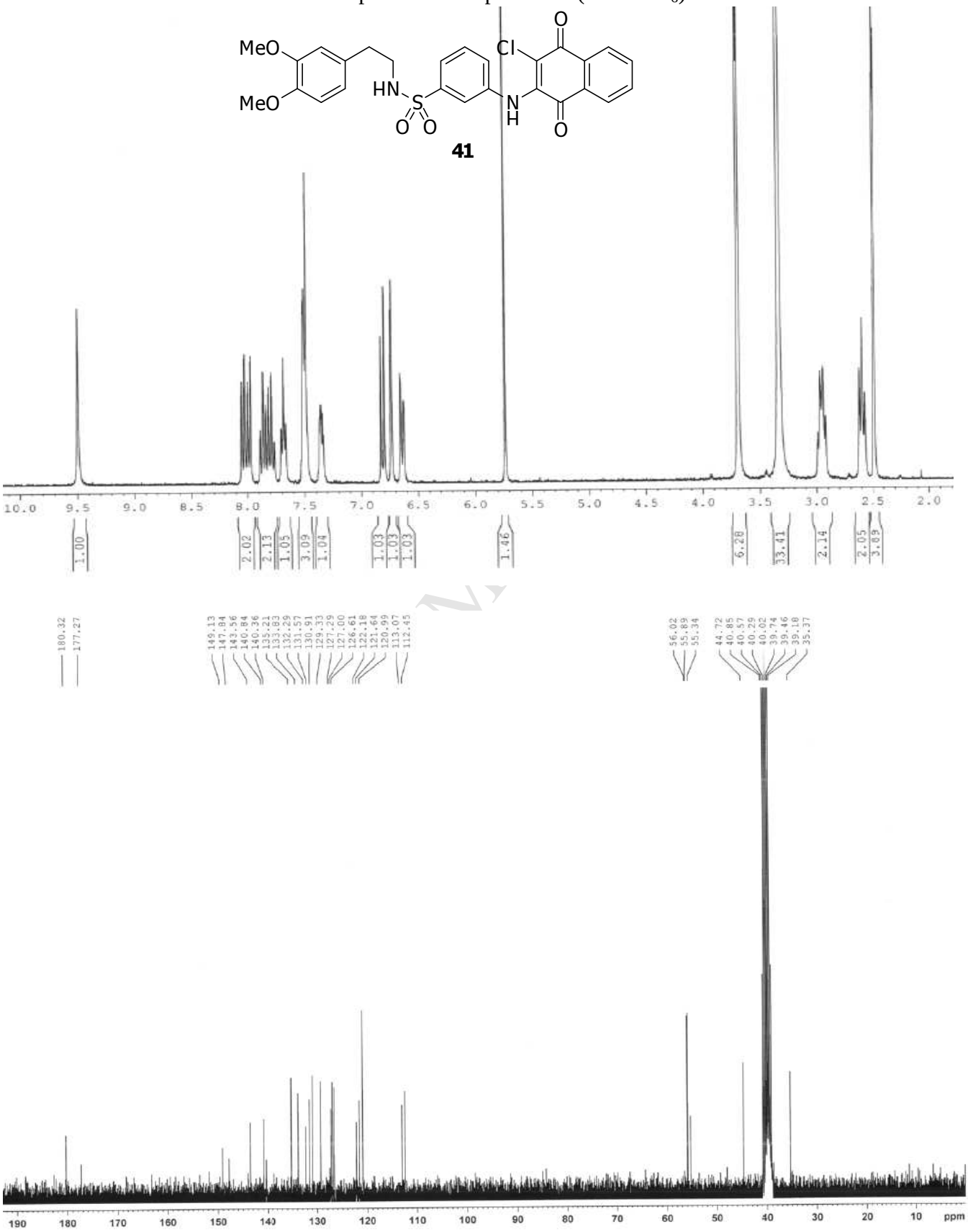

^{1}H and ^{13}C NMR spectra of compound **42** (DMSO-d_6)

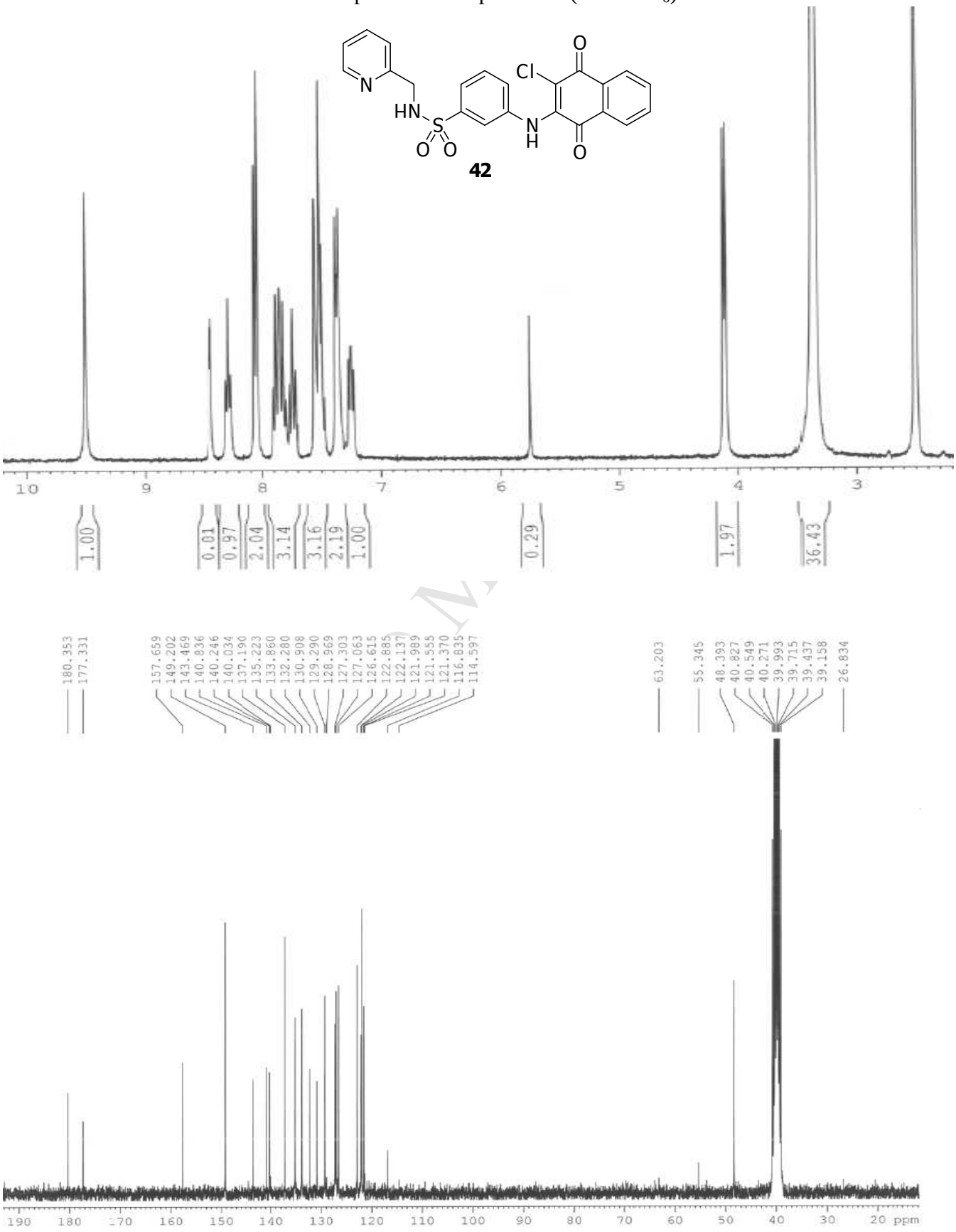

^{1}H and ^{13}C NMR spectra of compound **43** (DMSO-d_6)

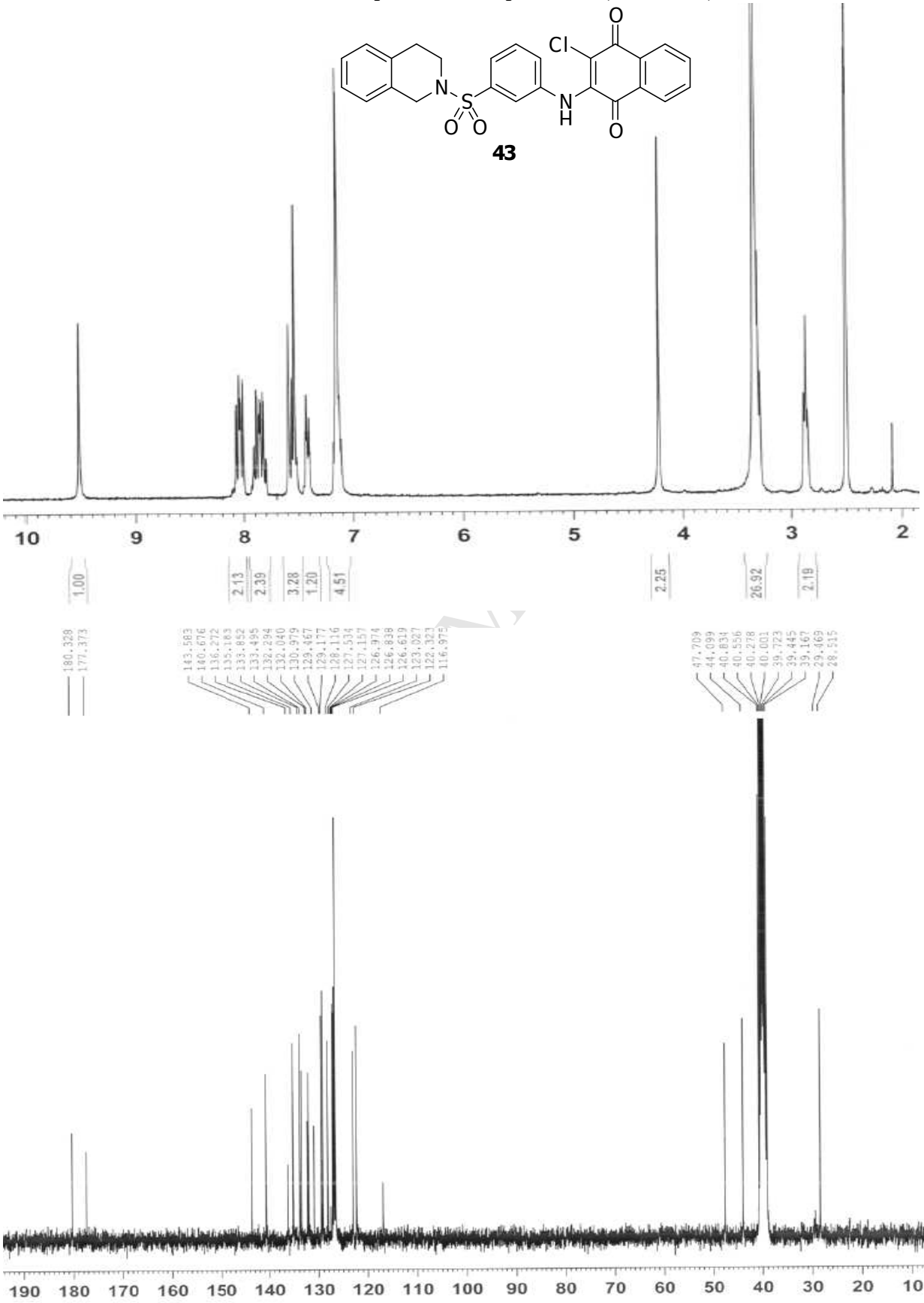

^{1}H and ^{13}C NMR spectra of compound **44** (DMSO-d_6)

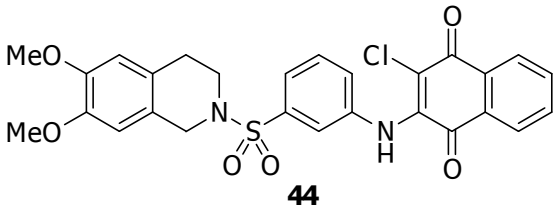

44